AFIT/GE/ENG/98M-01

IMPROVED MATHEMATICAL MODELING FOR GPS BASED NAVIGATION

THESIS

Salvatore Nardi
Captain, Canadian Forces

AFIT/GE/ENG/98M-01

19980409036

Approved for public release; distribution unlimited

The views expressed in this thesis are those of the author and do not reflect the official policy or position of the Department of Defense or the U. S. Government.

AFIT/GE/ENG/98M-01

IMPROVED MATHEMATICAL MODELING FOR GPS BASED NAVIGATION

THESIS

Presented to the Faculty of the School of Engineering
of the Air Force Institute of Technology
Air University
In Partial Fulfillment of the
Requirements for the Degree of
Master of Science in Electrical Engineering

Salvatore Nardi, B.Eng.
Captain, Canadian Forces

March, 1998

Approved for public release; distribution unlimited

Acknowledgements

First of all, I would like to thank my thesis advisor, Dr. Meir Pachter, for the outstanding guidance and support he provided. Even when the research outcome looked bleak, he remained enthusiastic, never lost hope, and somehow kept me motivated. His experience and insight were invaluable to the successful completion of this thesis.

I would also like to express my gratitude to my thesis committee members, Dr. Peter Maybeck and Captain Stewart DeVilbiss for the help they provided and for preparing me to undertake this research. I thank Mr. Donald Smith for being there for the occasional chat and for providing answers to some stupid questions when he could, but mostly for keeping the computer system in the guidance and control lab running, which at times required a great deal of creativity.

My greatest appreciation goes out to my wife, Maria, and my son, Daniel, for enduring my lack of attention while I was busy with class work and the thesis research. They supported me through this ordeal which was just as stressful on them as it was on me, so, I am grateful for their tolerance and understanding. Last but not least, I would like to thank my bird, Peewee, who at times seemed to be the only one I could relate to. When things got overly stressful, his pleasant, calm, and worryless nature helped ease my mind and kept me going.

Salvatore Nardi

Table of Contents

	Page
Acknowledgements	ii
List of Figures	vii
List of Tables	viii
Abstract	ix
I. Introduction	1-1
1.1 Background	1-1
1.2 Research Motivation	1-2
1.2.1 Improved User Positioning	1-3
1.2.2 Test Range Enhancement	1-3
1.2.3 Diversified Applications for GPS	1-4
1.2.4 Position Estimate Error Covariance	1-4
1.2.5 Computational Efficiency	1-5
1.3 Problem Statement	1-5
1.4 Scope	1-6
1.5 Assumptions	1-6
1.6 Methodology	1-7
1.6.1 Phase 1 - Development of a Closed Form Solution	1-7
1.6.2 Phase 2 - Implementation of the Algorithms	1-9
1.6.3 Phase 3 - Experimental Analysis	1-10
1.7 Thesis Overview	1-12

Page

II. Background 2-1

2.1 The Global Positioning System 2-1

2.1.1 GPS System Overview 2-1

2.1.2 The Earth Centered Earth Fixed (ECEF) Coordinate Frame 2-3

2.2 Summary of Current Knowledge 2-3

2.2.1 The GPS Pseudorange Equations 2-4

2.2.2 Conventional Iterative Solution to the GPS Pseudorange Equations 2-5

2.2.3 Closed-Form Solutions to the GPS Pseudorange Equations 2-8

2.2.4 Stochastic Modeling 2-9

2.2.5 The Stochastic Estimation Problem 2-11

2.2.6 Conclusion of Literature Review 2-12

III. Mathematical Derivations 3-1

3.1 Stochastic Closed-Form Solution 3-1

3.1.1 Basic Concepts 3-1

3.1.2 Linear Regression 3-2

3.1.3 Noise Statistics 3-6

3.1.4 Minimum Variance Estimate Solution 3-10

3.1.5 Estimate Error Covariance 3-12

3.2 Maximum Likelihood Estimate 3-13

3.2.1 Maximum Likelihood Concept 3-13

3.2.2 Mathematical Development 3-15

3.3 Kalman Update Solution 3-19

3.3.1 Kalman Update Concept 3-19

3.3.2 Linearized Measurement 3-20

Page

3.3.3 Noise Statistics 3-22

3.3.4 The Augmented Linear Regression 3-24

3.4 Alternate Stochastic Closed-form Solution 3-34

3.4.1 New Linear Regression in n Equations 3-35

3.4.2 Noise Statistics 3-37

3.5 Conclusion of Mathematical Derivations 3-45

IV. Experimental Results and Analysis 4-1

4.1 Overview 4-1

4.2 Data Set Generation, Simulated GPS Test Environment 4-3

4.3 Simulation of the Ground-Based Pseudolite Test Environment 4-4

4.4 Experimental Data Description 4-6

4.5 The Monte Carlo Runs 4-10

4.6 Experimental Observations, Simulated GPS Test Environment 4-10

4.7 Conventional Iterative Algorithms 4-10

4.7.1 Analysis of Results 4-11

4.8 Closed-Form Algorithm 4-13

4.8.1 Limitations 4-14

4.8.2 Analysis of Results 4-15

4.8.3 Experimental Results, Alternate Closed-Form Algorithm 4-20

4.9 Maximum Likelihood 4-21

4.9.1 Limitations 4-21

4.9.2 Analysis of Results 4-22

4.10 Kalman Update 4-23

4.10.1 Analysis of Results 4-23

Page

4.11 Experimental Results, Ground-Based Pseudolite Test Environment 4-38

4.11.1 Analysis of Results, Conventional Iterative Least Squares Algorithm 4-38

4.11.2 Analysis of Results, Closed-Form Algorithm . 4-40

4.11.3 Analysis of Results, Kalman Update 4-42

4.12 Summary of Experimental Results 4-42

V. Conclusions and Recommendations 5-1

5.1 Typical Near-Earth GPS Applications 5-1

5.2 Unconventional GPS Applications 5-3

5.3 Estimation Error Covariance 5-5

5.4 Condition Number of the Regressor 5-7

5.5 Recommendations 5-8

5.5.1 GPS Measurement Noise Levels Investigation 5-8

5.5.2 Alternate Stochastic Closed-Form Algorithms 5-9

5.5.3 Computational Effectiveness 5-10

Bibliography BIB-1

Vita VITA-1

List of Figures

Figure		Page
3.1.	Maximum Likelihood of Gaussian Probability Distribution Subject to a Linear Constraint	3-14
4.1.	Scenario B, Optimum Ground-Based Planar Array	4-6
4.2.	Geometry Effects on Miss Distance	4-12
4.3.	Geometry Effects on Standard Deviation	4-14
4.4.	Closed-Form Algorithm Performance versus Condition Number	4-16
4.5.	Estimation of σ Using Scenario Concatenation	4-19
4.6.	Skyplot, Scenario 1	4-26
4.7.	Skyplot, Scenario 2	4-27
4.8.	Skyplot, Scenario 3	4-28
4.9.	Skyplot, Scenario 4	4-29
4.10.	Skyplot, Scenario 5	4-30
4.11.	Skyplot, Scenario 6	4-31
4.12.	Skyplot, Scenario 7	4-32
4.13.	Skyplot, Scenario 8	4-33
4.14.	Skyplot, Scenario 9	4-34
4.15.	Skyplot, Scenario 10	4-35
4.16.	Skyplot, Scenario 11	4-36
4.17.	Skyplot, Scenario 12	4-37

List of Tables

Table		Page
4.1.	Monte Carlo Simulation Results, Scenario 1	4-26
4.2.	Monte Carlo Simulation Results, Scenario 2	4-27
4.3.	Monte Carlo Simulation Results, Scenario 3	4-28
4.4.	Monte Carlo Simulation Results, Scenario 4	4-29
4.5.	Monte Carlo Simulation Results, Scenario 5	4-30
4.6.	Monte Carlo Simulation Results, Scenario 6	4-31
4.7.	Monte Carlo Simulation Results, Scenario 7	4-32
4.8.	Monte Carlo Simulation Results, Scenario 8	4-33
4.9.	Monte Carlo Simulation Results, Scenario 9	4-34
4.10.	Monte Carlo Simulation Results, Scenario 10	4-35
4.11.	Monte Carlo Simulation Results, Scenario 11	4-36
4.12.	Monte Carlo Simulation Results, Scenario 12	4-37
4.13.	Monte Carlo Simulation Results, Ground Test Environment	4-39

Abstract

In order to enhance the accuracy of the Global Positioning System (GPS) it is proposed to improve the GPS position determination algorithm used in the GPS receiver to solve the trilateration equations. The use of direct, or closed-form, solutions based on stochastic modeling and estimation techniques is investigated to achieve this improvement. The objective of this thesis research is the development and experimental analysis of new closed-form position determination algorithms that work in the presence of pseudorange measurement noise. The mathematical derivation of two closed-form solution algorithms, based entirely on linear mathematics, is presented. The closed-form algorithms provide an estimate of the GPS solution parameters (viz., the user position and the user clock bias) as well as the associated parameter estimation error covariance. The experimental results are based on 5000 Monte Carlo runs and are produced through realistic simulations of typical NAVSTAR GPS low noise, near-earth navigation scenarios and of ground-based pseudolite planar array scenarios. Analysis of the experimental results is accomplished through direct comparison to the baseline results from the conventional Iterative Least Squares (ILS) algorithm, which is currently used in GPS. To ensure fair comparitive analysis, all the algorithms are tested under identical noise and geometry conditions. The closed-form algorithms, both of which produce identical results, are extremely sensitive to noise in typical NAVSTAR GPS scenarios, making them unsuitable for stand-alone use; however, they perform very well at estimating horizontal position parameters in ground-based pseudolite planar array scenarios where the ILS algorithm breaks down due to poor geometry. For the near-earth GPS scenarios, the use of an additional nonlinear measurement in a supplementary algorithm is required to refine the solution produced by the closed-form algorithm. Thus, the derivation of two supplementary algorithms is presented. The first supplementary algorithm is based on a

maximum likelihood approach and the second uses a Kalman-like update approach. The maximum likelihood algorithm is capable of producing solutions with accuracy equivalent to that of the conventional ILS algorithm, both in terms of mean estimation errors and experimental estimation parameter standard deviations; however, the capability to predict its estimation error covariance is lost. The performance of the Kalman update algorithm is marginally degraded, most notably in its user clock bias estimation errors, but it is capable of predicting its estimation error covariance. The capability to predict the estimation error covariance is dependent on how well the closed-form algorithm estimates the pseudorange measurement noise variance, which in turn is a function of satellite availability. The performance of the closed-form, supplemented by the Kalman update, algorithm is comparable to the ILS algorithm's performance. The advantages introduced by the developed algorithm are: 1) The capability to estimate its estimation error covariance, and 2) The potential for computational efficiency due to the direct, closed-form, nature of the solution.

IMPROVED MATHEMATICAL MODELING FOR GPS BASED NAVIGATION

I. Introduction

1.1 Background

The NAVSTAR Global Positioning System (GPS) is an extremely accurate navigation system; nevertheless, there are errors associated with the GPS position fix, leaving room for further improvements. The GPS is a space based satellite radio navigation system that provides three dimensional (3-D) user positioning by solving a set of nonlinear pseudorange trilateration equations. A common approach to solving the nonlinear equations is to linearize the pseudorange equations and calculate the user position iteratively, starting with a user provided initial position guess [27]. For near-earth navigation, the center of the earth is a good initial guess which guarantees that the iterative algorithm will quickly converge towards the correct GPS solution. An area of potential improvement, that has been the topic of several papers in recent years, is the use of closed-form solutions to the nonlinear GPS pseudorange equations. The use of closed-form or direct solutions has been motivated by the fact that direct solutions shorten the computational cycle and that they do not depend on an initial position guess. Closed-form solution algorithms have been developed by Bancroft [2], Krause [14], Abel and Chaffee [1], Chaffee and Abel [6], and Hoshen [11] using different approaches.

The recent derivations of the closed-form solutions considered only the exactly determined case in which four of the available pseudorange measurements are used to obtain exact positioning solutions. The motivation for considering only four satellites is questionable since, if a five degree elevation mask angle is assumed, it has been

shown that for near-earth navigation, there are at least five satellites in view at all times and at least seven satellites in-view 80 % of the time [28]. An elevation mask angle is used to mask satellites close to the horizon. Although satellite vehicles close to the horizon are in-view by line-of-sight, their transmitted data is prone to a large amount of atmospheric interference caused by the long propagation path through the ionosphere and troposphere. In airborne applications, satellite visibility will tend to improve with altitude, potentially increasing the number of satellite pseudorange measurements available. In addition, some receivers have access to signals from the GLONASS constellation, the former USSR's satellite-based global navigation system, potentially doubling satellite availability.

Previous works on closed-form solutions of the GPS pseudorange equations did not make use of the pseudorange measurements from all in-view satellites. This research differs from previous works in that it will treat an overdetermined system, making use of all in-view satellites. Furthermore, the research specifically addresses the issue of developing a reliable closed-form solution that works in the presence of noise. With the exception of [8], the pseudorange equations have been treated as a deterministic set of equations. Benefits can be gained by recognizing that pseudorange measurements are noise corrupted; hence, the stochastic nature of the measurements should be reflected in the GPS pseudorange equations from the onset to develop a stochastically sound position solution estimate. Furthermore, it would allow for obtaining an estimate of the covariance of the position estimation error.

1.2 Research Motivation

The goal in the design of a navigation system is to obtain the best possible positioning accuracy by eliminating or at least minimizing the impact of error sources. The GPS system errors can be attributed to seven basic sources of error: satellite clock errors, atmospheric delays, group delay, ephemeris errors, receiver noise and resolution, multipath errors, and receiver vehicle dynamics [21]. These sources of

error are briefly addressed in the discussion of the stochastic modeling of the pseudorange equations in Chapter II. Although not the only, or most intuitive, approach to improving positioning accuracy, improvement of the GPS position determination algorithm used within the receiver to produce the position estimate from the pseudorange measurements undoubtedly impacts the achievable accuracy of the solution. Improvements to the algorithm will complement any other system improvements to reduce errors in any of the seven basic error sources. There are numerous potential benefits that encourage improvements to the GPS position determination algorithm; a few that provided the motivation to this thesis are discussed in this section.

1.2.1 Improved User Positioning. GPS plays an extremely important role in positioning applications, both military and civilian. Regardless of whether precise positioning service (PPS) or standard positioning service (SPS) is being used, an improved GPS position determination algorithm that provides a closed-form solution to the GPS pseudorange equations considering all in-view satellites can improve the accuracy of the GPS position fix. The improvement is expected to be achieved as a result of computing an exact solution to the nonlinear equation as opposed to introducing approximations by linearizing the equations.

1.2.2 Test Range Enhancement. The Submeter Accuracy Reference System (SARS) navigation test reference system being developed at the 746^{th} Test Squadron at Holoman Air Force Base, is used primarily in the flight testing of integrated navigation systems [20]. With the improvement of GPS, the accuracy of the integrated aircraft navigation systems is also improving. Since the test reference system must provide much higher accuracy than the system being tested, the importance of improved test range accuracy can never be overemphasized. The use of an improved GPS position estimation algorithm can enhance the accuracy of the SARS.

1.2.3 Diversified Applications for GPS. Current iterative GPS algorithms are guaranteed to converge to a correct position solution for near-earth users, initializing the iterations at the earth's center and assuming a zero user clock bias [1]. In space applications, inverted GPS applications such as the SARS [25], [20], and unconventional applications that involve the use of both pseudolites and satellites, the lack of a sufficiently good initial guess may lead to convergence towards the wrong solution. Pseudolite are ground-based transmitters that provide GPS-like positioning data and can be used for augmentation. Inverted GPS applications, and the use of pseudolites are applications that are currently being considered by the 746^{th} Test Squadron for the SARS as a result of work performed at AFIT by McKay [20]. The fact that a closed-form solution will not require an initial position guess is an advantage for these applications.

1.2.4 Position Estimate Error Covariance. By stochastically modeling the GPS pseudorange equations, solving for position becomes a stochastic estimation problem. The use of correct stochastic modeling and of Kalman Filtering like techniques to solve the estimation problem will lead to a GPS solution that provides accurate estimates of the position estimation error covariance in addition to the position estimate itself. This will introduce a new confidence factor into GPS positioning and is critical for the integration of GPS with additional sensors for integrated navigation systems. This will specifically enhance the accuracy of navigation systems that are integrated using a federated approach but will not help in deep integration schemes as discussed in [16], where the raw pseudorange signals are being used for system integration. Federated system integration is done at processed data levels using computed positioning data from the navigation sensors. This approach is common when system integration is performed as an upgrade on existing sensors that do not provide access to raw data signals required for deep integration [9].

1.2.5 Computational Efficiency. The use of direct, or closed-form solution algorithms tend to be more computationally efficient than iterative or recursive algorithms. This efficiency results in reduction of the computational cycle which is most advantageous for fast moving vehicles. The use of a positioning algorithm with short computation cycles is of extreme importance to space vehicles where the earth's rotation and the vehicle movement, in the computation interval, needs to be taken into account.

1.3 Problem Statement

The objective of this thesis is to provide a closed-form solution to the GPS pseudorange equations and present a way of using it effectively in the presence of GPS measurement noise. This thesis work develops an improved closed-form mathematical solution to the GPS pseudorange equations, implements an algorithm based on the mathematical solution, and performs an experimental analysis of the algorithm using realistic Monte Carlo simulations. The mathematical derivation of the closed-form solution used in this research is closely based on notes provided by Dr. Meir Pachter [22].

The closed-form positioning solution will consider pseudorange measurements from all available satellites, to obtain a position fix, since they are readily handled by the closed-form solution algorithm. A minimum of five satellites will be needed to obtain an initial 3-D position fix using the algorithm developed in this thesis, but this is not a serious problem since there are always more than four satellites in-view when the NAVSTAR GPS constellation is fully operational. The thesis work will emphasize the proper use of stochastic modeling and estimation in order to provide appropriate weighting of satellite pseudorange data in producing a positioning solution.

1.4 Scope

The focus of this research is on the improvement of the GPS algorithm to obtain better positioning accuracy and to obtain shorter computation cycles. There are numerous other factors in GPS receiver design that affect GPS positioning accuracy that will not be addressed in this thesis. The GPS will be considered at the system level, hence the inner workings of the GPS receiver will not be considered. The GPS pseudoranges that will be used in the research are *corrected pseudoranges.* The *corrected pseudoranges* will represent the pseudoranges as they would be provided by the receiver after all known correction factors have been applied and known errors modeled out of the raw pseudorange measurements. The corrections of these errors are GPS receiver design issues beyond the scope of this thesis. Throughout this thesis, the term *pseudoranges* is treated as meaning *corrected pseudoranges.*

The experimental analysis will be limited to obtaining positioning performance indexes relative to the conventional ILS GPS algorithm. The experimental analysis will not encompass any computational and numerical performance issues that would have to be addressed prior to using the algorithm in real-time applications. Due to the proprietary nature of the algorithms in current commercially available GPS receivers, comparisons to actual GPS receiver performance will not be attempted.

1.5 Assumptions

Assumptions must be made about the noise corrupting the pseudorange measurements in order to allow the use of a simple stochastic model and to simplify the stochastic estimation problem. The following assumptions are used in this thesis:

1. After all known corrections are applied to the pseudorange measurements, the residual noise corrupting the pseudorange measurement is a zero-mean Gaussian distributed noise.
2. The noises on all the pseudorange measurements have equal variance.

3. The noises on the pseudorange measurements are uncorrelated with one another.
4. The effects of Selective Availability (SA) on pseudorange noise is not considered.
5. A 10 degree elevation angle is always achievable for determination of in-view GPS satellites.
6. The GPS satellite constellation has 24 fully operational satellites.

The extent to which the assumptions are valid is not exactly known; consequently, the impact of using these assumptions can't be determined beforehand. Some of the assumptions made are necessary to obtain the solution to the pseudorange equations. Others are required to establish a realistic baseline for satellite availability used for the experimental simulations. Attempts will be made to qualify the significance of these assumptions on the positioning solution through experimental analysis.

1.6 Methodology

This thesis contains three distinct phases. The first phase is the development of the closed-form solution to the pseudorange equations. The second phase is the implementation of the experimental algorithms based on the developed solutions. The third phase is the experimental analysis which can only be initiated after the algorithms in the second phase are fully completed, implemented, and debugged. The approach will be iterative in nature since rework of the mathematical solution may be required after some experimental analysis is performed, which in turn will require changes to the algorithms and the performing of new simulations.

1.6.1 Phase 1 - Development of a Closed Form Solution. This phase consists of the mathematical derivation of a closed-form solution to the GPS pseudorange

equations. The solution will consider $n \geq 5$ satellites and will capture the stochastic nature of the pseudorange measurement.

The corrected pseudorange can be modeled as the true Euclidean range with an unknown clock bias and some measurement noise superimposed; thus, the stochastic pseudorange measurement equation is given by

$$R_i \equiv \sqrt{(u_x - x_i)^2 + (u_y - y_i)^2 + (u_z - z_i)^2} + b + w_i, \tag{1.1}$$

where R_i is the corrected pseudorange corresponding to the i^{th} satellite, (u_x, u_y, u_z) are the user position coordinates, (x_i, y_i, z_i) are the known coordinates of the i^{th} satellite, b is the range-equivalent user clock bias defined as the error in the receiver clock times the speed of light, and w_i is zero-mean Gaussian pseudorange measurement noise. It is reasonable to assume that all measurements are subject to the same noise; therefore, they will have the same variance, σ^2. However, the noise terms are not correlated between satellites. The point of departure for the mathematical derivation of the closed-form stochastic solution is Equation (1.1).

One such measurement equation is available for each of the n in-view satellites. The n equations will be referred to as the GPS pseudorange equations. All positions used in the derivation will be expressed in Earth Centered Earth Fixed (ECEF) coordinates. These n nonlinear equations will be solved algebraically for the estimated user position, (u_x, u_y, u_z) and user clock bias, b. This will be achieved through algebraic manipulation to reduce the GPS pseudorange equations into a linear regression in the form of the standard linear measurement model as defined in [18]. The linear regression is given by

$$\vec{Z} = H\vec{X} + \vec{V}, \tag{1.2}$$

where $\vec{Z}$ is the measurement vector, $\vec{X}$ is the vector of unknown quantities comprising the user position coordinates (u_x, u_y, u_z) and the user clock bias (b), H is

the regressor, an $(n \times 4)$ measurement matrix, and $\vec{V}$ is a Gaussian noise vector, or equation error vector, whose covariance matrix must be determined. The solution is obtained by solving the static estimation problem. The covariance of the estimation error of the user position and user clock bias is also obtained.

1.6.2 Phase 2 - Implementation of the Algorithms. Matlab [17] algorithms based on the solution processes to the GPS pseudorange equations developed in Phase 1 are implemented. The main algorithm will be referred to as the *closed-form* algorithm to distinguish it from conventional iterative algorithms. The *closed-form* algorithm will expect as inputs pseudorange measurements from $n \geq 5$ satellites and will provide as a solution the estimates of the user position coordinates, user clock bias, and the associated estimation error covariance matrix. The *closed-form* algorithm, as implied by its name, will be non-iterative in nature; hence, will not be using an initial guess of the receiver position and clock bias.

Two additional algorithms based on conventional iterative solutions to the GPS pseudorange equations will also be implemented in Matlab. Both algorithms will be iterative in nature and will both use the linearized pseudorange equation approach described in [27]. These algorithms will expect the same input that was provided to the direct algorithm, the pseudorange measurements from $n \geq 5$ satellites. Since these algorithms require an initial guess of the receiver position and clock bias, the initial guess will be built into the algorithms. Due to the lack of a better guess it is common practice to use the center of the earth as the initial position guess and zero as the initial clock bias guess.

The first iterative algorithm will use all available pseudorange measurements to calculate a least squares solution; the algorithm will be referred to as the Iterative Least Squares (ILS) algorithm. The second algorithm will provide a solution based on only the best four pseudorange measurements based on geometry *strength.* Dilution of Precision (DOP) is used as a measure of geometrical strength [5]; thus, a frequently

used approach is to select the four satellites whose geometry yields the smallest Position Dilution of Precision (PDOP), which considers only the effect of the three ECEF axis position errors [27]. To simplify the experimental data collection, the Geometric Dilution of Precision (GDOP) will be used to evaluate the geometry since GDOP will be the same as PDOP if a zero receiver clock drift rate is assumed. GDOP is defined as,

$$GDOP \equiv \sqrt{tr\{(H^T H)^{-1}\}}, \tag{1.3}$$

where H is the matrix of direction cosines associated with the conventional iterative algorithms. The algorithm which considers only the four satellites which yield the lowest GDOP is referred to as the Iterative Best Four (IBF) algorithm. Both algorithms provide a solution that includes the estimated receiver position coordinates, and the receiver clock bias. These algorithms do not have the capability of providing an indication of how good the calculated estimates actually are unless they are artificially informed of the pseudorange noise strength. Since in a simulated experiment the noise strength is known, it is possible to inform the algorithm of the value of σ to verify how well the algorithm's predicted performance compares to its actual performance based on the experimentally obtained covariance yielded over the 5000 Monte Carlo runs. A discussion of how the number of Monte Carlo runs was selected is presented in Chapter IV.

1.6.3 Phase 3 - Experimental Analysis. The experimental analysis phase will contain the bulk of the work of this study. The object of this phase is to provide thorough and realistic performance analyses of the closed-form algorithm implemented in the second phase. In addition to evaluating how good the position and clock bias estimates are, particular emphasis will be placed on how well the algorithm believes it is doing. The provision of the estimation error covariance is the key innovation to the algorithm developed in this thesis; hence, it is of extreme importance that the validity of this feature be established. Some performance comparisons

between the direct algorithm and the two iterative algorithms will be performed to provide an appreciation of the relative performance.

GPS ephemeris data will be generated using GPS simulation tools available in the GPSoft Satellite Navigation Toolbox for Matlab [10]. This will provide realistic data from which true ranges from all in-view GPS satellites to an arbitrarily selected receiver position can be calculated. After adding an arbitrary clock bias to all the ranges, a zero-mean random noise of preselected variance is superimposed to represent the Gaussian measurement noise. These generated pseudoranges will serve to perform the analysis of the GPS algorithm through the running of 5000 Monte Carlo trials. Using the Satellite Navigation Toolbox, the capability exists of simulating realistic noise corrupted pseudorange measurements which could be applied directly to the GPS position determination algorithm as would be the case in a real world scenario. The approach used of simulating just the GPS satellite ephemeris data and producing the simulated pseudoranges was preferable for the following reasons:

1. It provides a more structured data set for analysis of the algorithms since only the desired effects are being considered and the amount of corruption on the pseudorange measurements is exactly known; and
2. Since the pseudoranges are produced starting from exactly known position coordinates, comparisons against the true position for determining accuracy are possible.

Numerous trials will be run under different scenarios to provide a thorough picture of the performance. As an end result of the Monte Carlo simulations in Matlab, an estimate of the position fix accuracy attainable using the developed algorithm will be obtained and consequently compared to that achievable using the conventional algorithms. Recognizing that a large number of Monte Carlo trials are required to achieve statistically reliable experimental results, all simulations will be based on 5000 Monte Carlo runs.

Through the experimental trials the issue of geometry will also be analyzed. Experimental scenarios with varying degrees of GDOP will be used for the trials to bring out the effects of geometry on GPS positioning. GDOP is commonly used as a measure of GPS satellite geometry, whereby a lower GDOP is an indication of better geometry; hence, lower positioning error. As suggested by McKay, GDOP may not be the best measure of geometry [20]; therefore, the condition number of the regressor matrix will also be examined and attempts will be made to bring forth any relationships to the accuracy bounds. It is expected that, through the investigation of satellite geometry, some interesting issues related to the accuracy of the GPS positioning calculations will arise. The validity of considering only the four satellites that yield the best GDOP to calculate a position fix, as well as the validity of using GDOP as the measure of geometry, will be examined.

1.7 Thesis Overview

Chapter II presents the background theory upon which this research will be based. The first part includes a thorough literature review that provides a summary of current knowledge in the field of closed-form GPS algorithms and the application of stochastic modeling to the GPS pseudorange equations. The second part discusses the basic concepts of GPS technology. Particular emphasis is placed on the formulation of the GPS pseudorange equations and the theory behind the current iterative algorithms.

Chapter III presents a thorough development of the *closed-form* mathematical solution to the GPS pseudorange equations. The development of supplementary algorithms that make use of a nonlinear measurement equation and that were deemed essential to enhance the performance of the *closed-form* algorithm is also addressed. The purpose of these enhanced algorithms is to produce an improvement to the solution achieved by the *closed-form* algorithm; they are not capable of providing, nor are they intended to provide, stand-alone solutions. The two stage algorithms that are

presented are the *Maximum Likelihood* approach and the *Kalman Update* approach. The background theory and the operating concept behind each approach is discussed and the complete mathematical derivations are presented. The development of an *alternate closed-form* algorithm is also presented.

Chapter IV presents the experimental portion of the thesis. The first part discusses how the experiment was set up and how the Monte Carlo trials were run. Next is presented a brief discussion of how the results are intended to be interpreted. The experimental results are then presented and the chapter sums up with a detailed analysis of the results.

Chapter V presents a brief summary of the performance related issues of the *closed-form* algorithm and the supporting algorithms developed for this thesis research. Emphasis is placed on the identifying the areas of strength for the algorithms and suggesting applications for which they are best suited. The shortcomings seen in the Chapter IV related to algorithm deficiency and inconclusive findings are discussed, and potential approaches to correcting the problems are presented. The chapter sums up with recomendations for future work that can prove rewarding in bringing the concept of using a stochastic closed-form GPS position determination algorithm closer to reality.

II. Background

This chapter presents the background theory upon which this research will be based. The first part includes a thorough literature review that provides a summary of current knowledge in the field of closed-form GPS algorithms and the application of stochastic modeling to the GPS pseudorange equations. The second part discusses the basic concepts of GPS technology. Particular emphasis is placed on the formulation of the GPS pseudorange equations and the theory behind the current iterative algorithms.

2.1 The Global Positioning System

This section presents an overview of the Global Positioning System to provide some insight into the complexity of the system. This section serves to focus attention to the specific portions of GPS of interest in this thesis, namely the position determination algorithm within the GPS receiver, and shows how it fits into context of the overall GPS system. GPS specific terminology and the coordinate systems used in this thesis are discussed as well.

2.1.1 GPS System Overview. GPS is a satellite based radio-navigation system that provides worldwide, virtually continuous, three-dimensional (3-D) positioning and accurate timing. The beauty of the system is in its apparent simplicity since, from the user's perspective, extremely accurate positioning can be achieved with the use of a simple, fairly inexpensive GPS receiver. For these reasons, GPS is rapidly becoming the positioning sensor of choice for both military and civilian users. The continuous worldwide coverage provided by GPS makes it ideally suited for air, land, and sea navigation applications. It must be recognized that there is much more to GPS than the portion that the typical user is dealing with in obtaining a GPS position fix. GPS is composed of three segments: the space segment, the control segment, and the user segment. Each segment is essential to the proper

functioning of GPS as an accurate and reliable navigation tool. The typical GPS user is concerned with the user segment only.

The GPS space segment refers to the GPS satellite constellation. The GPS constellation consists of 24 satellites, 21 active satellites plus three active spares, in six orbital planes. Each of the satellites has an orbital period of approximately 12 hours (half a sidereal day). A healthy GPS constellation provides satellite coverage such that, for near-earth locations, there are always at least five satellites in-view and at least seven satellites in-view 80 percent of the time [28]. The satellites transmit time-tagged navigation messages which the GPS receivers (user segment) use to calculate their positions. The navigation message information required by the receivers to perform their function, includes GPS time, satellite ephemeris data, correction data, and system almanac data [27].

The control segment is composed of five stations spread over the world, which monitor and control the satellite orbits and GPS time. Only one of the five stations is the master control station and only three of the remaining four stations are uplink stations capable of transmitting data back to the satellites. The five stations receive the same signals seen by all users and collect pseudoranges to all the satellites. All pseudorange measurements collected by the stations are transmitted to the master control station which then computes the true satellite positions and true GPS time. This is possible since the stations are situated at very well surveyed positions. The master control station then calculates corrections for the satellites and transmits them to the uplink stations where the corrections are transmitted to the satellites [26].

The user segment is the GPS receiver. The receiver receives the navigation message, extracts the data and applies the corrections to obtain the pseudorange and pseudorange rate measurements. The user position, velocity, and time are then obtained through an algorithm that calculates a solution from the corrected pseudo-

range measurements. The proposed research will specifically address an algorithm that can be used by a GPS receiver to obtain a position fix.

2.1.2 The Earth Centered Earth Fixed (ECEF) Coordinate Frame. The ECEF coordinate frame is an orthogonal frame with its origin at the earth's center of mass. The ECEF frame is fixed to the earth and therefore rotates with the earth. This frame consists of three axes: x, y, and z. The z axis is aligned with the earth's spin axis directed north and the x and y axes lie in the equatorial plane. The x axis is directed through the Greenwich Meridian (0 longitude) and the y axis through the 90 east longitude [27]. ECEF coordinatization is commonly used in GPS since, in near-earth navigation, the navigator wants to know his positioning with respect to the earth. Calculations in the GPS receiver are normally performed in the ECEF frame for convenience but are converted, in the GPS receiver, to a coordinate system the user selects for display. Geographic coordinates (Latitude, Longitude and Altitude) are commonly used for display purposes.

2.2 Summary of Current Knowledge

The proposed thesis research involves the development and evaluation of a closed-form solution to the GPS pseudorange equations using stochastic modeling and estimation. A thorough literature review was required to identify areas and approaches that have not yet been explored in the field of closed-form GPS solutions and to establish the framework for this thesis research. This review of current literature on the NAVSTAR GPS emphasizes the development of closed-form solutions to the pseudorange equations and stochastic estimation.

Relevant papers related to GPS closed-form solutions published over the past twelve years, past theses, articles, and books covering more general aspects of GPS, were reviewed. The information collected is critical to establishing that a problem exists and that the proposed thesis research is a potential solution for improved

mathematical modeling for GPS. The literature review covers the following areas: GPS Overview, GPS equations, conventional GPS positioning solutions, and recent alternate approaches to GPS positioning solutions. Upon completion of the literature review, areas of interest that have not yet been addressed will be identified and the viability of pursuing the thesis research will be confirmed.

2.2.1 The GPS Pseudorange Equations. GPS uses radio signal timing to measure the ranges between the satellites and the GPS receiver, making it a time-difference-of-arrival system. If ranges were being measured directly, we would be dealing with a multilateration system described by a spherical geometry and obtaining a position fix would be trivial [6]. Under ideal error and noise-free conditions, if both the satellite and the GPS receiver's clock were perfectly synchronized on GPS time with no error, then the measured range would be the true range [29]. The GPS receiver actually measures pseudoranges which are corrupted by the receiver clock bias, noise, and other error sources. The errors include atmospheric delays, satellite clock errors, ephemeris errors, and receiver induced errors. The receiver clock bias caused by the difference between the receiver clock time and GPS time is by far the largest contributor to the difference between pseudorange and range. However, the receiver clock bias is common to a set of simultaneous measurements, making it possible to treat it as an unknown variable to be estimated along with the receiver position, hence the GPS solution considers space and time.

According to Parkinson [24], the GPS pseudorange equation that reflects all the known sources of error is given by

$$R_i \equiv \sqrt{(u_x - x_i)^2 + (u_y - y_i)^2 + (u_z - z_i)^2} + c(b_u - B_i) + c(T + I) + E + W, \quad (2.1)$$

where R_i is the raw pseudorange from the user to the i^{th} satellite, (u_x, u_y, u_z) are the user position ECEF coordinates, (x_i, y_i, z_i) are the ECEF coordinates of the i^{th} satellite as calculated from the Keplerian parameters in the satellite's ephemeris data,

c is the speed of light in vacuum, b_u is the receiver clock bias, B_i is the error in satellite time, T is the tropospheric delay, I is ionospheric delay, E are ephemeris errors, and W represents other errors that can attributed to the receiver including receiver noise, code loop quantization error, multipath effects, and interchannel errors.

Ephemeris corrections provided to the satellites from the control segment can be used to eliminate the satellite time error and the ephemeris errors partially. Known tropospheric and ionospheric error model corrections can be applied to compensate for tropospheric and ionospheric delay errors partially. Improved receiver design techniques are used to minimize the effects of the receiver related errors, including multipath errors. Given the current state of GPS receiver design technology, the residual errors that remain uncompensated can be assumed to be negligibly small. Furthermore, if the residual errors are grouped together under one random variable w the equation reduces to the expression presented as Equation (1.1) known as the GPS pseudorange equation. If the residual errors are neglected entirely, the ideal GPS pseudorange equation can be expressed as:

$$R_i \approx \sqrt{(u_x - x_i)^2 + (u_y - y_i)^2 + (u_z - z_i)^2} + b. \tag{2.2}$$

The ideal GPS pseudorange equation is a nonlinear equation in four unknowns, the three receiver position coordinates, (u_x, u_y, u_z) and the receiver clock bias, b. This equation is the basis for deriving the conventional iterative GPS position solutions. At least four GPS pseudorange equations are required to calculate the four unknowns, (u_x, u_y, u_z, b) and obtain a solution.

2.2.2 Conventional Iterative Solution to the GPS Pseudorange Equations. The conventional approach to solving the GPS pseudorange equations is to linearize Equation (2.2) about a nominal solution for the vector of unknowns. The vector of

unknowns, and its associated nominal values, are defined as:

$$\vec{X} \equiv [u_x \; u_y \; u_z \; b]^T$$

and

$$\vec{X_n} \equiv [u_{xn} \; u_{yn} \; u_{zn} \; b_n]^T$$

respectively.

As described in [27], performing a Taylor series expansion of the GPS pseudorange equation and ignoring the second and higher order terms, the following equation is obtained:

$$R_i \approx R_{ni} + \frac{u_{xn} - x_i}{R_{ni} - b_n}\Delta u_x + \frac{u_{yn} - y_i}{R_{ni} - b_n}\Delta u_y + \frac{u_{zn} - z_i}{R_{ni} - b_n}\Delta u_z + \Delta b, \qquad (2.3)$$

Considering the exactly determined case of four pseudorange equations, the linearized pseudorange equations can be written in matrix form as:

$$\begin{bmatrix} a_{1x} & a_{1y} & a_{1z} & 1 \\ a_{2x} & a_{2y} & a_{2z} & 1 \\ a_{3x} & a_{3y} & a_{3z} & 1 \\ a_{4x} & a_{4y} & a_{4z} & 1 \end{bmatrix} \begin{bmatrix} \Delta u_x \\ \Delta u_y \\ \Delta u_z \\ \Delta b \end{bmatrix} = \begin{bmatrix} R_1 - R_{n1} \\ R_2 - R_{n2} \\ R_3 - R_{n3} \\ R_4 - R_{n4} \end{bmatrix} = \begin{bmatrix} \Delta R_1 \\ \Delta R_2 \\ \Delta R_3 \\ \Delta R_4 \end{bmatrix} \qquad (2.4)$$

where,

$$\begin{aligned} a_{ix} &= \frac{u_{xn} - x_i}{R_{ni} - b_n} \\ a_{iy} &= \frac{u_{yn} - y_i}{R_{ni} - b_n} \\ a_{iz} &= \frac{u_{zn} - z_i}{R_{ni} - b_n} \end{aligned}$$

The a_{ij} entries in the H matrix are recognized as the cosine of the angle between the line-of-sight vector from the receiver to the i^{th} satellite and the j^{th} axis of the ECEF coordinate frame [27].

The linearized pseudorange equations can be written in a more compact form as $H\Delta X = \Delta R$. Solving for ΔX gives the result $\Delta X = H^{-1}\Delta R$. This equation can be solved iteratively using the following procedure:

1. Estimate an initial X_n, a nominal receiver position and clock bias.
2. Calculate nominal pseudoranges and difference them with measured pseudoranges to obtain ΔR.
3. Compute direction cosines to form the H matrix.
4. Compute $\Delta X = H^{-1}\Delta R$.
5. Add ΔX to X_n forming a new corrected X_n and go back to step 2.
6. Continue process until convergence to a solution is achieved by verifying that $\|\Delta X\| \approx 0$ or that an established threshold is attained.

Upon completion, X_n, the nominal position and bias, represents the best estimate of receiver position and receiver clock bias. This method converges to a solution within three to five iterations even when the initial position guess is nowhere close to the true position [14], for instance the center of the earth. Drawbacks of using this iterative approach include the approximative nature of the linearized equations, computational loading associated with the inversion of a four by four matrix, the requirement for an initial guess, and the possibility of converging to the wrong solution if the initial position guess were not sufficiently close to the true position [1] [14]. The last concern is not an issue for near-earth navigation since a unique solution is guaranteed if the earth's center is used as the initial position guess and a zero initial clock bias is assumed, but is a serious concern if the receiver position is outside the GPS satellite constellation where a unique solution is not guaranteed. The same

applies to certain inverted GPS arrangements. To alleviate such concerns, direct closed-form solutions to the GPS pseudorange equations are sought.

2.2.3 Closed-Form Solutions to the GPS Pseudorange Equations. Although closed-form solutions to the GPS pseudorange equations are attractive, the concept is not new. Joseph Hoshen [11] proposed that a closed-form solution to two-dimensional equations in the form of the GPS pseudorange equations may have been available since the third century BC in the form of the Problem of Apollonius. Since GPS is a fairly recent system, the first article in the open literature concerned with closed-form solutions specifically tailored to the GPS pseudorange equations is Stephen Bancroft's in 1985 [2]. Bancroft [2] developed an algebraic solution to the GPS pseudorange equations that was noniterative in nature. His method provides an exact solution in the exactly determined system using four satellites; like the iterative solution, however, it provides a least squares solution in an overdetermined system. The motivation to this solution was accuracy improvement and the possibility of space applications since an initial position-clock bias guess was not required. Bancroft's solution involves solving a quadratic equation, where each of the two roots leads to a potential solution, one of which does not satisfy the pseudorange equations and can be readily eliminated. This solution had a great deal of merit and motivated a number of papers in the years that followed. Driven by accuracy and computational issues including lower dimensionality and speed, Lloyd Krause [14] formulated a direct solution to the GPS pseudorange equation of the exactly determined system based on difference linearization. By differencing the satellite position vectors, a new basis is formed by using any two adjacent difference vectors, forming a measurement plane, and a vector orthogonal to the plane. The four nonlinear pseudorange equations expressed in the new basis are reduced to three linear equations that are independent of the user clock bias and are used to solve for the user position directly. A quadratic auxiliary equation is then formed to solve for the user clock bias. Krause's paper demonstrated a brilliant approach by which differencing

is used to linearize quadratic equations and remove dependence on variables. A similar approach will be used in the development of the *closed-form* algorithm for this thesis research.

Abel and Chaffee [1] demonstrated that in both closed-form solutions presented by Bancroft [2]and by Krause [14], a position fix may not exist and if it does exist, it may not be unique. Abel and Chaffee's paper concluded that, in order to guarantee a unique position fix, an overdetermined system using at least five satellites must be considered. In a subsequent paper [6], Abel and Chaffee suggest that in a pseudorange system such as GPS, the geometry is hyperbolic, unlike the spherical geometry of a ranging system. In a ranging system, ranges are measured directly, unlike the case for GPS in which the pseudoranges include the unknown receiver clock bias. The solution to range equations is obtained geometrically through the intersection of spheres, but this method does not generalize to pseudorange equations because of the unknown bias in each pseudorange; hence, it is not possible to determine the spheres. In view of the fact that the pseudoranges are not only corrupted by an unknown clock bias but also by some measurement noise, caution must be taken in dealing with the pseudorange equations when it comes to the use of solutions based on spherical geometry.

2.2.4 Stochastic Modeling. Pseudorange noise that corrupts the pseudorange measurements is caused by the residual errors discussed earlier. In order to model the GPS pseudorange equations statistically, tremendous effort would have to be dedicated towards the development of reliable noise models. This noise is actually the manifestation of receiver noise and residuals of various measurement errors that remain unmodelled and uncompensated. The major contributors to pseudorange noise that warrant consideration will be discussed.

Although Gaussian-like, receiver noise is better modeled by a longer tailed mixture of Gaussian distributions that can be expressed as:

$$F(x) = (1 - \epsilon)\Phi(x) + \epsilon\Phi(\frac{x}{3}),$$

where Φ is a Gaussian distribution and the parameter ϵ is generally between 0.01 and 0.1 [7]. In a multichannel receiver, receiver noise can be considered to be uncorrelated across satellites. Consideration must also be given to the receiver clock bias which tends to correlate the pseudorange measurements. The uncompensated residuals of tropospheric and ionospheric errors may have nonzero means that also add to the modeling difficulties. Noise on the satellite position from the ephemeris data will also have some effect on pseudorange noise, but it is likely to be non-Gaussian and have a nonzero mean.

Given the number of contributing factors to pseudorange noise and our lack of knowledge of their characteristics, it is reasonable to propose that the overall pseudorange noise will have a zero-mean Gaussian distribution by invoking the Central Limit Theorem. The Central Limit Theorem states that the sum of many independent random variables, regardless of their distribution, will approach a Gaussian distribution [18]. The Gaussian pseudorange noise will not be white due to the correlated nature of the encompassed errors and noise. This concern is alleviated since there is no requirement for the pseudorange measurements to be uncorrelated in time because the positioning problem will be treated as a static estimation problem, where each snapshot in time is treated as a new static estimation problem. On the other hand, it is desirable to the development of the stochastic estimation that pseudorange noise be uncorrelated across satellites. A solid argument for this is not available, but this will not hinder the development of the stochastic closed-form solution to the GPS pseudorange equations in this thesis since the pseudorange measurements will be differenced, thereby eliminating some of the effects of correlated noise. The uncorrelated noise after differencing can only be justified if the effects

of Selective Availability (SA) that are highly time correlated in nature are not considered [30]. The choice to overlook the effects of SA in this thesis is not overly restrictive since authorized military users of GPS are not subject to the effects of SA and it is believed that the use of SA will be abolished in the near future.

The assumption that the noise across pseudoranges can be modeled as an independent zero-mean, σ^2 variance random variable is used by Dailey and Bell [8] without any solid justification. The assumption is used to derive statistics for the pseudorange equations position solution errors similar to what is being proposed for this thesis research; however, their approach does not consider a closed-form solution.

2.2.5 The Stochastic Estimation Problem. The components of an estimation problem are the variables to be estimated, the measurements, and a mathematical model describing relationship between the measurements and the variables to be estimated [18]. Given the lack of dynamics in the GPS pseudorange equations at any given time instant, a static estimation problem can be formulated from the stochastically modeled pseudorange equations. The variables to be estimated and the measurement noise on the pseudoranges can be represented by random variables. The stochastic estimation process will not only provide an optimal estimate of the unknown variables, the user coordinates and user clock bias; but, will also provide the estimation error covariance. This is the most significant motivation to pursuing a stochastic approach to solving the GPS pseudorange equations. However, the error covariance accuracy will be limited by the quality of the measurement noise statistics. In a stochastic estimation problem, this emphasizes the requirement for good noise models. In this research the measurement noise is modeled as a zero-mean, σ^2 variance Gaussian noise, which is believed to be adequate. Due to the lack of knowledge of the variance σ^2 and the fact that it is dependent on receiver design, location, orientation and time of day, attempting to model the noise variance is not a viable option. The approach that is proposed in this research is to determine the variance, (σ^2), of the Gaussian measurement noise, by using the return difference or

measurement residual. It is suggested that, if sufficient measurements are available, reliable data-driven noise statistics can be extracted by evoking ergodic approxitions. The question at hand is determining how many measurements are sufficient and if that is a reasonable number in the context of the NAVSTAR GPS constellation.

2.2.6 Conclusion of Literature Review. The literature review supports the proposed approach for this thesis research. There are problems associated with the currently used iterative approach to GPS positioning and there is potential for improvement with an exact closed-form solution. With the exception of one recent paper [8], the pseudorange equations have generally been treated as a deterministic set of equations. The lack of effort in the area of stochastic modeling applied to GPS pseudorange equations is evident from the lack of literature on the subject. Previous works on closed-form solutions for the GPS pseudorange equations did not make use of the pseudorange measurements from all in-view satellites; the derivations considered the exactly determined case using only four of the available pseudorange measurements to obtain positioning solutions. Based on the literature review, the development and evaluation of a closed-form solution to the GPS pseudorange equations using stochastic modeling and estimation, and making use of all in-view satellites, is warranted.

III. Mathematical Derivations

This chapter presents a thorough development of the *closed-form* mathematical solution to the GPS pseudorange equations. The development of supplementary algorithms that make use of a nonlinear measurement equation and that were deemed essential to enhance the performance of the *closed-form* algorithm is also addressed. The purpose of these enhanced algorithms is to produce an improvement to the solution achieved by the *closed-form* algorithm; they are not capable of providing, nor are they intended to provide, stand-alone solutions. The two stage algorithms that are presented are the *Maximum Likelihood* approach and the *Kalman Update* approach. The background theory and the operating concept behind each approach is discussed and the complete mathematical derivations are presented. The development of an *alternate closed-form* algorithm is also presented.

3.1 Stochastic Closed-Form Solution

The mathematical derivation of the stochastic *closed-form* solution is developed in four parts. The first part presents the algebraic manipulations to transform the stochastic GPS pseudorange equation as shown in Equation (1.1) into the desired matrix linear regression form as shown in Equation (1.2). The second part involves the derivation of statistics for the equation error in the linear regression. The third part presents the development of the static stochastic estimator based on a minimum variance estimate that will provide an estimate of the user position coordinates and user clock bias. The final part presents the derivation of the estimation error covariance matrix.

3.1.1 Basic Concepts. Prior to initiating the mathematical derivation, it is necessary to present some basic concepts and notation that will be used in the sequel:

- $x \sim N(\mu, \sigma^2)$ is the notation used to represent a random variable (x) that has a Gaussian (Normal) probability distribution function with mean (μ) and variance (σ^2).
- E is used to represent the expectation operator. The expectation of a random variable y is given by $E\{y\} = \int_{-\infty}^{\infty} \rho f_y(\rho) d\rho$, where $f_y(\rho)$ is the density of y [18]. This also defines the mean (μ), the first moment of the random variable.
- Expectation is a linear operation; therefore, for any two random variables x and y, then $E\{x + y\} = E\{x\} + E\{y\}$.
- If two random variables x and y are uncorrelated, then $E\{xy\} = E\{x\}E\{y\}$.
- The variance of the i^{th} element of a random vector $\vec{x}$ can be expressed as, $P_{ii} \equiv E\{(x_i - \mu_i)^2\}$, which make up the diagonal elements of the covariance matrix. The off-diagonal elements P_{ij} are zero if the i^{th} and j^{th} elements of the random vector $\vec{x}$ are uncorrelated.
- For a random variable $x \sim N(0, \sigma^2)$, the moments of x are expressed as $E\{x^k\}$ for $k = (1, 2, \cdots, \infty)$. An odd k denotes an odd moment and an even k denotes an even moment. All odd moments are zero and even moments are given by $(k-1)\sigma^k$ [23].

3.1.2 Linear Regression. The derivation of the *closed-form* solution to the pseudorange equations begins with Equation (1.1). The general form solution with $n \geq 5$ satellites is presented.

$$R_i = \sqrt{(u_x - x_i)^2 + (u_y - y_i)^2 + (u_z - z_i)^2} + b + w_i,$$

represents the i^{th} pseudorange equation of n equations where w_i is Gaussian measurement noise with statistics $w_i \sim N(0, \sigma^2)$ and $E\{w_i w_j\} = 0$ for $(i \neq j)$. The

pseudorange equation can also be rewritten as:

$$(u_x - x_i)^2 + (u_y - y_i)^2 + (u_z - z_i)^2 = (R_i - b - w_i)^2$$

By expanding both sides of the above equation and rearranging the terms such that only the known terms and the noise terms are on the left hand side, the equation becomes:

$$u_x^2 + u_y^2 + u_z^2 - b^2 - 2x_i u_x - 2y_i u_y - 2z_i u_z + 2R_i b =$$

$$R_i^2 - x_i^2 - y_i^2 - z_i^2 - 2R_i w_i + 2bw_i + w_i^2 \tag{3.1}$$

It is noted that the first four terms in Equation (3.1) are simply the unknown variables squared and that they are common to all n equations. This presents an opportunity of eliminating the nonlinear terms by differencing; hence, the n^{th} equation is subtracted from the remaining $n-1$ equations. The resulting $n-1$ equations are linear in the unknown variables and can be expressed as:

$$(x_n - x_i)u_x + (y_n - y_i)u_y + (z_n - z_i)u_z + (R_i - R_n)b =$$

$$\frac{1}{2}(R_i^2 - R_n^2 + x_n^2 - x_i^2 + y_n^2 - y_i^2 + z_n^2 - z_i^2) + R_n w_n - R_i w_i + bw_i - bw_n + \frac{1}{2}(w_i^2 - w_n^2) \tag{3.2}$$

As a by-product of the preceding operation, the nonlinear n^{th} pseudorange equation remains.

$$R_n = \sqrt{(u_x - x_n)^2 + (u_y - y_n)^2 + (u_z - z_n)^2} + b + w_n \tag{3.3}$$

The n^{th} equation will remain unused for this section of the derivation but will be used subsequently as an auxiliary equation for developing a *maximum likelihood* solution and for use in the *Kalman update* solution.

To simplify Equation (3.2) further, an average pseudorange expression is introduced by defining:

$$\bar{R} \equiv \frac{1}{n}\sum_{i=1}^{n} R_i \tag{3.4}$$

The following approximation is also introduced as a first attempt at reducing Equation (3.2) by simplifying the noise terms $R_n w_n - R_i w_i$:

$$R_i \approx R_n \approx \bar{R} \tag{3.5}$$

In the GPS constellation it is not possible to produce a scenario with more than five satellites in which all pseudoranges are the same; therefore, the approximation in Equation (3.5) introduces a source of error whereby some geometrical scenarios will be more prone to errors than others. The impact of introducing the approximation is not known but it will undoubtedly affect the accuracy of the *closed-form* solution being developed. If the effect is found to be significant through experimental analysis, this approximation must be revisited. To minimize the impact of the approximation in Equation (3.5), the measured pseudoranges will be ordered such that the pseudorange closest to $\bar{R}$ will be used as the n^{th} measurement. By introducing the approximation in Equation (3.5) into the noise terms of Equation (3.2), the equation becomes:

$$(x_n - x_i)u_x + (y_n - y_i)u_y + (z_n - z_i)u_z + (R_i - R_n)b \approx$$

$$\frac{1}{2}(R_i^2 - R_n^2 + x_n^2 - x_i^2 + y_n^2 - y_i^2 + z_n^2 - z_i^2) - \bar{R}(w_i - w_n) + b(w_i - w_n) + \frac{1}{2}(w_i^2 - w_n^2)$$

From this point on in the derivation, the exactness of the solution has been lost due to the approximation that has been introduced. The equation is further reduced to obtain:

$$(x_n - x_i)u_x + (y_n - y_i)u_y + (z_n - z_i)u_z + (R_i - R_n)b \approx$$

$$\frac{1}{2}(R_i^2 - R_n^2 + x_n^2 - x_i^2 + y_n^2 - y_i^2 + z_n^2 - z_i^2) + (b - \bar{R})(w_i - w_n) + \frac{1}{2}(w_i^2 - w_n^2)$$

The following noise terms are redefined to allow for further simplification of the equation:

- $(w_i - w_n) \Rightarrow \tilde{v}_i$
- $(w_i^2 - w_n^2) \Rightarrow \tilde{w}_i$

The equation can then be rewritten as:

$$(x_n - x_i)u_x + (y_n - y_i)u_y + (z_n - z_i)u_z + (R_i - R_n)b \approx$$

$$\frac{1}{2}(R_i^2 - R_n^2 + x_n^2 - x_i^2 + y_n^2 - y_i^2 + z_n^2 - z_i^2) + (b - \bar{R})\tilde{v}_i + \tilde{w}_i$$

By redefining the following terms:

- $(b - \bar{R})\tilde{v}_i + \tilde{w}_i \Rightarrow V_i$;
- $\frac{1}{2}(R_i^2 - R_n^2 + x_n^2 - x_i^2 + y_n^2 - y_i^2 + z_n^2 - z_i^2) \Rightarrow Z_i$,

the equation reduces to a linear regression form of $(n-1)$ equations in four unknowns and is expressed as:

$$(x_n - x_i)u_x + (y_n - y_i)u_y + (z_n - z_i)u_z + (R_i - R_n)b \approx Z_i + V_i \tag{3.6}$$

The linear regression in Equation (3.6) can be compactly written in matrix notation form as:

$$\vec{Z} = H\vec{X} + \vec{V}, \tag{3.7}$$

where

- $\vec{Z}$ is the $(n-1)$-dimensional measurement vector given by:

$$\vec{Z} \equiv \begin{bmatrix} Z_1 \\ Z_2 \\ \vdots \\ \vdots \\ Z_{n-1} \end{bmatrix}$$

- H is the $(n-1) \times 4$ regressor matrix given by:

$$H \equiv \begin{bmatrix} x_n - x_1 & y_n - y_1 & z_n - z_1 & R_1 - R_n \\ x_n - x_2 & y_n - y_2 & z_n - z_2 & R_2 - R_n \\ \vdots & \vdots & \vdots & \vdots \\ \vdots & \vdots & \vdots & \vdots \\ x_n - x_{n-1} & y_n - y_{n-1} & z_n - z_{n-1} & R_{n-1} - R_n \end{bmatrix}$$

- $\vec{X}$ is the vector of unknowns given by:

$$\vec{X} \equiv \begin{bmatrix} u_x \\ u_y \\ u_z \\ b \end{bmatrix}$$

- $\vec{V}$ is the $(n-1)$ equation error vector given by:

$$\vec{V} \equiv \begin{bmatrix} V_1 \\ V_2 \\ \vdots \\ \vdots \\ V_{n-1} \end{bmatrix}$$

3.1.3 Noise Statistics. Using the linear regression obtained in Section 3.1.2 as shown in Equation (3.7), it is possible to obtain an estimate of $\vec{X}$ if the statistics of the noise vector $\vec{V}$ are given. The noise vector statistics are not known; however, the composition of the noise vector elements is known. The statistics of $\vec{V}$ must be derived from the known statistics of the pseudorange measurements noise, w_i.

For the statistical derivations that follow, when the subscript i and the subscript j are used together it is implied that $(i \neq j)$.

Statistics for w where $(i, j = 1, 2, \cdots, n)$:

$$\begin{aligned} E\{w_i\} &= 0 \\ E\{w_i^2\} &= \sigma^2 \\ E\{w_i w_j\} &= 0 \ (i \neq j) \end{aligned}$$

Statistics for $\tilde{v}$ and $\tilde{w}$ where $(i, j = 1, 2, \cdots, n-1)$:

$$\begin{aligned} \tilde{v}_i &\equiv (w_i - w_n) \\ \tilde{w}_i &\equiv \frac{1}{2}(w_i^2 - w_n^2) \end{aligned}$$

$$\begin{aligned} E\{\tilde{v}_i\} &= E\{(w_i - w_n)\} \\ &= E\{w_i\} - E\{w_n\} \\ &= 0 - 0 \ = \ 0 \end{aligned}$$

$$\begin{aligned} E\{\tilde{v}_i^2\} &= E\{(w_i - w_n)^2\} \\ &= E\{w_i^2\} + E\{w_n^2\} - 2E\{w_i w_n\} \\ &= \sigma^2 + \sigma^2 - 0 = 2\sigma^2 \end{aligned}$$

$$\begin{aligned} E\{\tilde{v}_i \tilde{v}_j\} &= E\{(w_i - w_n)(w_j - w_n)\} \\ &= E\{w_i w_j\} - E\{w_i w_n\} - E\{w_j w_n\} + E\{w_n^2\} \\ &= 0 - 0 - 0 + \sigma^2 = \sigma^2 \ (i \neq j) \end{aligned}$$

$$
\begin{aligned}
E\{\tilde{w}_i\} &= \frac{1}{2}E\{(w_i^2 - w_n^2)\} \\
&= \frac{1}{2}(E\{w_i^2\} - E\{w_n^2\}) \\
&= \frac{1}{2}(\sigma^2 - \sigma^2) = 0
\end{aligned}
$$

$$
\begin{aligned}
E\{\tilde{w}_i^2\} &= E\{(\frac{1}{2}(w_i^2 - w_n^2))^2\} \\
&= \frac{1}{4}(E\{w_i^4\} + E\{w_n^4\} - 2E\{w_i^2 w_n^2\}) \\
&= \frac{1}{4}(3\sigma^4 + 3\sigma^4 - 2\sigma^4) = \sigma^4
\end{aligned}
$$

$$
\begin{aligned}
E\{\tilde{w}_i\tilde{w}_j\} &= E\{\frac{1}{2}(w_i^2 - w_n^2)\frac{1}{2}(w_j^2 - w_n^2)\} \\
&= \frac{1}{4}(E\{w_i^2 w_j^2\} + E\{w_n^4\} - E\{w_i^2 w_n^2\} - E\{w_j^2 w_n^2\}) \\
&= \frac{1}{4}(\sigma^4 + 3\sigma^4 - \sigma^4 - \sigma^4) = \frac{1}{2}\sigma^4 \ (i \neq j)
\end{aligned}
$$

$$
\begin{aligned}
E\{\tilde{v}_i\tilde{w}_i\} &= E\{(w_i - w_n)\frac{1}{2}(w_i^2 - w_n^2)\} \\
&= \frac{1}{2}(E\{w_i^3\} + E\{w_n^3\} - E\{w_i w_n^2\} - E\{w_i^2 w_n\}) \\
&= \frac{1}{2}(0 + 0 - 0 - 0) = 0
\end{aligned}
$$

$$
\begin{aligned}
E\{\tilde{v}_i\tilde{w}_j\} &= E\{(w_i - w_n)\frac{1}{2}(w_j^2 - w_n^2)\} \\
&= \frac{1}{2}(E\{w_i w_j^2\} + E\{w_n^3\} - E\{w_i w_n^2\} - E\{w_j^2 w_n\}) \\
&= \frac{1}{2}(0 + 0 - 0 - 0) = 0 \ (i \neq j)
\end{aligned}
$$

Statistics for V where $(i, j = 1, 2, \cdots, n-1)$:

$$V_i \equiv (b - \bar{R})\tilde{v}_i + \tilde{w}_i$$

$$\begin{aligned} E\{V_i\} &= E\{(b - \bar{R})\tilde{v}_i + \tilde{w}_i\} \\ &= (b - \bar{R})E\{\tilde{v}_i\} + E\{\tilde{w}_i\} \\ &= 0 + 0 = 0 \end{aligned}$$

$$\begin{aligned} E\{V_i^2\} &= E\{((b - \bar{R})\tilde{v}_i + \tilde{w}_i)((b - \bar{R})\tilde{v}_i + \tilde{w}_i)\} \\ &= (b - \bar{R})^2 E\{\tilde{v}_i^2\} + 2(b - \bar{R})E\{\tilde{v}_i\tilde{w}_i\} + E\{\tilde{w}_i^2\} \\ &= (b - \bar{R})^2(2\sigma^2) + 2(b - \bar{R})(0) + \sigma^4 \\ &= 2(b - \bar{R})^2\sigma^2 + \sigma^4 \end{aligned} \tag{3.8}$$

$$\begin{aligned} E\{V_i V_j\} &= E\{((b - \bar{R})\tilde{v}_i + \tilde{w}_i)((b - \bar{R})\tilde{v}_j + \tilde{w}_j)\} \\ &= (b - \bar{R})^2 E\{\tilde{v}_i\tilde{v}_j\} + (b - \bar{R})E\{\tilde{v}_i\tilde{w}_j\} + (b - \bar{R})E\{\tilde{v}_j\tilde{w}_i\} + E\{\tilde{w}_i\tilde{w}_j\} \\ &= (b - \bar{R})^2(\sigma^2) + (b - \bar{R})(0) + (b - \bar{R})(0) + \frac{1}{2}\sigma^4 \\ &= (b - \bar{R})^2\sigma^2 + \frac{1}{2}\sigma^4 \ (i \neq j) \end{aligned} \tag{3.9}$$

From the results obtained in Equation (3.8) and Equation (3.9) it can be seen that the covariance of the noise vector $\vec{V}$ has diagonal elements that are twice the off-diagonal elements. Indeed, the covariance matrix of the equation error vector, $\vec{V}$, can be expressed as:

$$P_V = \sigma^2(\frac{1}{2}\sigma^2 + (b - \bar{R})^2)R_n, \tag{3.10}$$

where R_n is a $(n-1) \times (n-1)$ matrix defined as follows:

$$R_n \equiv \begin{bmatrix} 2 & 1 & 1 & \cdots & 1 \\ 1 & 2 & 1 & \cdots & 1 \\ 1 & 1 & 2 & & \vdots \\ \vdots & \vdots & & \ddots & \vdots \\ 1 & 1 & \cdots & \cdots & 2 \end{bmatrix} \tag{3.11}$$

An interesting characteristic of the R_n matrix is that its determinant is always equal to n which allows it to be easily inverted analytically. The inverse of R_n is required to find the inverse covariance matrix that is given by:

$$P_V^{-1} = \frac{1}{\sigma^2(\frac{1}{2}\sigma^2 + (b - \bar{R})^2)} R_n^{-1}, \tag{3.12}$$

and where R_n^{-1} is the matrix inverse of R_n explicitly given by:

$$R_n^{-1} = \frac{1}{n} \begin{bmatrix} n-1 & -1 & -1 & \cdots & -1 \\ -1 & n-1 & -1 & \cdots & -1 \\ -1 & -1 & n-1 & & \vdots \\ \vdots & \vdots & & \ddots & \vdots \\ -1 & -1 & \cdots & \cdots & n-1 \end{bmatrix} \tag{3.13}$$

3.1.4 Minimum Variance Estimate Solution. Using the linear regression from Equation (3.7) as a starting point, the aim is to obtain an estimate $\hat{\vec{X}}$ of the vector of unknown parameters $\vec{X}$. The $\hat{\vec{X}}$ that minimizes the estimation error as weighted by the inverse covariance of the noise must be obtained. Recognizing that the estimation error, also known as the return difference or measurement residual, is $(\vec{Z} - H\vec{X})$, the estimation problem can be formulated as follows:

$$min_{\vec{X}}[(\vec{Z} - H\vec{X})^T P_V^{-1} (\vec{Z} - H\vec{X})] \tag{3.14}$$

Equation (3.14) can be expanded to obtain:

$$\vec{Z}^T P_V^{-1} \vec{Z} + \vec{X}^T H^T P_V^{-1} H \vec{X} - 2\vec{X}^T H^T P_V^{-1} \vec{Z} \tag{3.15}$$

Since a minimization over $\vec{X}$ is needed, Equation (3.15) is differentiated with respect to $\vec{X}$ and set equal to zero yielding the following expression:

$$0 + 2H^T P_V^{-1} H \vec{X} - 2H^T P_V^{-1} \vec{Z} = 0$$

Rearranging the expression and solving for $\vec{X}$ produces the desired solution:

$$\hat{\vec{X}} = (H^T P_V^{-1} H)^{-1} H^T P_V^{-1} \vec{Z} \tag{3.16}$$

In order to demonstrate that the stationary point solution in Equation (3.16) is indeed a minimum, the hessian matrix of Equation (3.15) must be verified. The resulting hessian matrix is $(H^T P_V^{-1} H)$, which by definition is always positive definite, providing the necessary and sufficient conditions for minimization. Furthermore, since the existance of the hessian inverse in Equation (3.16) is guaranteed, the existance of a solution is also guaranteed.

Equation (3.16) is a *closed-form* solution to the GPS pseudorange equations. The solution is not dependent on σ, the pseudorange measurement noise standard deviation. To simplify the solution for implementation, it is noted that Equation (3.10) shows the noise covariance P_V as simply R_n premultiplied by a scalar quantity. In Equation (3.16) the scalar premultiplier of P_V will cancel out; therefore, the estimation solution shown in Equation (3.16) can be rewritten in an equivalent form as:

$$\hat{\vec{X}} = (H^T R_n^{-1} H)^{-1} H^T R_n^{-1} \vec{Z} \tag{3.17}$$

Equation (3.17) is used for coding the experimental Matlab algorithm. It must be noted that there are no big matrix inversions associated with this solution

since R_n^{-1} has been determined analytically and can be coded directly into the algorithm. The only inversion that needs to be performed is that of the (4×4) matrix, $(H^T R_n^{-1} H)$, which can be hardwired into the receiver's algorithm.

3.1.5 Estimate Error Covariance. It follows from Equations (3.14) and (3.16) that the covariance of the estimate error is given by:

$$\begin{aligned} P_X &\equiv E\{(\vec{X} - \hat{\vec{X}})(\vec{X} - \hat{\vec{X}})^T\} \\ &= \sigma^2(\frac{1}{2}\sigma^2 + (\hat{b} - \bar{R})^2)(H^T R_n^{-1} H)^{-1} \end{aligned} \tag{3.18}$$

Unlike the solution estimate, the covariance P_X *is* dependent on σ; hence, σ must be known or estimated, in order to compute the error covariance. If a sufficiently large number of GPS pseudorange measurements are available, the following approach of using an ergodic assumption, whereby an ensemble average is approximated by a time average, can attempted:

$$\begin{aligned} E\{\vec{V}^T\vec{V}\} &= \sum_{i=1}^{n-1} E\{V_i^2\} \\ &= (n-1)E\{V_i^2\} \\ &= (n-1)(2(\hat{b} - \bar{R})^2\sigma^2 + \sigma^4) \end{aligned} \tag{3.19}$$

Using the return difference from the measurement data and using an ergodic approximation, an expression equivalent to Equation (3.19) can also be obtained as follows:

$$E\{\vec{V}^T\vec{V}\} \approx (\vec{Z} - H\hat{\vec{X}})^T(\vec{Z} - H\hat{\vec{X}}) \tag{3.20}$$

By equating Equations (3.19) and (3.20) and re-arranging the terms, a quadratic equation in σ^2 is obtained:

$$\sigma^4 + 2(\hat{b} - \bar{R})^2\sigma^2 - \frac{1}{n-1}(\vec{Z} - H\hat{\vec{X}})^T(\vec{Z} - H\hat{\vec{X}}) = 0$$

Solving the quadratic equation yields the following data driven estimate of σ^2:

$$\hat{\sigma^2} = -(\bar{R} - \hat{b})^2 + \sqrt{(\bar{R} - \hat{b})^4 + \frac{1}{n-1}(\vec{Z} - H\hat{\vec{X}})^T(\vec{Z} - H\hat{\vec{X}})} \tag{3.21}$$

If Equations (3.19) and (3.20) are accepted as being equivalent through evoking ergodicity, the expression for the error covariance matrix given in Equation (3.18) can be rewritten in terms of the measurement data driven return difference as follows:

$$P_X = \frac{1}{2(n-1)}(\vec{Z} - H\hat{\vec{X}})^T(\vec{Z} - H\hat{\vec{X}})(H^T R_n^{-1} H)^{-1} \tag{3.22}$$

It must be recognized that the validity of Equation (3.22) is dependent on the validity of the ergodic approximation introduced at Equation (3.20); hence, a yet-to-be-determined minimum satellite availability (n_{min}) must be present to validate this solution for the estimation error covariance. An acceptable value for (n_{min}) must be determined experimentally.

3.2 Maximum Likelihood Estimate

This section presents the background theory behind the *maximum likelihood* solution and a potential estimation algorithm is developed. It is important to note that the solution that is presented in this section is not a stand-alone solution to the GPS pseudorange equations; it is a supplementary process that improves on the *closed-form* solution presented in Section 3.1.

3.2.1 Maximum Likelihood Concept. The concept behind the *maximum likelihood* solution approach is simple and ideally suited as a natural continuation to the *closed-form* solution. Given a known probability density function of a random vector and some equality constraint(s) on the random vector, it is possible using optimization techniques to find the maximum value of the density function subject to the constraint(s). The optimized maximum value of the probability density function

corresponds to the most likely realizations of the random vector. Hence the solution approach will be referred to as *Maximum Likelihood.* The concept is clearly demonstrated in the two dimensional illustration in Figure 3.1. Figure 3.1 shows a Gaussian probability distribution function in two variables subject to a linear constraint on the two variables. Given the constraint, the values for the two random variables that maximize the probability function is readily observed as the intersection of the constraint with the highest constant probability contour line.

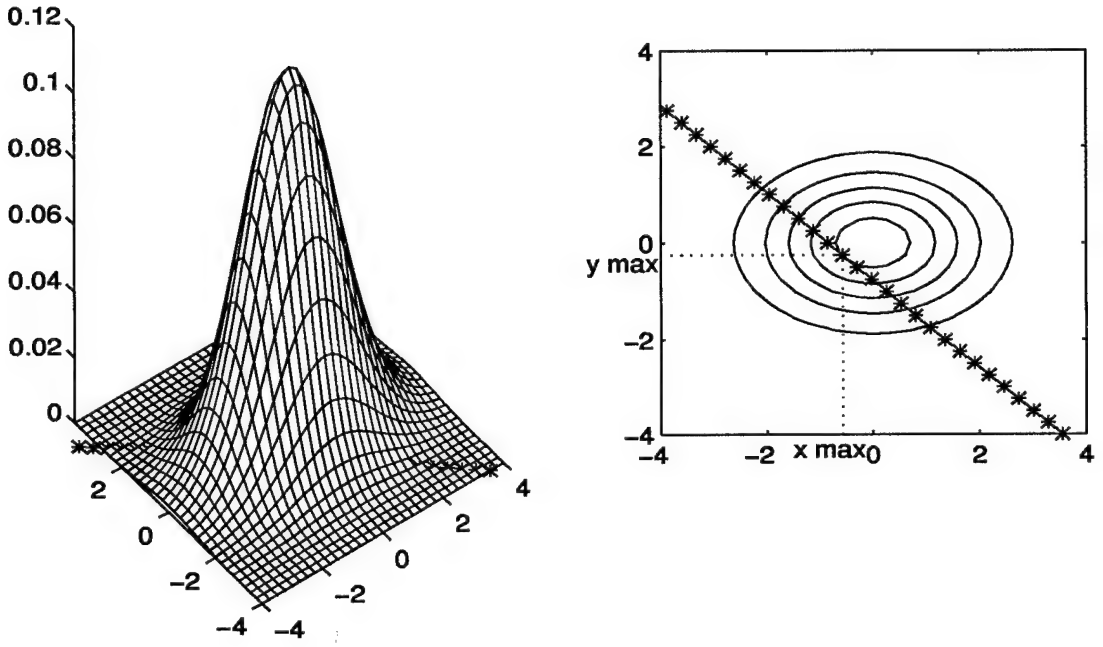

Figure 3.1 Maximum Likelihood of Gaussian Probability Distribution Subject to a Linear Constraint

The *closed-form* solution to the GPS pseudorange equations developed in Section 3.1 of this thesis proposed that the four dimensional random vector $\vec{X}$ has a Gaussian probability density function. The *closed-form* solution provided the mean $\hat{\vec{X}}$ and covariance P_X which can be represented as:

$$\vec{X} \sim N(\hat{\vec{X}},\ P_X),$$

or in expanded form as:

$$[u_x,\ u_y,\ u_z,\ b]^T \sim N([\hat{u}_x,\ \hat{u}_y,\ \hat{u}_z,\ \hat{b}]^T,\ P_X).$$

A Gaussian probability density function is fully described by its first two moments; hence, although it is impossible to visualize the four dimensional density function in our three dimensional world, it can be represented mathematically along with an equality constraint to formulate an optimization problem.

3.2.2 Mathematical Development. The Gaussian probability density function of a k-dimensional random vector $(\vec{Y})$ whose realizations are represented by the vector $\vec{\gamma}$ is described by [18]:

$$f_y(\vec{\gamma}) \equiv \frac{1}{(2\pi)^{\frac{k}{2}}|P|^{\frac{1}{2}}}\ e^{\{-\frac{1}{2}[\vec{\gamma}-\vec{m}]^T P^{-1}[\vec{\gamma}-\vec{m}]\}}, \tag{3.23}$$

where P is the $(k \times k)$ covariance matrix and m is the $(k \times 1)$ mean vector. It follows from Equation (3.23) that, in the context of the GPS solution estimate, the Gaussian probability density function for the random vector $(\vec{X})$ can be expressed as:

$$f(\vec{X}) = \frac{1}{(2\pi)^2|P_X|^{\frac{1}{2}}}\ e^{\{-\frac{1}{2}[\vec{X}-\hat{\vec{X}}]^T P_X^{-1}[\vec{X}-\hat{\vec{X}}]\}}. \tag{3.24}$$

The goal in this section is to find the GPS solution $(\vec{X})$ that maximizes the probability density function $f(\vec{X})$ in Equation (3.24). In order to maximize the function $f(\vec{X})$, $(\vec{X})$ must be selected such that the following part of the exponential's exponent is minimized:

$$[\vec{X} - \hat{\vec{X}}]^T P_X^{-1}[\vec{X} - \hat{\vec{X}}]$$

The exponent to be minimized can be rewritten in expanded form as:

$$\begin{bmatrix} u_x - \hat{u}_x \\ u_y - \hat{u}_y \\ u_z - \hat{u}_z \\ b - \hat{b} \end{bmatrix}^T P_X^{-1} \begin{bmatrix} u_x - \hat{u}_x \\ u_y - \hat{u}_y \\ u_z - \hat{u}_z \\ b - \hat{b} \end{bmatrix} \tag{3.25}$$

At this point it is necessary to introduce the n^{th} pseudorange measurement equation described in Equation (3.3). The exponent term in Equation (3.25) must be minimized subject to the constraint imposed by Equation (3.3). Equation (3.3) cannot be used as a constraint in its present form due to the noise term it contains. The zero-mean noise term, w_n, in the n^{th} pseudorange measurement equation is neglected to obtain a simple equality constraint. A minimization problem can now be formulated as follows:

$$min_{(u_x,u_y,u_z,b)} \begin{bmatrix} u_x - \hat{u}_x \\ u_y - \hat{u}_y \\ u_z - \hat{u}_z \\ b - \hat{b} \end{bmatrix}^T P_X^{-1} \begin{bmatrix} u_x - \hat{u}_x \\ u_y - \hat{u}_y \\ u_z - \hat{u}_z \\ b - \hat{b} \end{bmatrix}, \tag{3.26}$$

subject to:

$$R_n = \sqrt{(u_x - x_n)^2 + (u_y - y_n)^2 + (u_z - z_n)^2} + b \tag{3.27}$$

The constrained optimization problem specified in equations 3.26 and 3.27 can be solved; however, it is desirable to use the equality constraint to solve explicitly for one of the optimization parameters, thereby reducing the order of the optimization problem as suggested by Maybeck [19]. Equation (3.27) can be rearranged to solve for the user clock bias (b):

$$b = R_n - \sqrt{(u_x - x_n)^2 + (u_y - y_n)^2 + (u_z - z_n)^2} \tag{3.28}$$

Equation (3.28) should be showing a non-unique solution for b caused by the positive and negative roots; however, the positive root has been dropped since it leads to a physically impossible solution. Substituting Equation (3.28) into the minimization problem defined in Equation (3.26) will reduce the optimization problem to an unconstrained minimization in three variables which can be solved with greater ease.

$$min_{(u_x,u_y,u_z)} \begin{bmatrix} u_x - \hat{u}_x \\ u_y - \hat{u}_y \\ u_z - \hat{u}_z \\ (R_n - \sqrt{(u_x - x_n)^2 + (u_y - y_n)^2 + (u_z - z_n)^2}) - \hat{b} \end{bmatrix}^T P_X^{-1}$$

$$\begin{bmatrix} u_x - \hat{u}_x \\ u_y - \hat{u}_y \\ u_z - \hat{u}_z \\ (R_n - \sqrt{(u_x - x_n)^2 + (u_y - y_n)^2 + (u_z - z_n)^2}) - \hat{b} \end{bmatrix} \tag{3.29}$$

After Equation (3.29) is solved for the optimization parameters (u_x, u_y, u_z) which correspond to the Maximum Likelihood GPS user position estimate, (u_x, u_y, u_z) must be substituted into Equation (3.28) to obtain the Maximum Likelihood GPS user clock bias estimate (b).

The unconstrained minimization problem in Equation (3.29) can be solved using a number of different optimization approaches. Solving the actual optimization problem is beyond the scope of this thesis; however, the function used for the experimental implementation of the Maximum Likelihood solution needs to be discussed. The experimental algorithm implemented in Matlab [17] produced the most desirable results using the function *fmins*. The search initialization point used experimentally was $(\hat{u_x},\ \hat{u_y},\ \hat{u_z})$ corresponding to the previous best GPS position solution estimate provided by the *closed-form* solution from Section 3.1. The *fmins* Matlab function

uses the simplex search method of Nelder and Mead [17]. The simplex search method does not use any derivative or gradient information, rather it involves the use of a simplex. In m-dimensional space, where m corresponds to the order of the optimization problem, the simplex is characterized by $(m+1)$ distinct vertices. At each step in the search, one of the vertices is replaced by a new point reducing the size of the simplex. The search continues until the size of the simplex is less than the stopping tolerance [17]. The *fmins* function consistently produces a solution to the minimization problem regardless of how good the previous estimate used for initialization was. The *fminu* function which uses a quasi-Newton search method was also tried in the experimental algorithm but it was not as robust as the *fmins* function. The *fminu* function occasionally failed to produce a minimum when the search initialization point was not close enough to the true user position.

The Maximum Likelihood approach described makes effective use of the stochastic estimation solution produced by the *closed-form* algorithm presented in Section 3.1 and of the n^{th} pseudorange equation, that had not previously been used, to provide a better GPS solution estimate. If the constraint formed from the n^{th} pseudorange equation were truly a deterministic equation as was assumed in Equation (3.27), the Maximum Likelihood approach would produce the true user position and user clock bias as its GPS solution estimate. Unfortunately, the n^{th} pseudorange equation is noise corrupted, as are the other $(n-1)$ pseudorange equations; therefore, the Maximum Likelihood estimate is prone to the effects of the noise on the n^{th} pseudorange measurement. Perhaps the largest disadvantage of taking a *maximum likelihood* approach is that there is no simple way of determining the error covariance of the the solution estimate it produces. The capability to estimate the error covariance is traded off to obtain an improved GPS solution estimate.

3.3 Kalman Update Solution

This section presents the development of the *Kalman update* GPS position determination algorithm. As was the case for the *maximum likelihood* algorithm developed in Section 3.2, the *Kalman update* solution is not a stand-alone solution to the GPS pseudorange equations; it is a supplementary process that improves on the *closed-form* solution presented in Section 3.1. The concept behind the Kalman Update solution is discussed followed by the complete mathematical derivation of the solution itself. The *Kalman update* algorithm presented in this section is an alternate to the maximum likelihood algorithm to enhancing the GPS solution produced by the *closed-form* algorithm by using the previously unused n^{th} pseudorange equation. However, the *Kalman update* algorithm is capable of obtaining the estimation error covariance which is not readily obtainable using the *maximum likelihood* algorithm.

3.3.1 Kalman Update Concept. The concept behind the *Kalman update* solution approach is similar to that of a conventional Kalman Filter. The *closed-form* solution in Section 3.1 provides a GPS solution estimate ($\hat{\vec{X}}$) and the associated estimation error covariance matrix (P_X). Recalling that this solution was produced without making use of the n^{th} pseudorange equation in Equation (3.3), the n^{th} pseudorange equation can be perceived as a new measurement which can be used to update the previous estimate the same way that it would be accomplished during the update cycle of an extended Kalman Filter. The approach that is used begins with the linearization of Equation (3.3) about a nominal position estimate. The linearized equation is then manipulated into the standard linear measurement form as described in [18], and used to update the estimate. It may be necessary for the process to continue in an iterative manner until convergence within a predefined tolerance is achieved; however, it is expected that the algorithm will converge to a solution in a few iterations.

The *Kalman update* algorithm that is presented in this section differs from the basic Kalman Filter developed by Kalman [12] [13] in that the measurement that is used to update the previous estimate is correlated with the previous estimate. The conventional Kalman Filter update equation does not allow for correlation between the new measurement and the previous estimate; hence, a Kalman-like update equation that can account for this correlation is presented for use in the experimental algorithm.

3.3.2 Linearized Measurement. The first step in the mathematical development of the *Kalman update* algorithm is to linearize Equation (3.3) about a nominal user position $(u_{x_0}, u_{y_0}, u_{z_0})$ by performing a Taylor series expansion and neglecting second and higher order terms. The linearized equation obtained is given by

$$\begin{aligned} R_n \approx & \frac{(u_{x_0} - x_n)}{\sqrt{(u_{x_0} - x_n)^2 + (u_{y_0} - y_n)^2 + (u_{z_0} - z_n)^2}}(u_x - u_{x_0}) \\ & + \frac{(u_{y_0} - y_n)}{\sqrt{(u_{x_0} - x_n)^2 + (u_{y_0} - y_n)^2 + (u_{z_0} - z_n)^2}}(u_y - u_{y_0}) \\ & + \frac{(u_{z_0} - z_n)}{\sqrt{(u_{x_0} - x_n)^2 + (u_{y_0} - y_n)^2 + (u_{z_0} - z_n)^2}}(u_z - u_{z_0}) \\ & + \sqrt{(u_{x_0} - x_n)^2 + (u_{y_0} - y_n)^2 + (u_{z_0} - z_n)^2} + b + w_n \end{aligned}$$

By defining the regressor h for this scalar measurement equation as follows:

$$h \equiv \begin{bmatrix} \frac{(u_{x_0} - x_n)}{\sqrt{(u_{x_0} - x_n)^2 + (u_{y_0} - y_n)^2 + (u_{z_0} - z_n)^2}} \\ \frac{(u_{y_0} - y_n)}{\sqrt{(u_{x_0} - x_n)^2 + (u_{y_0} - y_n)^2 + (u_{z_0} - z_n)^2}} \\ \frac{(u_{z_0} - z_n)}{\sqrt{(u_{x_0} - x_n)^2 + (u_{y_0} - y_n)^2 + (u_{z_0} - z_n)^2}} \\ 1 \end{bmatrix}, \tag{3.30}$$

the linearized equation can be rewritten as

$$
\begin{aligned}
R_n &\approx h^T\vec{X} + w_n \\
&- \frac{(u_{x_0} - x_n)u_{x_0} + (u_{y_0} - y_n)u_{y_0} + (u_{z_0} - z_n)u_{z_0}}{\sqrt{(u_{x_0} - x_n)^2 + (u_{y_0} - y_n)^2 + (u_{z_0} - z_n)^2}} \\
&+ \sqrt{(u_{x_0} - x_n)^2 + (u_{y_0} - y_n)^2 + (u_{z_0} - z_n)^2}
\end{aligned}
$$

where $\vec{X}$ is the vector of unknowns, $[u_x, u_y, u_z, b]^T$. The goal is to reduce the above equation into the form of a linear measurement model described by:

$$
Z_n = h^T\vec{X} + w_n \tag{3.31}
$$

In order to achieve this goal, Z_n must be defined as:

$$
\begin{aligned}
Z_n &\equiv R_n - \sqrt{(u_{x_0} - x_n)^2 + (u_{y_0} - y_n)^2 + (u_{z_0} - z_n)^2} \\
&+ \frac{(u_{x_0} - x_n)u_{x_0} + (u_{y_0} - y_n)u_{y_0} + (u_{z_0} - z_n)u_{z_0}}{\sqrt{(u_{x_0} - x_n)^2 + (u_{y_0} - y_n)^2 + (u_{z_0} - z_n)^2}},
\end{aligned}
$$

which can be simplified into the following:

$$
Z_n = R_n + \frac{(u_{x_0} - x_n)x_n + (u_{y_0} - y_n)y_n + (u_{z_0} - z_n)z_n}{\sqrt{(u_{x_0} - x_n)^2 + (u_{y_0} - y_n)^2 + (u_{z_0} - z_n)^2}} \tag{3.32}
$$

Now that the n^{th} pseudorange measurement equation is approximated into the appropriate linear measurement model form defined in Equation (3.31), it can be used to update the solution obtain from the *closed-form* algorithm using a Kalman-like update approach. Using a linear measurment model simplifies the solution by allowing the use of linear Kalman filtering techniques, as apposed to using an Extended Kalman filter or increasing the order of the filter to accomodate a nonlinear measurement equation. Keeping in mind that Z_n is actually part of the measurements that were used to obtain the *closed-form* solution and not a new measurement

as would be the case in a conventional Kalman Filter application, hence the *new measurement* and the previous estimate are correlated. This is a violation to the basic assumptions used in the derivation of the conventional Kalman Filter update equations. A Kalman-like update equation that can accommodate correlation between the new measurement and the previous estimate needs to be derived.

3.3.3 Noise Statistics. In order to derive the new Kalman-like update equation, it is necessary to know the relationship between the noise in the *new measurement* (w_n) and the previous estimate being the solution obtained from the *closed-form* algorithm. The linear regression used for the *closed-form* algorithm was defined in Equation (3.7) as,

$$\vec{Z} = H\vec{X} + \vec{V},$$

and the statistics of the noise vector $\vec{V}$ were derived in Section 3.1.3. The *closed-form* algorithm produced an estimate of the GPS unknown parameter, ($\hat{\vec{X}}$), defined in Equation (3.17) and an estimate of the covariance matrix associated with estimation, (P_X), defined in Equation (3.22). Using the knowledge of the estimated GPS solution, the true GPS parameter vector can be defined as,

$$\vec{X} \equiv \hat{\vec{X}} + \vec{W}, \tag{3.33}$$

where $\vec{W} \sim N(0, P_X)$. The correlation of interest between w_n and $\vec{W}$ can be defined as:

$$p \equiv E\{\vec{W}w_n\} = E\{w_n\vec{W}\} \tag{3.34}$$

To determine the relationship between $\vec{W}$ and $\vec{V}$, the linear regression in Equation (3.7) is multiplied from the left by $H^T R_n^{-1}$ yielding the following expression:

$$H^T R_n^{-1}\vec{Z} = H^T R_n^{-1} H\vec{X} + H^T R_n^{-1}\vec{V}$$

The expression can be solved for $\vec{X}$ to obtain:

$$\vec{X} = (H^T R_n^{-1} H)^{-1} H^T R_n^{-1} \vec{Z} - (H^T R_n^{-1} H)^{-1} H^T R_n^{-1} \vec{V} \tag{3.35}$$

The first term on the right hand side of Equation (3.35) is recognized from Equation (3.17) as $\hat{\vec{X}}$; therefore, by equating Equation (3.35) and Equation (3.33) an expression for $\vec{W}$ in terms of $\vec{V}$ is obtained:

$$\vec{W} = (H^T R_n^{-1} H)^{-1} H^T R_n^{-1} \vec{V} \tag{3.36}$$

Next the relationship between $\vec{V}$ and w_n is determined be exploiting the noise statistics derived in Section 3.1.3.

$$\begin{aligned} E\{V_i w_n\} &= E\{((b-\bar{R})\tilde{v}_i + \tilde{w}_i) w_n\} \\ &= (b-\bar{R}) E\{\tilde{v}_i w_n\} + E\{\tilde{w}_i w_n\} \\ &= (b-\bar{R}) E\{(w_i - w_n) w_n\} + \frac{1}{2} E\{(w_i^2 - w_n^2) w_n\} \\ &= (b-\bar{R}) E\{w_i w_n - w_n^2\} + \frac{1}{2} E\{w_i^2 w_n - w_n^3)\} \\ &= (b-\bar{R})(0-\sigma^2) + \frac{1}{2}(0-0) \\ &= (\bar{R}-b)\sigma^2. \end{aligned} \tag{3.37}$$

Equation (3.37) which represents the variance between any single element of $\vec{V}$ and w_n. The relationship can be generalized to obtain the following covariance matrix:

$$E\{\vec{V} w_n\} = (\bar{R}-b)\sigma^2 \begin{bmatrix} 1 \\ 1 \\ \vdots \\ 1 \end{bmatrix}_{((n-1)\times 1)} \tag{3.38}$$

Using Equation (3.36) and the relationship in Equation (3.38), an expression for the covariance between $\vec{W}$ and w_n is determined:

$$\begin{aligned} E\{\vec{W}w_n\} &= (H^T R_n^{-1} H)^{-1} H^T R_n^{-1} E\{\vec{V}w_n\} \\ &= (\bar{R} - b)\sigma^2 (H^T R_n^{-1} H)^{-1} H^T R_n^{-1} \begin{bmatrix} 1 \\ 1 \\ \vdots \\ 1 \end{bmatrix}_{((n-1)\times 1)} \end{aligned} \tag{3.39}$$

3.3.4 The Augmented Linear Regression. An augmented linear regression can be formulated by combining Equation (3.33) and Equation (3.31). The augmented linear regression is expressed as:

$$\vec{Z}_a = H_a \vec{X} + \vec{V}_a \tag{3.40}$$

where,

- $\vec{Z}_a$ is the (5×1) augmented measurement vector defined as:

$$\vec{Z}_a \equiv \begin{bmatrix} \hat{\vec{X}} \\ Z_n \end{bmatrix}$$

- H_a is the (5×4) augmented regressor defined as:

$$H_a \equiv \begin{bmatrix} I \\ h^T \end{bmatrix}$$

- $\vec{V}_a$ is the (5×1) augmented measurement noise vector defined as:

$$\vec{V}_a \equiv \begin{bmatrix} \vec{W} \\ w_n \end{bmatrix}$$

The goal is to derive a Kalman-like update equation to refine the unknown GPS parameters vector estimate, $(\hat{\vec{X}})$, and its covariance matrix, (P_X), both produced by the *closed-form* algorithm developed in Section 3.1. In the derivation that follows, to distinguish the estimates $\hat{\vec{X}}$ and P_X as produced by the *closed-form* algorithm from the estimates that will be obtained through the Kalman update, the following notation is used:

- $\hat{\vec{X}}^-$ and P_X^- represent the estimate and the estimation error covariance prior to the update; and
- $\hat{\vec{X}}^+$ and P_X^+ represent the estimate and the estimation error covariance following the update.

In order to obtain the updated estimates from the augmented linear regression in Equation (3.40), it is necessary to derive the covariance of the augmented noise vector $\vec{V}_a$. Since the statistics of the noise components in $\vec{V}_a$ have already been determined, the equation error covariance matrix, R_a, is derived as follows:

$$\begin{aligned} R_a &\equiv E\{\vec{V}_a\vec{V}_a^T\} \\ &= E\{\begin{bmatrix} \vec{W} \\ w_n \end{bmatrix} [\vec{W}^T \; w_n]\} \\ &= E\{\begin{bmatrix} \vec{W}\vec{W}^T & \vec{W}w_n \\ w_n\vec{W}^T & w_n^2 \end{bmatrix}\} \\ &= \begin{bmatrix} P_X^- & p \\ p^T & \sigma^2 \end{bmatrix} \end{aligned} \tag{3.41}$$

The updated minimum variance GPS solution estimate and associated covariance matrix are given by the expressions:

$$\hat{\vec{X}}^+ = P_X^+ H_a^T R_a^{-1} \vec{Z}_a \tag{3.42}$$

$$P_X^+ = (H_a^T R_a^{-1} H_a)^{-1} \tag{3.43}$$

The expressions in Equation (3.42) and Equation (3.43) are sufficient to obtain the required updates but it is desirable to manipulate and reduce the equations into the more familiar and computationally efficient form of the classical Kalman filter update equations. The expressions can be rewritten in expanded form as:

$$\hat{\vec{X}}^{+} = [I\ h]\begin{bmatrix} P_X^- & p \\ p^T & \sigma^2 \end{bmatrix}^{-1}\begin{bmatrix} \hat{\vec{X}}^- \\ Z_n \end{bmatrix} \tag{3.44}$$

$$P_X^+ = [[I\ h]\begin{bmatrix} P_X^- & p \\ p^T & \sigma^2 \end{bmatrix}^{-1}\begin{bmatrix} I \\ h^T \end{bmatrix}]^{-1} \tag{3.45}$$

To assist in the reduction of the expressions, the parameters are redefined by scaling them as follows:

$$\begin{aligned} P_X^- &\Rightarrow \sigma^2 P_X^- \\ P_X^+ &\Rightarrow \sigma^2 P_X^+ \\ p &\Rightarrow \sigma^2 p \end{aligned}$$

In terms of the redefined parameters, the expressions become:

$$\hat{\vec{X}}^{+} = P_X^+[I\ h]\begin{bmatrix} P_X^- & p \\ p^T & 1 \end{bmatrix}^{-1}\begin{bmatrix} \hat{\vec{X}}^- \\ Z_n \end{bmatrix}$$

$$P_X^+ = [[I\ h]\begin{bmatrix} P_X^- & p \\ p^T & 1 \end{bmatrix}^{-1}\begin{bmatrix} I \\ h^T \end{bmatrix}]^{-1}$$

The inverse of the redefined noise covariance matrix is calculated by defining a piecewise matrix inverse and algebraically determining the inverse of each piece:

$$\begin{bmatrix} P_X^- & p \\ p^T & 1 \end{bmatrix}^{-1} \equiv \begin{bmatrix} A & a \\ a^T & c \end{bmatrix} \tag{3.46}$$

From Equation (3.46), it is obvious that,

$$\begin{bmatrix} P_X^- & p \\ p^T & 1 \end{bmatrix} \begin{bmatrix} A & a \\ a^T & c \end{bmatrix} = \begin{bmatrix} I & 0 \\ 0 & 1 \end{bmatrix} \tag{3.47}$$

The following four equations are obtained by piecewise equating the members of the matrix on the left hand side of Equation (3.47) to those on the right hand side:

- $P_X^- A + pa^T = I$
- $p^T A + a^T = 0$
- $P_X^- a + cp = 0$
- $p^T a + c = 1$

From the four equations above, expressions for A, a, and c are determined algebraically in terms of only P_X^- and p.

$$A = (P_X^- - pp^T)^{-1} \tag{3.48}$$

$$a = -(P_X^- - pp^T)^{-1} p \tag{3.49}$$

$$c = 1 + p^T (P_X^- - pp^T)^{-1} p \tag{3.50}$$

With A, a, and c known, it is possible to describe R_a^{-1}. Further to the above equations the following relationships are noted:

$$a = -Ap \tag{3.51}$$

$$c = 1 + p^T Ap \tag{3.52}$$

Using Equations (3.51) and (3.52), the following two expressions that will be extremely useful in the simplification of Equations (3.44) and (3.45) are formed:

$$A + ha^T = A - hp^T A = (I - hp^T)A$$

$$a + ch = -Ap + h + hp^T Ap = h - (I - hp^T)Ap$$

The expressions in Equations (3.44) and (3.45) can be rewritten by substituting R_a^{-1} by its equivalent form as defined in Equation (3.46) and simplified by multiplying out the matrices.

$$\begin{aligned}
\hat{\vec{X}}^+ &= P_X^+ [I \; h] \begin{bmatrix} A & a \\ a^T & c \end{bmatrix} \begin{bmatrix} \hat{\vec{X}}^- \\ Z_n \end{bmatrix} \\
&= P_X^+ [(A + ha^T)\hat{\vec{X}}^- + (a + ch)Z_n] \\
&= P_X^+ (A + ha^T)\hat{\vec{X}}^- + P_X^+ (a + ch)Z_n \\
&= P_X^+ (I - hp^T)A\hat{\vec{X}}^- + P_X^+ [h - (I - hp^T)Xp]Z_n
\end{aligned} \tag{3.53}$$

$$\begin{aligned}
P_X^+ &= [[I \; h] \begin{bmatrix} A & a \\ a^T & c \end{bmatrix} \begin{bmatrix} I \\ h^T \end{bmatrix}^{-1} \\
&= [A + chh^T + ha^T + ah^T]^{-1} \\
&= [A + (a + ch)h^T + ha^T]^{-1} \\
&= [A + (h - (I - hp^T)Ap)h^T + ha^T]^{-1} \\
&= [A + hh^T - (1 - hp^T)Aph^T + ha^T]^{-1} \\
&= [A + hh^T - Aph^T + hp^T Aph^T - hp^T A]^{-1} \\
&= [hh^T + (I - hp^T)A - (I - hp^T)Aph^T]^{-1} \\
&= [hh^T + (I - hp^T)A(I - ph^T)]^{-1}
\end{aligned} \tag{3.54}$$

The inverse of the $(I - ph^T)$ matrix in the P_X^+ expression in Equation (3.54) is calculated by applying the Matrix Inversion Lemma (MIL):

$$(I - ph^T)^{-1} = I + h(1 - p^T h)^{-1} p^T = I + \frac{1}{1 - p^T h} hp^T$$

By using the above result and introducing the expression for A in Equation (3.48), Equation (3.54) becomes:

$$\begin{aligned} P_X^+ &= [hh^T + (I + \frac{1}{1-p^Th}hp^T)^{-1}A(I + \frac{1}{1-p^Th}ph^T)^{-1}]^{-1} \\ &= [hh^T + (I + \frac{1}{1-p^Th}hp^T)^{-1}(P_X^- - pp^T)^{-1}(I + \frac{1}{1-p^Th}ph^T)^{-1}]^{-1} \end{aligned}$$

To simplify the expression for P_X^+ further, it is necessary to define a new intermediate variable, Y:

$$Y \equiv (I + \frac{1}{1-p^Th}hp^T)(P_X^- - pp^T)(I + \frac{1}{1-p^Th}ph^T) \tag{3.55}$$

The expression for Y defined in Equation (3.55) is further simplified as follows:

$$\begin{aligned} Y &= (I + \frac{1}{1-p^Th}hp^T)(P_X^- - pp^T + \frac{1}{1-p^Th}P_X^-hp^T - \frac{1}{1-p^Th}p^Thpp^T) \\ &= (I + \frac{1}{1-p^Th}hp^T)(P_X^- - \frac{1}{1-p^Th}pp^T + \frac{1}{1-p^Th}P_X^-hp^T) \\ &= P_X^- + \frac{h^TP_X^-h - h^Tp + p^Th - 1}{(1-p^Th)^2}pp^T + \frac{1}{1-p^Th}(P_X^-hp^T + ph^TP_X^-) \\ &= P_X^- + \frac{h^TP_X^-h - 1}{(1-p^Th)^2}pp^T + \frac{1}{1-p^Th}(P_X^-hp^T + ph^TP_X^-) \end{aligned} \tag{3.56}$$

By introducing the expression for Y defined in Equation (3.55) and applying the MIL, the expression for P_X^+ is further simplified:

$$\begin{aligned} P_X^+ &= (Y^{-1} + hh^T)^{-1} \\ &= Y - Yh(1 + h^TYh)^{-1}h^TY \\ &= Y - \frac{1}{1+h^TYh}Yhh^TY \end{aligned} \tag{3.57}$$

It is noted from the simplified expression for P_X^+ given in Equation (3.57) that no matrix inversion operation is required for the update of the covariance matrix since both Equations (3.56) and (3.57) do not involve any matrix inversion.

Attention must now be turned towards the update equation for the GPS solution estimate ($\hat{\vec{X}}$). In Equation (3.53) the term, $\{P_X^+(I - hp^T)A\}$, is algebraically manipulated to allow for further simplification of the equation. The manipulation involves using the result obtained in the covariance update equation in Equation (3.57):

$$\begin{aligned}
P_X^+(I - hp^T)A &= (I - P_X^+hh^T)(I - ph^T)^{-1} \\
&= (I - P_X^+hh^T)(I + \frac{1}{1 - p^Th}ph^T) \\
&= I - P_X^+hh^T + \frac{1}{1 - p^Th}ph^T - \frac{h^Tp}{1 - p^Th}P_X^+hh^T \\
&= I + \frac{1}{1 - p^Th}ph^T - \frac{1}{1 - p^Th}P_X^+hh^T \\
&= I + \frac{1}{1 - p^Th}(p - P_X^+h)h^T \qquad (3.58)
\end{aligned}$$

The expressions in Equation (3.58) and Equation (3.48) are replaced into Equation (3.53) and the equation is further manipulated to obtain:

$$\begin{aligned}
\hat{\vec{X}}^+ &= P_X^+(I - hp^T)A\hat{\vec{X}}^- + P_X^+[h - (I - hp^T)Ap]Z_n \\
&= P_X^+(I - hp^T)A\hat{\vec{X}}^- + P_X^+hZ_n - P_X^+(I - hp^T)ApZ_n \\
&= P_X^+(I - hp^T)A\hat{\vec{X}}^- + P_X^+hZ_n - (I + \frac{1}{1 - p^Th}(p - P_X^+h)h^T)pZ_n \\
&= P_X^+(I - hp^T)A\hat{\vec{X}}^- + P_X^+hZ_n - pZ_n - \frac{1}{1 - p^Th}(p - P_X^+h)h^TpZ_n \\
&= P_X^+(I - hp^T)A\hat{\vec{X}}^- + P_X^+hZ_n - pZ_n - \frac{h^Tp}{1 - p^Th}(p - P_X^+h)Z_n \\
&= P_X^+(I - hp^T)A\hat{\vec{X}}^- + P_X^+hZ_n - pZ_n - \frac{p^Th}{1 - p^Th}(pZ_n) + \frac{p^Th}{1 - p^Th}(P_X^+hZ_n) \\
&= P_X^+(I - hp^T)A\hat{\vec{X}}^- + P_X^+hZ_n - \frac{1}{1 - p^Th}(pZ_n) + \frac{p^Th}{1 - p^Th}(P_X^+hZ_n)
\end{aligned}$$

$$
\begin{aligned}
&= P_X^+(I - hp^T)A\hat{\vec{X}}^- - \frac{1}{1-p^Th}(pZ_n) + \frac{1}{1-p^Th}(P_X^+hZ_n) \\
&= (I + \frac{1}{1-p^Th}(p - P_X^+h)h^T)\hat{\vec{X}}^- - \frac{1}{1-p^Th}(pZ_n) + \frac{1}{1-p^Th}(P_X^+hZ_n) \\
&= \hat{\vec{X}}^- + \frac{1}{1-p^Th}(p - P_X^+h)h^T\hat{\vec{X}}^- - \frac{1}{1-p^Th}(pZ_n) + \frac{1}{1-p^Th}(P_X^+hZ_n) \\
&= \hat{\vec{X}}^- - \frac{1}{1-p^Th}(P_X^+hh^T\hat{\vec{X}}^-) + \frac{1}{1-p^Th}p(h^T\hat{\vec{X}}^- - Z_n) + \frac{1}{1-p^Th}(P_X^+hZ_n) \\
&= \hat{\vec{X}}^- + \frac{1}{1-p^Th}p(h^T\hat{\vec{X}}^- - Z_n) - \frac{1}{1-p^Th}(P_X^+h)(h^T\hat{\vec{X}}^- - Z_n) \\
&= \hat{\vec{X}}^- + \frac{1}{1-p^Th}(P_X^+h - p)(Z_n - h^T\hat{\vec{X}}^-) \qquad (3.59)
\end{aligned}
$$

By comparing the expression in Equation (3.59) to the classical Kalman filter estimate update equation, it is noted that by defining a filter gain K:

$$K \equiv \frac{1}{1-p^Th}(P_X^+h - p),$$

Equation (3.59) is reduced to the form of the classical estimate update equation and it can be rewritten as:

$$\hat{\vec{X}}^+ = \hat{\vec{X}}^- + K(Z_n - h^T\hat{\vec{X}}^-) \qquad (3.60)$$

Although Equation (3.60) has the same form as that of the classical Kalman filter, it must be noted that the filter gains K are not the same. The main difference is due to the introduction of the correlation p between the new measurement and the previous estimate which in the case of the classical Kalman filter is zero. As is the case for the Kalman filter update equations, an equivalent expression for the filter gain K must be obtained in terms of the covariance prior to the update (P_X^-). Using the previous result obtained for P_X^+ in Equation (3.57), it is most convenient to express the filter gain K in terms of Y as defined in Equation (3.55), which is a function of (P_X^-).

$$K \equiv \frac{1}{1-p^Th}(P_X^+h - p)$$

$$
\begin{aligned}
&= \frac{1}{1-p^Th}[(Y - \frac{1}{1+h^TYh}Yhh^TY)h - p] \\
&= \frac{1}{1-p^Th}[Yh - \frac{1}{1+h^TYh}Yh(h^TYh) - p] \\
&= \frac{1}{1-p^Th}[\frac{1}{1+h^TYh}Yh - p] \qquad (3.61)
\end{aligned}
$$

Using the new expression for K obtained in Equation (3.61), the covariance update equation (Equation (3.57)) must be rewritten in terms of the filter gain K. By manipulating Equation (3.61), the following expression is obtained:

$$(1-p^Th)K + p = \frac{1}{1+h^TYh}Yh$$

This expression is inserted into Equation (3.57) to obtain the covariance update equation in the desired form:

$$
\begin{aligned}
P_X^+ &= Y - [(1-p^Th)K + p]h^TY \\
&= \{I - [(1-p^Th)K + p]h^T\}Y \qquad (3.62)
\end{aligned}
$$

The derivation of the Kalman-like update equations in the desired form is now complete.

To summarize the results obtained, the final Kalman update equations as presented in Equation (3.56), Equation (3.61), Equation (3.60), and Equation (3.62) are:

$$
\begin{aligned}
Y &= P_X^- + \frac{h^TP_X^-h - 1}{(1-p^Th)^2}pp^T + \frac{1}{1-p^Th}(P_X^-hp^T + ph^TP_X^-) \\
K &= \frac{1}{1-p^Th}[\frac{1}{1+h^TYh}Yh - p] \\
\hat{\vec{X}}^+ &= \hat{\vec{X}}^- + K(Z_n - h^T\hat{\vec{X}}^-) \\
P_X^+ &= \{I - [(1-p^Th)K + p]h^T\}Y
\end{aligned}
$$

The above equations are used in the Matlab implementation of the *Kalman update* experimental algorithm. The *Kalman update* algorithm is intended to refine the GPS solution estimate in a direct and non-iterative manner. Although this can be achieved in most cases, it was determined experimentally that sometimes a second application of the algorithm is required to obtain a better solution estimate. Recalling that the *new measurement* used by the *Kalman update* algorithm is actually the n^{th} pseudorange equation in Equation (3.3) that has been linearized about the position estimate produced by the *closed-form* algorithm, implies that how well the linearization fits the true unknown GPS parameters is dependent on how good the solution produced by the *closed-form* algorithm is to start. In order to alleviate this undesired dependency, after the Kalman Update algorithm has been applied once, and produces an improved solution estimate, Equation (3.3) is once again linearized about the improved position estimate producing a better *new measurement.* The *Kalman update* algorithm is applied a second time keeping in mind that the estimate prior to the update ($\hat{\vec{X}}^{-}$) and the covariance prior to the update ($P_{\vec{X}}^{-}$) are the estimates produced by the *closed-form* algorithm, not the solution obtained as a result of the previous application of the *Kalman update.* Theoretically, this process can be continued recursively until convergence to the best possible solution is achieved; however, it was shown experimentally that after the second application of the algorithm, the change in the solution estimate is insignificant. Consequently, continued iterations are not required; the algorithm needs to be applied just twice. The first application is strictly to obtain a suitable position estimate about which to perform a valid linearization of the n^{th} pseudorange equation and the second application is to calculate the final GPS solution estimate and its covariance.

A quick verification of the derived update equations in Equations (3.56), (3.61), (3.60), and (3.62) is carried out to confirm the validity of the new equations. The special case of the classical Kalman filter where $p = 0$ is considered. For this special case of no correlation, the well known classical Kalman update formulae, are

recovered:

$$
\begin{aligned}
Y &= P_X^- \\
K &= \frac{1}{1 + h^T P_X^- h} P_X^- h \\
\hat{\vec{X}}^+ &= \hat{\vec{X}}^- + K(Z_n - h^T \hat{\vec{X}}^-) \\
P_X^+ &= (I - Kh^T) P_X^-
\end{aligned}
$$

3.4 Alternate Stochastic Closed-form Solution

This section presents the mathematical derivation of an alternate stochastic *closed-form* solution that is closely related to the *closed-form* algorithm developed in Section 3.1. This *alternate closed-form* algorithm attempts to alleviate some of the undesirable characteristic associated with the *closed-form* algorithm developed in Section 3.1. The development of this algorithm is presented strictly to demonstrate a potentially viable approach in producing an alternate stochastic closed-form solution. The main difference between this algorithm and the previous one is that the differencing of the n expanded pseudorange equations presented at Equation (3.1) will be done in a cyclical fashion. The concept of cyclical differencing is based on the *difference linearization* approach demonstrated by Krause [14] for the development of a deterministic closed-form solution. The solution in [14] uses differencing to formulate a computation basis from which the user position is backed out and uses a nonlinear auxiliary equation to compute the user clock bias; whereas, the goal in this development is to form a linear regression consisting of n equations in four unknowns, three user position coordinates and the user clock bias.

The cyclical differencing scheme involves subtracting the $(i+1)^{th}$ equation from the i^{th} equation for $i = 1, 2, ..., n-1$ where n is the number of available pseudorange measurements. The last, (n^{th}), linearized equation is formed by subtracting the first equation from the n^{th} equation. The most noteworthy motivation to attempt this

development is that the cyclical differencing will eliminate the nonlinear terms while retaining n linearized equations, unlike the previous *closed-form* solution presented in Section 3.1 which produced $(n-1)$ linearized equations and was left with the n^{th} nonlinear pseudorange equation for use as an auxiliary equation. It was initially anticipated that this *alternate closed-form* solution would be capable of producing estimates of the four GPS solution parameters with only four pseudorange measurements, unlike the *closed-form* algorithm presented in Section 3.1 which requires a minimum of five.

3.4.1 New Linear Regression in n Equations. The initial portion of the derivation of this *alternate closed-form* solution to the pseudorange equations is identical to that presented in Section 3.1. A natural starting point for this development is the point at which the developments differ. Consequently, the development of the *alternate closed-form* solution begins with Equation (3.1):

$$u_x^2 + u_y^2 + u_z^2 - b^2 - 2x_i u_x - 2y_i u_y - 2z_i u_z + 2R_i b =$$

$$R_i^2 - x_i^2 - y_i^2 - z_i^2 - 2R_i w_i + 2bw_i + w_i^2$$

The cyclical differencing is applied resulting in n equations that are linear in the unknown variables and can be expressed as:

$$(x_{i+1} - x_i)u_x + (y_{i+1} - y_i)u_y + (z_{i+1} - z_i)u_z + (R_i - R_{i+1})b =$$

$$\frac{1}{2}(R_i^2 - R_{i+1}^2 + x_{i+1}^2 - x_i^2 + y_{i+1}^2 - y_i^2 + z_{i+1}^2 - z_i^2) + R_{i+1}w_{i+1} - R_i w_i + bw_i - bw_{i+1} + \frac{1}{2}(w_i^2 - w_{i+1}^2) \tag{3.63}$$

Equation (3.63) is understood to encompass n equations for $i = 1...n$, where it is understood that the first equation also serves as the $(n+1)^{th}$ equation.

To simplify Equation (3.63), the approximation at Equation (3.5) is introduced as was done in the previous derivation and Equation (3.63) becomes:

$$(x_{i+1}-x_i)u_x+(y_{i+1}-y_i)u_y+(z_{i+1}-z_i)u_z+(R_i-R_{i+1})b\approx$$

$$\frac{1}{2}(R_i^2-R_{i+1}^2+x_{i+1}^2-x_i^2+y_{i+1}^2-y_i^2+z_{i+1}^2-z_i^2)+(b-\bar{R})(w_i-w_{i+1})+\frac{1}{2}(w_i^2-w_{i+1}^2) \quad (3.64)$$

By redefining the following terms :

- $(b-\bar{R})(w_i-w_{i+1})+\frac{1}{2}(w_i^2-w_{i+1}^2)\Rightarrow V_i$;
- $\frac{1}{2}(R_i^2-R_{i+1}^2+x_{i+1}^2-x_i^2+y_{i+1}^2-y_i^2+z_{i+1}^2-z_i^2)\Rightarrow Z_i$

Equation (3.64) reduces to a linear regression form of n equations in four unknowns expressed as:

$$(x_{i+1}-x_i)u_x+(y_{i+1}-y_i)u_y+(z_{i+1}-z_i)u_z+(R_i-R_{i+1})b\approx Z_i+V_i \quad (3.65)$$

At this point, the linear regression in Equation (3.65) can be written in matrix notation form as:

$$\vec{Z}=H\vec{X}+\vec{V}, \quad (3.66)$$

where

- $\vec{Z}$ is the measurement vector of dimension n given by:

$$\vec{Z}\equiv\begin{bmatrix} Z_1 \\ Z_2 \\ \vdots \\ \vdots \\ Z_n \end{bmatrix}$$

- H is the $(n \times 4)$ regressor matrix given by:

$$H \equiv \begin{bmatrix} x_2 - x_1 & y_2 - y_1 & z_2 - z_1 & R_1 - R_2 \\ x_3 - x_2 & y_3 - y_2 & z_3 - z_2 & R_2 - R_3 \\ \vdots & \vdots & \vdots & \vdots \\ \vdots & \vdots & \vdots & \vdots \\ x_n - x_{n-1} & y_n - y_{n-1} & z_n - z_{n-1} & R_{n-1} - R_n \\ x_1 - x_n & y_1 - y_n & z_1 - z_n & R_n - R_1 \end{bmatrix}$$

- $\vec{X}$ is the vector of unknowns given by:

$$\vec{X} \equiv \begin{bmatrix} u_x \\ u_y \\ u_z \\ b \end{bmatrix}$$

- $\vec{V}$ is the equation error vector of dimension n given by:

$$\vec{V} \equiv \begin{bmatrix} V_1 \\ V_2 \\ \vdots \\ \vdots \\ V_n \end{bmatrix}$$

It must be noted that the the $(n \times 4)$ regressor matrix (H) is rank deficient, viz., $rank(H) = 3$; therefore, this approach is incapable of producing a GPS solution in the deterministic case.

3.4.2 Noise Statistics. Using the linear regression obtained in Equation (3.66), it is possible to obtain an estimate of $\vec{X}$ if the statistics of the equation

error vector $\vec{V}$ are known. The statistics of $\vec{V}$ must be derived from the known statistics of the pseudorange measurements noise, w_i. The equation error vector $\vec{V}$ is known to be zero mean; therefore, only the covariance matrix of the equation error vector $\vec{V}$ needs to be derived. The covariance matrix is an $(n \times n)$ symmetrical matrix whose entries, in the most general form, are given by:

$$E\{V_i V_j\} \equiv E\{[(b-\bar{R})(w_i - w_{i+1}) + \frac{1}{2}(w_i^2 - w_{i+1}^2)][(b-\bar{R})(w_j - w_{j+1}) + \frac{1}{2}(w_j^2 - w_{j+1}^2)]\} \tag{3.67}$$

The subscripts i and j in Equation (3.67) take on values from 1 through n and it is understood that a subscript of $(n+1)$ is equivalent to a subscript of 1. There are three separate cases of covariance entries that must be considered:

1. $i = j$. These entries represent the diagonal elements of the covariance matrix and are annotated as P_{V_D}.
2. $i = j + 1$ or $j = i + 1$. These entries represent the adjacent elements and populate the matrix cells adjacent to the diagonal elements. Matrix elements $(1, n)$ and $(n, 1)$ are also adjacent elements since it is understood that $(n+1)$ is equivalent to 1. These adjacent elements are annotated as P_{V_A}.
3. $i \neq j + 1$ and $j \neq i + 1$ and $i \neq j$. These entries represent all the remaining elements of the covariance matrix and are annotated as P_{V_R}.

The noise covariance matrix P_V whose elements are described by $E\{V_i V_j\}$ is a symmetrical $(n \times n)$ matrix expressed as:

$$P_V = \begin{bmatrix} P_{V_D} & P_{V_A} & P_{V_R} & \cdots & P_{V_R} & P_{V_A} \\ P_{V_A} & P_{V_D} & P_{V_A} & P_{V_R} & \cdots & P_{V_R} \\ P_{V_R} & \ddots & \ddots & \ddots & \ddots & \vdots \\ \vdots & \ddots & \ddots & \ddots & \ddots & P_{V_R} \\ P_{V_R} & \cdots & P_{V_R} & P_{V_A} & P_{V_D} & P_{V_A} \\ P_{V_A} & P_{V_R} & \cdots & P_{V_R} & P_{V_A} & P_{V_D} \end{bmatrix} \tag{3.68}$$

By recognizing that the *expectation operator* (E) is a linear operator, the expression for $E\{V_iV_j\}$ in Equation (3.67) can be expanded as follows:

$$\begin{aligned} E\{V_iV_j\} &= E\{(b-\bar{R})^2(w_i-w_{i+1})(w_j-w_{j+1})\} + E\{\frac{1}{2}(b-\bar{R}) \\ &\quad [(w_i-w_{i+1})(w_j^2-w_{j+1}^2)+(w_j-w_{j+1})(w_i^2-w_{i+1}^2)]\} \\ &\quad +E\{\frac{1}{4}(w_i^2-w_{i+1}^2)(w_j^2-w_{j+1}^2)\} \\ &= (b-\bar{R})^2E\{(w_iw_j-w_iw_{j+1}-w_{i+1}w_j+w_{i+1}w_{j+1})\}+\frac{1}{2}(b-\bar{R}) \\ &\quad E\{(w_iw_j^2-w_iw_{j+1}^2-w_{i+1}w_j^2+w_{i+1}w_{j+1}^2+w_jw_i^2-w_jw_{i+1}^2-w_{j+1}w_i^2 \\ &\quad +w_{j+1}w_{i+1}^2)\}+\frac{1}{4}E\{(w_i^2w_j^2-w_i^2w_{j+1}^2-w_{i+1}^2w_j^2+w_{i+1}^2w_{j+1}^2)\} \end{aligned} \quad (3.69)$$

From Equation (3.69) it is possible to find the equation error statistics by using the defined elemental noise statistics of the pseudorange measurement noise, (w). In order to proceed, each of the three cases of the covariance matrix entries must be considered individually, where Equation (3.69) is further reduced for each case.

3.4.2.1 Noise Covariance, Diagonal Elements. The diagonal elements of the covariance matrix are represented by the case where $j=i$. Making this substitution into Equation (3.69) reduces the expression for the diagonal covariance elements to:

$$\begin{aligned} P_{V_D} &= (b-\bar{R})^2E\{(w_i^2-2w_iw_{i+1}+w_{i+1}^2)\} \\ &\quad +(b-\bar{R})E\{(w_i^3-w_iw_{i+1}^2-w_{i+1}w_i^2+w_{i+1}^3)\} \\ &\quad +\frac{1}{4}E\{(w_i^4-2w_i^2w_{i+1}^2-w_{i+1}^4)\} \\ &= (b-\bar{R})^2(\sigma^2-0+\sigma^2)+(b-\bar{R})(0)+\frac{1}{4}(3\sigma^4-2\sigma^4+3\sigma^4) \\ &= 2(b-\bar{R})^2\sigma^2+\sigma^4 \end{aligned}$$

3.4.2.2 Noise Covariance, Adjacent Elements. The adjacent elements of the covariance matrix are represented by the case where $j+1=i$. Making this

substitution into Equation (3.69) reduces the expression for the adjacent covariance elements to:

$$\begin{aligned} P_{V_A} &= (b-\bar{R})^2 E\{(w_i w_j - w_i^2 - w_{i+1}w_j + w_{i+1}w_i)\} + \frac{1}{2}(b-\bar{R}) \\ &\quad E\{(w_i w_j^2 - w_i^3 - w_{i+1}w_j^2 + w_{i+1}w_i^2 + w_j w_i^2 - w_j w_{i+1}^2 - w_i^3 + w_i w_{i+1}^2)\} \\ &\quad + \frac{1}{4}E\{(w_i^2 w_j^2 - w_i^4 - w_{i+1}^2 w_j^2 + w_{i+1}^2 w_i^2)\} \\ &= (b-\bar{R})^2(0-0-\sigma^2+0) + \frac{1}{2}(b-\bar{R})(0) + \frac{1}{4}(\sigma^4 - 3\sigma^4 - \sigma^4 + \sigma^4) \\ &= -(b-\bar{R})^2\sigma^2 - \frac{1}{2}\sigma^4 \;=\; -\frac{1}{2}P_{V_D} \end{aligned}$$

3.4.2.3 Noise Covariance, All Remaining Elements. Equation (3.69), in its current form, represents the case for all the remaining covariance matrix.

$$P_{V_R} \;=\; (b-\bar{R})^2(0) + \frac{1}{2}(b-\bar{R})(0) + \frac{1}{4}(\sigma^4 - \sigma^4 - \sigma^4 + \sigma^4) = 0$$

Since the individual covariance matrix elements P_{V_D}, P_{V_A}, and P_{V_R} have been determined, the covariance of the equation error vector $\vec{V}$ can be expressed as:

$$P_V = \sigma^2(\frac{1}{2}\sigma^2 + (b-\bar{R})^2)\tilde{R}_n, \tag{3.70}$$

where $\tilde{R}_n$ is a $(n \times n)$ matrix whose diagonal elements are 2, the elements adjacent to the diagonal elements are -1, and all the remaining elements are zero. As an example, the $\tilde{R}_n$ matrix for $n = 5$ is a (5×5) matrix defined as follows:

$$\tilde{R}_5 \equiv \begin{bmatrix} 2 & -1 & 0 & 0 & -1 \\ -1 & 2 & -1 & 0 & 0 \\ 0 & -1 & 2 & -1 & 0 \\ 0 & 0 & -1 & 2 & -1 \\ -1 & 0 & 0 & -1 & 2 \end{bmatrix}$$

An interesting characteristic of the $\tilde{R}_n$ matrix is that it is always positive semi-definite. $\tilde{R}_n$ always has exactly one eigenvalue equal to zero; hence, it is not invertible. Recalling the solution for the minimum variance estimate of the unknown parameter vector $\vec{X}$ derived in Equation (3.16), the inverse of $\tilde{R}_n$ is used as a weighting matrix. Since $\tilde{R}_n$ is not invertible, the unknown parameter estimation is obtained using the following equation where the inverse of $\tilde{R}_n$ is substituted by the generalized inverse of $\tilde{R}_n$:

$$\hat{\vec{X}} = (H^T \tilde{R}_n^\dagger H)^{-1} H^T \tilde{R}_n^\dagger \vec{Z}, \tag{3.71}$$

where $\tilde{R}_n^\dagger$ is the generalized inverse of $\tilde{R}_n$.

To get a deeper appreciation of the problem at hand, which is indeed more complex than it appears, the concept of the *generalized inverse* is examined closely. There are a number of possible approaches to obtaining a generalized inverse of a matrix, but given the symmetric characteristic of the $\tilde{R}_n$ matrix, using the Singular Value Decompostion (SVD) approach is the most convenient [4]. Performing a SVD on a real symmetric $\tilde{R}_n$ produces the following result:

$$\tilde{R}_n = USU^T \tag{3.72}$$

where S is a $(n \times n)$ diagonal matrix whose diagonal elements are simply the *singular values* or *eigenvalues* of $\tilde{R}_n$ and U is a $(n \times n)$ unitary matrix. Using the SVD results, the generalized inverse of $\tilde{R}_n$ is simply given by:

$$\tilde{R}_n^\dagger = US^\dagger U^T \tag{3.73}$$

where the generalized inverse of S is given by:

$$S^{\dagger} = \begin{bmatrix} \frac{1}{\lambda_1} & 0 & \cdots & \cdots & 0 \\ 0 & \frac{1}{\lambda_2} & 0 & \cdots & 0 \\ 0 & \ddots & \ddots & \ddots & 0 \\ 0 & \cdots & 0 & \frac{1}{\lambda_{n-1}} & 0 \\ 0 & \cdots & \cdots & \cdots & 0 \end{bmatrix}$$

The eigenvalues of $\tilde{R}_n$ are represented by λ_i but it must be reemphasized that $\tilde{R}_n$ has one eigenvalue ($\lambda_n = 0$).

The rank deficiency is now evident; furthermore, the last column of the unitary matrix, U, is arbitrary and insignificant. The impact of this rank deficiency is that although the linear regression in Equation (3.66) appears to be of order n, it is actually of order $(n-1)$. As was the case in the *closed-form* algorithm, a minimum of five pseudorange measurements are required to produce a solution using this *alternate closed-form* approach. To avoid the apparently excessive order of the linear regression and the requirement to work with a generalized inverse, the linear regression in Equation (3.66) can be transformed into an equivalent form of order $(n-1)$.

A transformation matrix, U^T, is defined and recalling that the last column of U is insignificant allows for the transformation matrix to be partitioned as follows:

$$U^T = \begin{bmatrix} T \\ \cdots \\ t \end{bmatrix}$$

where t is the last row of the U^T matrix. A new linear regression is obtained by premultiplying the linear regression in Equation (3.66) by the $((n-1) \times n)$ transformation matrix, T:

$$T\vec{Z} = TH\vec{X} + T\vec{V}, \tag{3.74}$$

A simple linear regression is formulated by redefining the terms in Equation (3.74) as follows:

- $T\vec{Z} \Rightarrow \vec{Z_T}$
- $TH \Rightarrow H_T$
- $T\vec{V} \Rightarrow \vec{V_T}$

The transformed linear regression is represented by :

$$\vec{Z_T} = H_T\vec{X} + \vec{V_T}, \tag{3.75}$$

where

- $\vec{Z_T}$ is the transformed measurement vector of dimension $(n-1)$
- H_T is the transformed regressor matrix of dimension $((n-1) \times 4)$
- $\vec{V_T}$ is the transformed equation error vector of dimension $(n-1)$

The covariance matrix of the equation error vector $\vec{V_T}$ is now calculated as follows:

$$\begin{aligned} E\{V_T V_T^T\} &= E\{TW(TW)^T\} \\ &= E\{TWW^T T^T\} \\ &= TE\{WW^T\}T^T \\ &= T\tilde{R}_n T^T \end{aligned} \tag{3.76}$$

The expression for the noise covariance obtained in Equation (3.76) is recognized as the diagonal S matrix obtained from the SVD operation in Equation (3.72) without its n^th row and n^th column of zeros. The covariance matrix can be defined

as $E\{V_T V_T^T\} \equiv S_{n-1}$, where S_{n-1} is given by:

$$S_{n-1} = \begin{bmatrix} \lambda_1 & 0 & \cdots & 0 \\ 0 & \lambda_2 & 0 & \vdots \\ \vdots & & \ddots & 0 \\ 0 & \cdots & 0 & \lambda_{n-1} \end{bmatrix}$$

The diagonal form of the transformed noise covariance simplifies the task of calculating its inverse which is explicitly given by:

$$S_{n-1}^{-1} = \begin{bmatrix} \frac{1}{\lambda_1} & 0 & \cdots & 0 \\ 0 & \frac{1}{\lambda_2} & 0 & \vdots \\ \vdots & & \ddots & 0 \\ 0 & \cdots & 0 & \frac{1}{\lambda_{n-1}} \end{bmatrix}$$

The minimum variance estimate of the unknown GPS parameter vector based on the transformed linear regression in Equation (3.75) can thereby be calculated using the following expression:

$$\hat{\vec{X}} = (H_T^T S_{n-1}^{-1} H_T)^{-1} H_T^T S_{n-1}^{-1} \vec{Z}_T \tag{3.77}$$

Equation (3.77) is the most convenient for use in the implementation of the experimental algorithm in Matlab. Preliminary experimental trials on the *alternate closed-form* algorithm demonstrated that the use of a supplementary algorithm is required to refine the solution produced by the *alternate closed-form* algorithm, as was the case for the *closed-form* algorithm. Both the *maximum likelihood* and the *Kalman update* algorithms can be used to supplement; however, now there is no obvious choice of auxiliary equation to use. Any of the original n pseudorange equations can be used as the auxiliary equation. The application of the *maximum likelihood* to the *alternate closed-form* solution is identical to that which was used for

the *closed-form* solution. In order to apply the *Kalman update* algorithm it would be necessary to determine the correlation between the solution produced by the *alternate closed-form* algorithm and the selected auxiliary equation. This correlation is not the same as the one determined for the *closed-form* solution; furthermore, the development is more involved due to the more complex form of the noise covariance matrix. The development of the *Kalman update* algorithm tailored for application to the *alternate closed-form* solution is not addressed in this thesis.

3.5 Conclusion of Mathematical Derivations

This chapter presented the derivations of the four algorithms that are used in the Matlab implementations for experimental analysis. The four algorithms are:

1. The *Closed-form* algorithm
2. The *Maximum likelihood* algorithm
3. The *Kalman update* algorithm
4. The *Alternate Closed-form* algorithm

The first three algorithms are thoroughly analyzed experimentally in Chapter 4; however, only the *Closed-form* algorithm developed in Section 3.1 provides a stand-alone GPS solution estimate, the two latter are used to refine the solution provided by the *closed-form* algorithm. The *maximum likelihood* algorithm developed in Section 3.2 accomplishes the task of refining the solution but it inherently possesses two serious drawbacks:

- It depends on optimization techniques that are recursive in nature hence the closed-form appeal is lost.
- It does not have the capability to provide the estimation error covariance readily.

As a result of these drawbacks, the more elegant *Kalman update* supplementary algorithm was developed.

The *Kalman update* algorithm maintains a closed-form approach despite the fact that a portion of the algorithm must be applied twice to ensure a *good* solution. The algorithm also retains the capability to calculate the estimation error covariance. Based strictly on the mathematical attributes of the *Kalman update* algorithm, it is the preferred supplementary algorithm. The performance of each of the algorithms is assessed experimentally to provide a broader comparison based also on performance.

The *alternate closed-form* algorithm based on cyclical differencing linearization, was expected to provide a more mathematically aesthetic and balanced solution than the *closed-form* solution. The algorithm produces a singular regressor matrix, H, preventing this approach from being used in the deterministic case. As well, in the stochastic case, the algorithm produces a positive semi-definite noise covariance matrix resulting in an undesirable rank deficiency; consequently, just like the *closed-form* algorithm, it still requires at least five pseudorange measurements in order to produce a GPS solution. The performance of the *alternate closed-form* algorithm needs to be compared to that of *closed-form* algorithm through experimental analysis to confirm which closed-form solution, if any, is preferable.

The most interesting realization that was brought to light through the mathematical development of the two stochastic closed-form solutions is the set of consequences of working with stochastic pseudorange equations. In both solutions, the average pseudorange approximation at Equation (3.5) is required in order to obtain an expression for the noise covariance in which the dependency on any of the estimation parameters can be eliminated. This approximation is not required in a deterministic development. It turned out that both solutions required at least five pseudorange measurements to produce a GPS solution. In the *closed-form* algorithm this was a direct result of the methodology used in differencing the pseudorange equations; however, the *alternate closed-form* algorithm was expected to resolve this problem

but was unable to do so due to the positive semi-definite noise covariance matrix, with a single zero eigenvalue guaranteed, obtained. In conclusion, when accounting for measurement noise, it is impossible to obtain a closed-form fix using linear mathematics only; furthermore, a direct (closed-form) solution can't be obtained using only four pseudorange measurements.

IV. Experimental Results and Analysis

This chapter presents the experimental portion of the thesis. The first part discusses how the experiment was set up and how the Monte Carlo trials were run. Next is presented a brief discussion of how the results are intended to be interpreted. The experimental results are then presented and the chapter sums up with a detailed analysis of the results.

4.1 Overview

The experimental results encompass the outcome from two test environments which were used to conduct the experimental trials. The first test environment consists of twelve simulated NAVSTAR GPS satellite scenarios chosen to represent conditions typically encountered in the real world. The twelve satellite scenarios were generated using the GPSoft Satellite Navigation Toolbox for Matlab [10]. The second test environment consists of three scenarios of pseudo-GPS transmitters in a ground-based planar array. The pseudo-GPS transmitters are referred to as *pseudolites* in this thesis. The second test environment is required to evaluate the performance of the GPS position determination algorithms developed in this thesis in relation to the performance achieved by conventional iterative GPS algorithms in other than typical GPS satellite geometries where current iterative algorithms tend to perform quite well. The test environment using pseudolites in ground-based planar arrays is indicative of the geometries that can be encountered in a test range such as the SARS [25], [20] where areas of high GDOP or poor geometry are typical. These high GDOP geometrical conditions are not very favorable to the conventional iterative GPS algorithms and restrictions on flight profiles and ground array patterns must be imposed to accommodate the deficiencies in the iterative algorithms [20]. The nonlinear closed-form algorithms are expected to be more accurate in regions of high GDOP than the conventional iterative algorithms [2].

The results associated with the first test environment are divided into four parts, each part related with a different approach used in obtaining the GPS solution estimate. The four parts include the *Closed-form* algorithm, *Maximum likelihood* algorithm, *Kalman update* algorithm, and Conventional Iterative algorithms. For the second test environment, only the results associated with the *Closed-form* algorithm, *Kalman update* algorithm, and the Iterative Least Squares (ILS) algorithm are presented. All the results presented are the cumulative representation of 5000 Monte Carlo runs. In order to provide an unbiased comparison basis between the results using the different algorithms, the Gaussian pseudorange noise for each satellite is maintained the same between the different approaches for any given Monte Carlo run. The pseudorange measurement noise for each visible satellite is randomly generated as an array with 5000 realizations, one for each Monte Carlo run. The simulated noise array has a zero-mean and a standard deviation of $\sigma = 100$ meters which is in a typical range but is arbitrarily selected for the purpose of the experimental trials.

It is not deemed necessary to carry out specific study measurements to confirm the validity of the selected standard deviation of $\sigma = 100$ meters because the experimental analysis is based strictly on relative performance of different algorithms under identical noise conditions. It is nonetheless essential that the Signal - to - Noise Ratio (SNR) used experimentally be in a typical range since there is a threshold level below which using stochastic estimation theory, where an inverse covariance matrix is used as a weighting matrix to obtain a minimum variance stochastic estimate, is of little or no benefit. Similarly, if an excessively small SNR is considered for experimental trials, it can lead to false conclusions because the stochastic approach will outperform the deterministic approach in these unrealistic conditions. This concept has been demonstrated by Brown for system identification applications whereby the stochastic weighted least squares was found to weight the estimates incorrectly when the SNR was above such a threshold [3]. This thesis does not attempt to determine a SNR threshold applicable specifically to GPS and of more importance to determine

if the current SNR encountered in typical GPS applications is above or below this threshold. It must be noted that if the threshold is at a SNR level much lower than that encountered by GPS, it is possible that there is no benefit in applying stochastic estimation theory.

Both GDOP and the condition number of the the regressor matrix (H), which is abbreviated as $cond(H)$, are considered in this thesis for the evaluation of how good the geometrical conditions in the test scenarios are relative to each other. GDOP is considered because it is the conventional, most widely accepted, and most familiar measure of geometrical strength for GPS. The $cond(H)$ is also being considered because it was shown that $cond(H)$ is a better measure of geometrical strength since, unlike the GDOP, it has no dependence on the satellite availability [20]. Cond(H) is a measure of strictly the geometry; furthermore, it reflects a worst case upper limit on error amplification that can be produced by the satellite geometry. The condition number of a matrix is defined as the ratio of the largest singular value to the smallest singular value. In the context of the GPS regressor matrix (H) the condition number is calculated as follows:

$$cond(H) \equiv \sqrt{\frac{\lambda_{max}(H^T H)}{\lambda_{min}(H^T H)}},$$

where $\lambda(\cdot)$ is used to represent the eigenvalues of a matrix.

4.2 Data Set Generation, Simulated GPS Test Environment

Spilker [28] shows that, with a five degree elevation angle, at least seven satellites are in view 80 percent of the time and there are always at least five satellites in view. In terms of satellite availability, the worst case scenario occurs at latitudes in the range of 35 to 55 degrees. In this latitude range there are at most six satellites available 20 percent of the time using a five degree elevation angle. Even if the worst case conditions with a ten degree elevation angle were considered, in the 35 to 55 degree latitude range, only four satellites are available less than 0.5 percent of the time. A ten degree elevation angle is extremely conservative since current technology

allows for better than five degree elevation angles at 0 altitude. The elevation angle can decrease to below 0 degrees with increasing altitude. Since satellite availability is not dependent on user position longitude, selecting a single user position in the 35 to 55 degree latitude range and assuming an elevation angle of 10 degrees will allow for simulating GPS data that is realistically indicative of worst case conditions. It is important that experimental scenarios be diverse in addition to being realistic; hence, using a fixed user position and using the satellite availability at different GPS times in a 24 hour period allows for a wide range of diversity.

An arbitrary user position in the 35 to 55 degree latitude range over the continental United States, 40° N latitude, 105° W longitude, at an altitude of 300 m was selected. The geographic coordinates are converted to ECEF coordinates and used to generate the experimental data sets with the Satellite Navigation Toolbox for Matlab [10]. Data sets are generated at one hour intervals and 12 scenarios which showed diversity in satellite availability and satellite geometry were selected to form the experimental data set. Satellite availability ranges from five to nine, which is indicative of real life scenarios. For a satellite availability of six, seven and eight where more than one scenario was selected, the different scenarios were selected to obtain the greatest diversity in satellite geometries.

To give an idea of the satellite geometry for each of the twelve selected satellite scenarios, a skyplot is generated for each scenario. The skyplot shows the relative position of the available satellites as seen at the user position by looking straight up at the sky. The center of the plot represents zenith, moving out from the center of the plot represents decreasing elevation angles, and the outer outline is the horizon. The skyplots for the 12 experimental scenarios are included at Figures 4.6 to 4.17.

4.3 Simulation of the Ground-Based Pseudolite Test Environment

The three ground-based pseudolite test scenarios are produced based on optimized ground-based planar arrays as presented by McKay [20]. An optimum ground

planar array of n transmitters has $(n-1)$ transmitters uniformly spread over the circumference of a circle of very large radius ideally at the horizon and one transmitter at the center of the circle. The optimum receiver location is directly above the transmitter at the center of the circle.

The following three guidelines were used in selecting the ground planar arrays for the test environment:

1. The optimum geometry for a planar array based on GDOP as described in [20] must be maintained to avoid geometries that may potentially be very unfavorable to the conventional iterative algorithms.
2. Maintaining the optimum geometry concept, the three scenarios represent a best possible condition, a degraded condition and a failure condition.
3. Without adversely effecting GDOP, sufficient transmitters are used in the planar array to allow the use of the ergodic assumption invoked in Equation (3.20) to estimate the equation error statistics.

The test environment includes 36 transmitters uniformly spread over the circumference of a circle of radius 10000 meters centered at the origin. It is recognized that a radius of 10000 meters is restrictive but it is used to reflect potential size restrictions due to terrain availability and/or line of sight visibility problems. The user is maintained stationary directly above the origin at an altitude of 10000 meters (i.e. user coordinates {0, 0, 10000}) for the three scenarios. To avoid confusion with the scenarios presented for the first test environment, the three scenarios are labeled Scenarios A, B, and C. The following differentiates each of the three scenarios:

- **Scenario A.** The ground array includes just the 36 GPS transmitters in the outer circular pattern.
- **Scenario B.** The ground array is the same as for Scenario A but an additional transmitter is included at the origin directly below the user receiver position.

This scenario represents the lowest achievable GDOP for the given number of receivers and ground area covered, or in other words, the most favorable conditions for the conventional ILS algorithm. The planar array depicted in Scenario B is shown in Figure 4.1.

- **Scenario C.** The ground array is the same as for Scenario A, but an additional transmitter is included 400 meters away from the origin; hence, below but not directly below the user receiver position, representing a degraded condition for the conventional ILS algorithm.

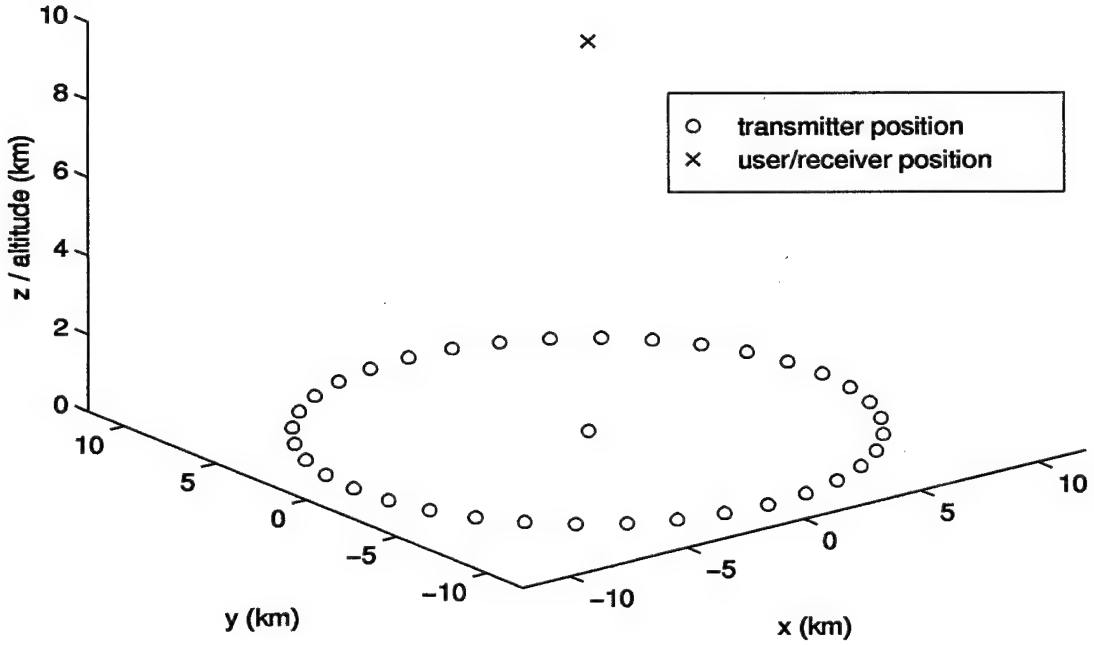

Figure 4.1 Scenario B, Optimum Ground-Based Planar Array

4.4 Experimental Data Description

The following provides a description of the data collected using the experimental GPS position determination algorithms. The descriptions are intended to facilitate interpretation of the experimental results. They are presented in the same

order that they appear in the tabulated results presented in Table 4.1 through Table 4.12:

- **Estimated σ.** This is an estimation of the standard deviation of the applied pseudorange measurement noise. A data-driven estimate of σ is calculated on each Monte Carlo run and the result shown is the average from all the runs. Only the *closed-form* algorithm has the capability to perform this calculation.
- **GDOP.** To demonstrate the diversity in geometry, the GDOP for each experimental scenario is shown. GDOP is a measure of geometry associated with the conventional iterative GPS position determination algorithms; hence, it is only presented in the results for the ILS and IBF algorithms. The GDOP is calculated using, $GDOP = \sqrt{trace((H^T H)^{-1})}$ where H is the matrix of direction cosines with ones populating the last column, as defined in Section 2.2.2 of this thesis. The GDOP for the ILS algorithm is calculated using the tall $(n \times 4)$ H matrix which reflects the n available satellites. The GDOP for the IBF algorithm is calculated using the (4×4) H matrix which reflects the set of four satellites amongst the available satellites, selected to yield the lowest value of GDOP. In order to obtain the lowest achievable GDOP, all the possible combinations of four satellite sets were tested for each scenario and the best combination was selected.
- **Condition (H).** This represents the condition number of the regressor H used in calculating the unknown GPS parameters. For the *closed-form* algorithm, the effective regressor is considered in the calculation as, $\sqrt{H^T R_n^{-1} H}$, where R_n represents the covariance of the measurement noise vector without the scalar premultiplier as defined in Equation (3.11). R_n is used as the noise strength weighting to obtain the *closed-form* estimate as defined in Equation (3.17). The calculated condition number is actually the condition number of $H^T \sqrt{R_n^{-1}}$ where the Cholesky decomposition of R_n^{-1} is used to calculate the matrix square root. For the iterative algorithms, the regressor H is the conventional matrix

of direction cosines with ones populating the last column. There is no regressor associated with the *maximum likelihood* approach or the *Kalman update* approach.

- **Error** $(x, y, z, bias)$. Errors are shown for user position ECEF coordinates (u_x, u_y, u_z) and for the range-equivalent user clock bias (b). For each parameter, the error is the difference between the sample average estimate produced by the respective position determination algorithm and the true value of the parameter. The parameter sample average estimates, produced by the algorithms, are obtained from averaging the parameter estimates from the 5000 Monte Carlo runs.

- **Miss distance.** The miss distance, or root mean square (rms) position error, is a measure of the positioning accuracy and is calculated from the user position ECEF coordinates sample average estimation errors. This measure reflects how far the estimated user position is from the true user position. The miss distance is calculated using, $md = \sqrt{error(x)^2 + error(y)^2 + error(z)^2}$. The estimate of the range-equivalent user clock bias has no effect on the miss distance which is a function of strictly the position parameter estimation errors.

- **Estimated std** $(x, y, z, bias)$. The average estimated standard deviation is a calculation associated with the estimate of the GPS solution itself. An estimate of standard deviation, for each parameter, is calculated on each Monte Carlo run and the result shown is the average from all the runs. This calculation is related to the estimate of σ and is performed within the *closed-form* algorithm only, since it is the only one with the capability. The *closed-form* algorithm is actually producing an estimate of the covariance matrix which is a fully populated matrix due to some unavoidable yet small and unknown level of cross correlation; however, the off-diagonal elements will be small. The standard deviation for each of the four estimated GPS parameters is obtained by taking

the square root of the diagonal elements in the predicted or estimated error covariance matrix.

- **Experimental std** $(x, y, z, bias)$. The experimental standard deviation corresponds to the actual standard deviation of the set of estimates collected over all the Monte Carlo runs. This data is essentially the most reliable and most critical measure of relative performance of the algorithms. The experimental standard deviation is a marker of how good the experimentally obtained estimates are in terms of spread, which is a direct indication of how sensitive the algorithm is to pseudorange measurement noise. The standard deviation is a more robust performance indicator than the parameter estimation errors or the miss distance since, the covariance of a random variable is readily recovered using a finite number of realizations and is very consistent. On the other hand, the mean is much more difficult to recover, which raises some concern over the results for the parameter estimation errors and the miss distance, despite the 5000 Monte Carlo runs. The experimental standard deviation also serves as a baseline to compare how well the *closed-form* algorithm predicts its parameter error standard deviations.

- **Expected std** $(x, y, z, bias)$. The *expected* standard deviation is shown to verify how well the standard deviation of an estimate can be calculated provided that the standard deviation of the pseudorange noise (σ) is known. The true value of σ is used in the calculation even though in reality the true value of σ could never be known. This measure is an interesting one since by comparing expected values to the experimentally obtained values, the algorithm used in the calculation can be validated. Expected standard deviation is calculated for all the approaches with the exception of the maximum likelihood approach which does not have the capability to produce an *expected* standard deviation. The only difference between the *expected* standard deviation and the estimated standard deviation is that the latter makes use of a data-driven estimate of

the pseudorange measurement noise variance (σ^2), which only the *closed-form* algorithm has the capability of producing.

4.5 The Monte Carlo Runs

The experimental trials consisted of 5000 Monte Carlo runs for each test scenario. Although 5000 Monte Carlo trials may appear over-abundant, it was observed experimentally that an extremely large number of runs is required in order to recover unbiased means of the estimated parameters. Using experimental noise arrays with zero-mean and a standard deviation of $\sigma = 100$ meters, the experimental covariance of the estimated parameters was found to converge to a steady value after a few hundred runs but it was not possible to determine the number of runs that would be required for the mean of the estimated parameters to converge to a steady state value. Under the experimental environments used for this thesis it is anticipated that over 10000 runs would have been required. Running the same experiment of 5000 Monte Carlo runs several times, using a different zero-mean, $\sigma = 100$ m simulated noise array each time, produced virtually identical covariance results but some small, yet significant, variations in the means were still being observed.

4.6 Experimental Observations, Simulated GPS Test Environment

The four sections that follow discuss results associated with the simulated GPS test environment. The results are presented in Table 4.1 through Table 4.12. The results are tabulated by scenario and each table is accompanied by a skyplot that reveals the satellite availability and geometry of each scenario.

4.7 Conventional Iterative Algorithms

The IBF and ILS algorithms are basically the conventional GPS position estimation algorithms currently being used. The IBF algorithm uses only a set of four satellite pseudorange measurements chosen from the available satellites based

on best GDOP. This approach yields a four by four regressor which must be inverted to obtain a solution. The ILS algorithm is essentially the same but all n available pseudorange measurements are used to obtain the GPS solution. The regressor is a $(n \times 4)$ tall matrix so the generalized inverse is used resulting in a least squares solution. The results for these two conventional approaches are presented to provide a comparison baseline. The ultimate aim is to improve on the GPS solutions produced by the two conventional iterative algorithms.

4.7.1 Analysis of Results. The results for both the IBF and ILS algorithms are presented to provide a comparison baseline for the results obtained by the *closed-form*, *maximum likelihood*, and *Kalman update* algorithms. Direct comparison under varying scenarios reveals how well the new algorithms are performing in relation to the conventional iterative algorithms.

Under some scenarios, the IBF algorithm yielded GPS solution estimates with smaller mean errors while the ILS algorithm yielded smaller mean errors under other scenarios. There was no strongly apparent geometry relationship that would indicate which of the two iterative algorithms yielded the smaller parameter estimation mean errors for any given scenario. For both iterative algorithms, a loose relationship was observed between the GDOP and the miss distance, in which the lower GDOP scenarios tended to yield smaller miss distances. These relationships are shown in Figure 4.2 which also shows that the relationship extended to the condition number of H. It was expected that a stronger relationship between GDOP and miss distance would have existed. The lack of the strong relationship in itself is an indicator of the weakness in using the parameter mean estimation errors as sole performance indicators. It is not possible to base comparisons conclusively on strictly the miss distance since the results obtained show small variations in the miss distances between the two iterative approaches for all the scenarios. These small differences in miss distances may also be partly due to the biases in the mean errors caused by insufficient Monte Carlo runs. It is safer to draw comparisons on the more robust experimental

standard deviations which tend to be much more consistent. The relationship between the standard deviation and GDOP or $cond(H)$ is extremely evident, as can be seen in Figure 4.3 which is a plot of the average standard deviation from the three position parameters. Regardless of which of the two iterative algorithms provided the smallest miss distance, the ILS algorithm always provided the smallest standard deviations. This implies that for any given scenario, there is less variation in the results yielded by the ILS algorithm, or in other words, the algorithm is less sensitive to the pseudorange noise. For the four estimated parameters, in all the scenarios, the standard deviations produced by the ILS algorithm varied between 55.56 and 289.14 meters. This will be used as the comparison baseline for the GPS position determination algorithms developed in this thesis.

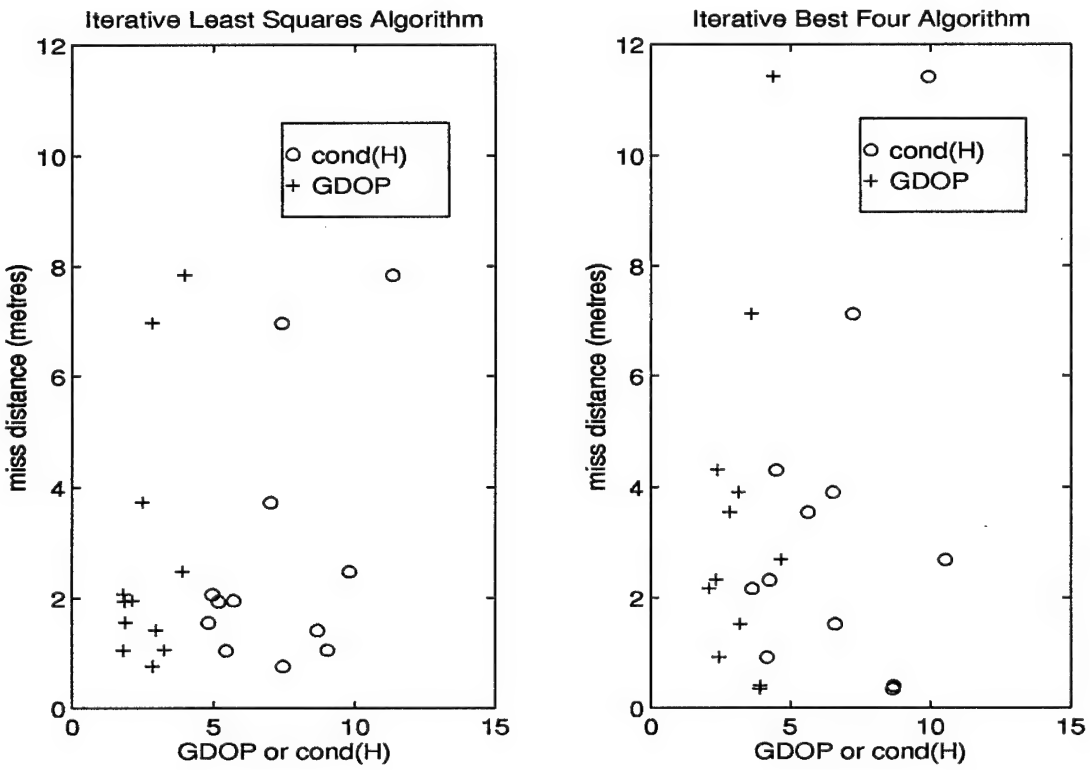

Figure 4.2 Geometry Effects on Miss Distance

The iterative algorithms do not have the capability of predicting the estimation error covariance; however, when the true value of σ is provided to either of the

conventional iterative algorithms, it is possible to calculate the *expected* covariance. This portion of the experimental trials is being included for academic discussions only since there is no way of knowing what the true value of σ is; furthermore, the iterative algorithms do not have the capability of producing a data-driven estimate of σ. Since the measurement noise on all pseudoranges is assumed independent, zero-mean, with equal variance σ^2, the covariance of the conventional iterative GPS solution is a function of σ given by, $cov(\vec{X}) = \sigma^2(H^T H)^{-1}$ [28]. It follows that the *expected* standard deviation of the GPS solution parameters can be calculated using the following expression, given in Matlab [17] notation:

$$\begin{aligned} [\sigma_{u_x},\ \sigma_{u_y},\ \sigma_{u_z},\ \sigma_b] &= \sqrt{diag(cov(\vec{X}))} \\ &= \sigma\sqrt{diag((H^T H)^{-1})} \end{aligned}$$

The calculated standard deviations of the GPS solution parameter estimates were remarkably close to the values obtained experimentally. For both iterative algorithms, the *expected* standard deviations calculated where within 2.25 percent of the experimentally obtained values.

4.8 Closed-Form Algorithm

The *closed-form* algorithm is based on the approach developed in Section 3.1 of this thesis. This approach provides a *closed-form* position estimate solution to a stochastically modeled set of n satellite pseudorange equations. The calculated user position estimate is not dependent on the equation error covariance, P_V, which can also be interpreted as the noise strength; however, the noise strength is required in the derivation of the estimate. This approach also provides an estimate of the covariance of the estimation error using the return differences or residuals. The return difference vector, as defined in Section 3.1.4, is used to obtain a data-driven estimate of the pseudorange measurement noise variance (σ^2), from which the estimation error covariance is readily calculated.

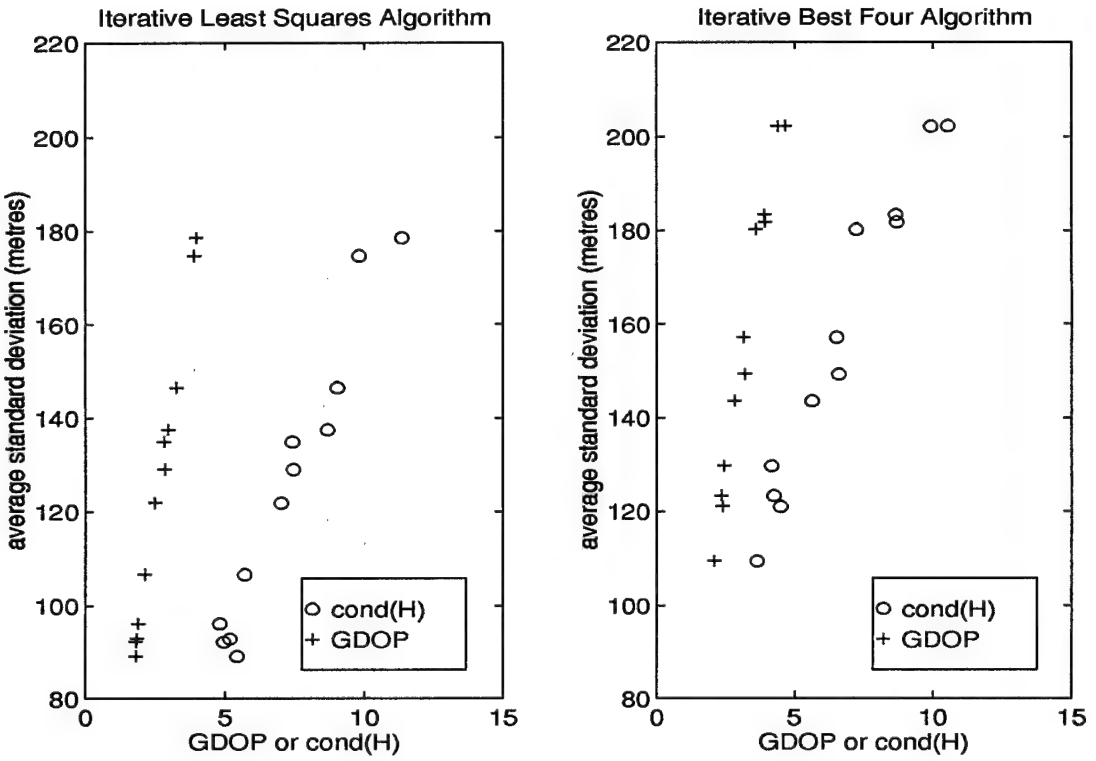

Figure 4.3 Geometry Effects on Standard Deviation

4.8.1 Limitations. Some known limitations associated with the *closed-form* algorithm must be emphasized to avoid misinterpretation of the experimental results. The following are the limitations that must be kept in mind in analyzing the experimental results:

1. n satellite pseudorange measurements are required to form a linear regression of $n-1$ equations. Since there are four unknown parameters, the user position ECEF coordinates and the range-equivalent user clock bias, a minimum of five pseudorange measurements are required.
2. When exactly five pseudorange measurements are available (i.e. $n = 5$), the linear regression takes the form of four equations in four unknowns. In this situation, return differences of essentially zero can be expected, thereby rendering the covariance estimation capability of the algorithm invalid.

3. In addition to the previous items, n must be large to determine σ experimentally. It is not known how large n must be before a reliable estimate of σ can be extracted from the return difference, but an unconfirmed rule of thumb from statistics suggests that $n_{min} = 2N^2$, where N is the number of variables. For GPS, $N = 4$ which implies an n_{min} of at least 32. The value of n_{min} serves only as a guideline because it is desirable to have n as large as possible since the ergodic assumption invoked in Equation (3.20) becomes more valid as the number of available satellites increases. The impact of this limitation can only be assessed through thorough experimentation.

4.8.2 Analysis of Results. The experimental results indicate that the *closed-form* algorithm developed in this thesis is extremely sensitive to noise. The sensitivity to pseudorange noise is reflected in the extremely large experimental standard deviations which ranged from 1078.08 m to 23864.01 m for the position parameter estimates as compared to ILS algorithm's baseline results of 55.56 m to 289.14 m. The standard deviations for the range-equivalent user clock bias estimates were significantly larger ranging between 19014.42 m and 111746.08 m. For the twelve scenarios under observation, the miss distance ranged between 4.93 m and 729.17 m compared to the baseline ILS results of 0.76 m to 7.84 m. The results loosely reflect tendencies that better results (i.e. lower mean errors and miss distance) are obtained when the condition number of the regressor H is lower. The relationship between the condition number of the regressor H and miss distance is plotted in Figure 4.4. In the twelve test scenarios the results both in terms of mean estimation errors and error standard deviations were significantly worse than those obtained by both conventional iterative algorithms.

The results show that the condition numbers for H yielded by the *closed-form* algorithm are all extremely large, ranging between 220.92 and 2172.53; however, an in depth appreciation of the algorithm has not yet been acquired to allow in distinguishing what could be considered a good range for the condition numbers.

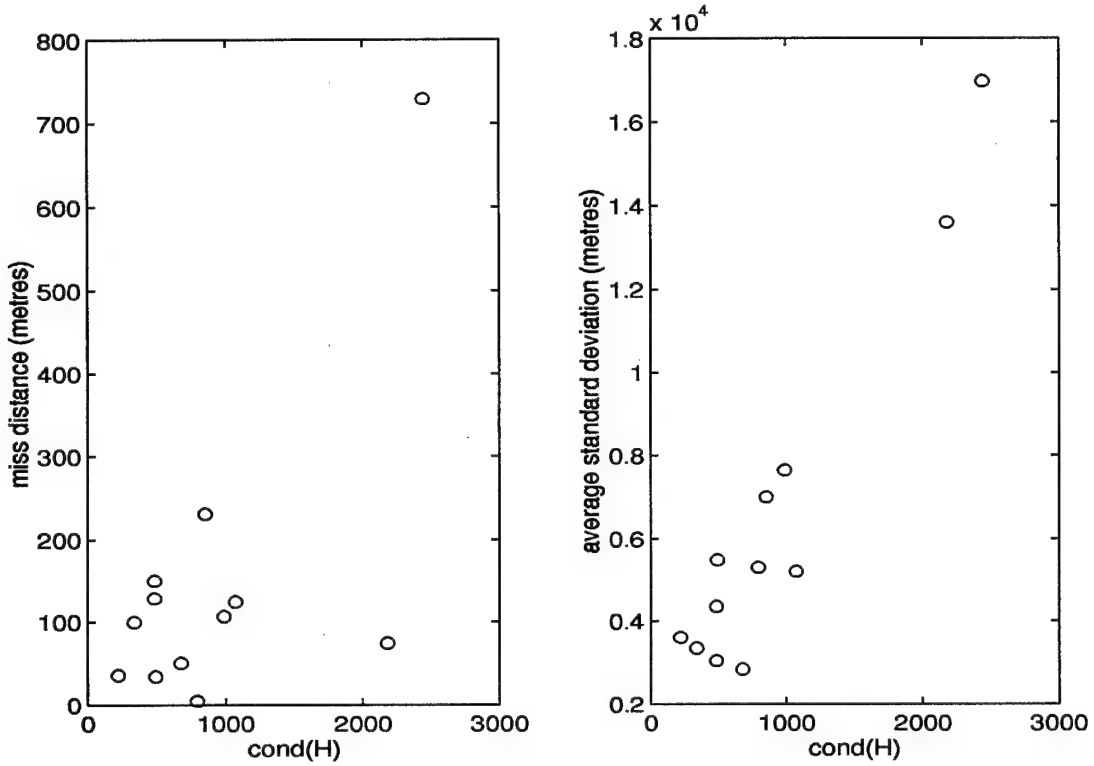

Figure 4.4 Closed-Form Algorithm Performance versus Condition Number

Consequently, it is unlikely that this algorithm can provide a GPS solution with small errors. The ill conditioning of the regressor is largely due to the last column which is made up of the difference between the pseudoranges. The first three columns are made up of differences in the three satellite position coordinates (u_x, u_y, u_z), respectively, which tend to produce much larger differences than the pseudorange differences. Based on the formulation of the H matrix, the lower condition numbers are achieved when the spread in the pseudorange measurements of the satellites in view is large. If all pseudoranges are equal, which is not a physically possible scenario in the NAVSTAR GPS satellite constellation, the last column of the H matrix would be all zeros, yielding a condition number of infinity. The poor scaling due to the last column of the H matrix manifests itself as extremely large errors in the range-equivalent user clock bias where the observed errors ranged between 2.04 m and 2500.71 m compared to baseline results of 0.03 m to 5.52 m. The errors

in the estimation of the range-equivalent user clock bias were generally in the range of one order of magnitude larger than the errors observed for the three coordinates of the user position estimate. The large errors in the clock bias estimates do not affect the miss distance which is strictly a function of the error in the estimated position.

An additional feature of the *closed-form* algorithm is its ability to provide a data-driven estimate of the covariance of the GPS solution estimate. This is achieved by using the return difference, or residuals, to estimate the variance of the pseudorange measurement noise (σ^2). It is recognized that when only five satellite pseudorange measurements are available, it is not possible to estimate the error covariance since the the return difference will be virtually zero. The results show that, with more than five satellites, an estimate of σ, the standard deviation of the experimental pseudorange measurement noise, is obtained. The estimates of σ are not reliable due to the small number of satellites available. As satellite availability increases, the estimate of σ improves accordingly. The experimental results show that, with six satellites in view, the estimated σ ranged between 23.51 m and 39.08 m. With seven satellites, the estimated σ ranged between 52.87 m and 56.26 m, showing some improvement. With eight satellites, the estimated σ ranged between 62.95 m and 64.01 m, showing some further improvement. Comparison of the estimated standard deviations obtained to the actual σ of 100 m used in the generation of the pseudorange measurement noise clearly indicates that a much larger number of satellites must be available before a reliable estimate of σ can be extracted from the return difference. This can present a serious obstacle since there are very rarely more than nine satellites in view from the NAVSTAR GPS constellation. This situation can change if consideration is given to GLONASS satellite augmentation or pseudolite augmentation.

The estimates of the error covariance yielded by the *closed-form* algorithm were poor as a direct consequence of the algorithm's inability to estimate σ accurately. There are large differences between the actual experimental standard deviations and

the estimated standard deviations; however, this was not due to any deficiency in the algorithm used in predicting the estimation error covariance. Although there would not be any way of knowing the true σ in the real world, in order to validate the algorithm used in estimating the error covariance, the actual σ of 100 m was provided for use in the calculations of the *expected* standard deviation. The *expected* standard deviation calculations yielded numbers extremely close to those observed experimentally. The *expected* standard deviations where all within 6.5 percent of the experimentally obtained values. This is sufficient to validate that the algorithm can be used to estimate the standard deviation of its GPS solution estimate, but it does not change the fact that the algorithm is plagued with extremely large GPS parameter estimate mean errors with extremely large standard deviations. It must be noted that when the true value of σ is provided to either of the conventional iterative algorithms, the *expected* standard deviations of the GPS unknown parameter estimates obtained were also remarkably close to the values obtained experimentally.

In order to appreciate the merits of the *closed-form* algorithm truly, particularly the ability to predict the estimation error covariance, it is necessary to increase the satellite availability. Nothing can be done to increase the actual satellite availability which is directly dependent on the constellation, but by applying some creative experimentation, it may be possible to increase the *effective* satellite availability. If it is assumed that the noise is predominantly receiver related and it is slowly varying, the estimate σ can be generated every k sample periods using a *moving window* type approach, in which only the most recent k data sets are used to establish the noise strength. This concept is actually more complex than it appears because, although it is possible to assume that the noise strength remains fairly constant over the window, the vehicle is moving continuously. This concept has not yet been evaluated experimentally; however, it proved to be extremely effective and reliable for estimating σ while the user position is maintained stationary. The experimental trials involved producing a concatenation of satellite scenarios generated at one hour time inter-

vals. The trials where run, incrementing the number of concatenated scenarios to determine the effective satellite availability required to produce reliable estimates of σ. Experimental results showed the estimated σ improving with increasing effective satellite availability until a steady state maximum was reached using six scenarios, giving an effective satellite availability of 42. These results are shown graphically in Figure 4.5. An estimated mean σ of 92.5 m was retrieved over 1000 Monte Carlo runs. An experimental standard deviation of 30.0 m was observed on the estimates of σ, which implies that 68.3 percent of the time the algorithm produces an estimate of σ between 62.5 m and 122.5 m. Although, the user position is stationary here, which is seldom the case in reality, it can be inferred that the concept of scenario concatenation can be modified and applied to increase the *effective* satellite availability even while the user position is not stationary. Being able to estimate σ, even if only while the receiver is stationary, can prove to be extremely useful for receiver calibration purposes.

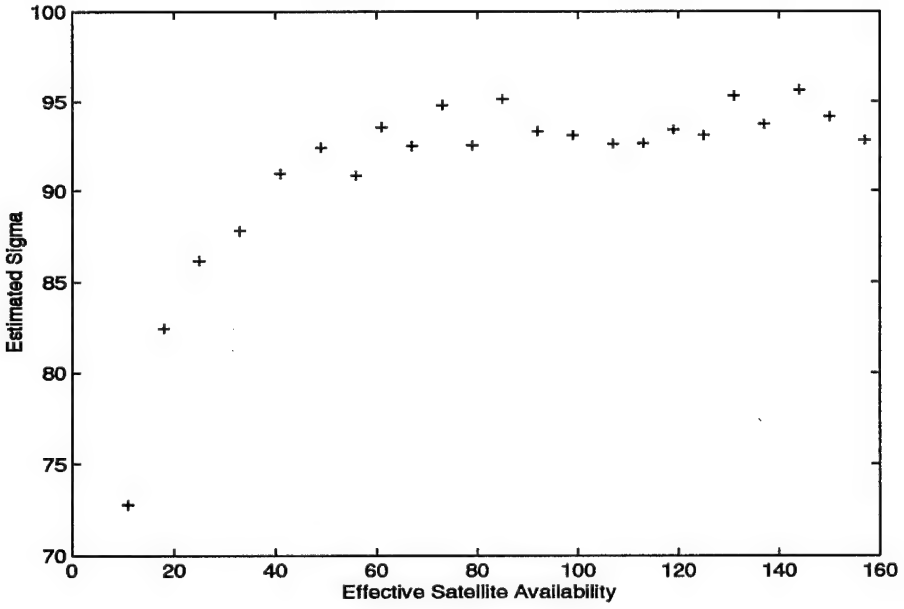

Figure 4.5 Estimation of σ Using Scenario Concatenation

4.8.3 Experimental Results, Alternate Closed-Form Algorithm. The experimental results obtained with the *alternate closed-form* algorithm developed in Section 3.4 are discussed. The *alternate closed-form* algorithm, as its name implies, is simply a variation on the closed-form algorithm which was motivated by the desire to obtain a more mathematically balanced algorithm that can produce a solution with only four pseudorange measurements as is the case for deterministic algorithms. The mathematical development showed that, due to the singularity in the noise covariance matrix, a minimum of five pseudorange measurements is required just as was the case in the *closed-form* solution. Given the apparent similarities between both closed-form algorithms, their relative performances were not expected to be much different. In fact, in all 12 experimental scenarios, the experimental results yielded by both versions of the *alternate closed-form* algorithm were identical to those obtained with the *closed-form* algorithm. The two versions of the *alternate closed-form* algorithm refers to:

1. The solution in Equation (3.71) based on the $(n \times n)$ linear regression with the singular noise covariance matrix.
2. The solution in Equation (3.77) based on the transformed $(n-1 \times n-1)$ linear regression with the diagonal noise covariance matrix.

The experimental results produced by the *alternate closed-form* algorithm are not presented explicitly since they are identical to the *closed-form* results; hence, the *closed-form* results presented in Tables 4.1 through 4.12 can be interpreted as being the results from the *alternate closed-form* algorithm as well. Contrary to the original expectations, the *alternate closed-form* algorithm does not offer any additional benefits over the the *closed-form* algorithm; hence, given its complex structure and the inherited singularities in the equation error covariance and regressor matrices, its use is not recommended.

4.9 Maximum Likelihood

The *maximum likelihood* algorithm was developed as a supplement to the *closed-form* algorithm and is not intended to provide a GPS solution on its own. The *maximum likelihood* algorithm is initiated when the *closed-form* algorithm has produced a solution and the *closed-form* solution is used as a starting point or initialization for the *maximum likelihood* algorithm. The estimate of the unknown GPS parameter vector and the associated error covariance obtained from the *closed-form* algorithm is sufficient to describe the Gaussian probability distribution function entirely. A constrained optimization problem is formulated by using the last pseudorange equation at Equation (3.3) which was not fully employed in the linear regression. The goal of the optimization problem is to obtain a new estimate of the GPS parameters that maximizes the probability subject to the constraint imposed by the n^{th} pseudorange measurement equation; hence, the name *maximum likelihood.*

4.9.1 Limitations. The following are some known limitations associated with the *maximum likelihood* algorithm which must be kept in mind in analyzing the experimental results:

1. Optimization algorithms are iterative in nature, hence the *closed-form* appeal is lost.
2. The *maximum likelihood* algorithm can provide an improved estimate of the GPS unknown parameter vector, but there is no simple way of predicting the estimation error covariance.
3. The pseudorange measurement associated with the last satellite is noise corrupted but the constraint equation used in the development of the algorithm must be a deterministic equation. Disregarding the noise in the n^{th} equation will bias the solution and can have an adverse impact on the error since the solution becomes extremely dependent on the noise of that one single pseudorange measurement. Some of this concern is alleviated by recalling that the last

pseudorange equation is actually the one closest to the average pseudorange as defined in Equation (3.4). As such, it is likely that the last satellite is somewhat in the vicinity of zenith where lower levels of pseudorange measurement noise can be expected.

4.9.2 Analysis of Results. The results produced by the *maximum likelihood* algorithm demonstrate the necessity of using the last GPS pseudorange measurement. In all twelve scenarios, regardless of what the GPS solution errors where when the algorithm was initiated, the errors are reduced drastically to essentially the same level as obtained with ILS method. The most remarkable difference is in the errors of the range-equivalent user clock bias which were extremely large in the initial conditions provided. There is no direct relationship between the *closed-form* results and the *maximum likelihood* results in that the smaller initial errors do not necessarily yield better results. The miss distances yielded ranged from 0.89 m to 8.22 m and followed the ILS results quite closely for the four GPS solution parameters in all twelve scenarios. The miss distances yielded by the *maximum likelihood* algorithm, when compared to those yielded by the ILS algorithm, are a fraction of a meter either above or below and the largest difference was 0.56 m observed in Scenario 8.

The experimental standard deviations observed for the three position estimation parameters are essentially the same as those observed for the ILS. The performance in terms of to the estimation of the range-equivalent user clock bias is slightly worse than the baseline established by the ILS algorithm both in terms of the mean error and the error covariance. If only the user position estimation parameters, (u_x, u_y, u_z), are considered, the *maximum likelihood* algorithm demonstrates performance equivalent to the baseline. The fundamental limitation with the *maximum likelihood* approach is its inability to predict its estimation error covariance; furthermore, unlike the iterative approaches, even if the standard deviation of the

pseudorange measurement noise is somehow known, the *expected* standard deviation of the estimation parameters cannot be calculated.

The results yielded by the *maximum likelihood* algorithm provide some hope that a stochastic estimation approach to the GPS pseudorange equations is feasible and that performance comparable to that currently being achieved by the ILS algorithm is attainable. However, the limitations associated with the *maximum likelihood* algorithm outweigh the advantages that motivated this research in the first place. Consequently, another supplementary algorithm that is noniterative and more elegant in form and that can refine the solution produced by the *closed-form* algorithm while maintaining the capability to provide the estimation error covariance is needed, which leads to the *Kalman update* algorithm presented in Section 3.3.

4.10 Kalman Update

The *Kalman update* algorithm was developed as an alternate supplement to the *closed-form* algorithm and, as was the case for the *maximum likelihood* algorithm, it is not intended to provide a GPS solution on its own. The *Kalman update* algorithm requires the *closed-form* solution for initialization. The last pseudorange equation at Equation (3.3) which was not fully employed in the linear regression is manipulated into the form of a *new* linear measurement and is used to update the solution yielded by the *closed-form* algorithm through an update cycle closely resembling that of a conventional Kalman filter.

4.10.1 Analysis of Results. The *Kalman update* algorithm produced results comparable to the baseline results. Again, the errors on the estimation parameters and the miss distance obtained are extremely close to the baseline results. The miss distances yielded by the *Kalman Update* algorithm when compared to those yielded by the ILS algorithm are a fraction of a meter either above or below and the largest difference was 0.77 m observed in Scenario 8. Given the lack of confidence that can

be placed on just the mean error results, the results are considered equivalent to the baseline in terms of parameter estimation errors. For the three position estimation parameters, the experimental standard deviations are also equivalent to the baseline; however, the standard deviation associated with the error on the range-equivalent user clock bias is noticeably larger than the baseline. The standard deviation on the user clock bias was consistently marginally larger than those obtained with the *maximum likelihood* algorithm. Unlike the *maximum likelihood* algorithm, the *Kalman update* algorithm has the capability of predicting its estimation error covariance, and its performance is reasonably good. The calculated standard deviations for the three position estimation parameters where all within 14.02 percent of the experimentally obtained values. The performance in producing the *expected* standard deviation on the user clock bias estimation error was poorer and differed from the experimentally obtained values by as much as 44.2 percent.

Overall, the performance of the *Kalman update* algorithm is good and truly deserving of further consideration. The only shortcoming of this algorithm is that it produces user clock bias estimation error standard deviations larger than the baseline and the algorithm is incapable of predicting the standard deviation, associated with the user clock bias estimation error, accurately. For the most part, the performance of the *Kalman update* algorithm is comparable to that of the baseline; furthermore, the algorithm retained all the attractive features that motivated the development of the *closed-form* algorithm. Looking at the *closed-form* algorithm as supplemented by the *Kalman update* algorithm as a single GPS position determination algorithm has produced an algorithm with the following attributes:

1. The algorithm is closed-form, hence it can be used under any geometrical conditions without the need for externally provided initialization.
2. The algorithm has the potential to benefit from computational efficiencies due to its non-recursive nature.

3. The algorithm has the capability to produce an estimate of the estimation error covariance.

4. The algorithm can produce a GPS solution estimate without the knowledge of the pseudorange measurement noise standard deviation (σ).

5. The performance under typical navigation scenarios, using only the NAVSTAR GPS satellite constellation, is for the most part equivalent to the performance achieved by the conventional ILS algorithm used as a baseline.

EXPERIMENTAL SCENARIO DATA

GPS time: t = 20700 sec
User Position: 40 N, 105 W, 300 m
Satellite Availability: N = 9
Satellites for best GDOP: 5 17 20 23

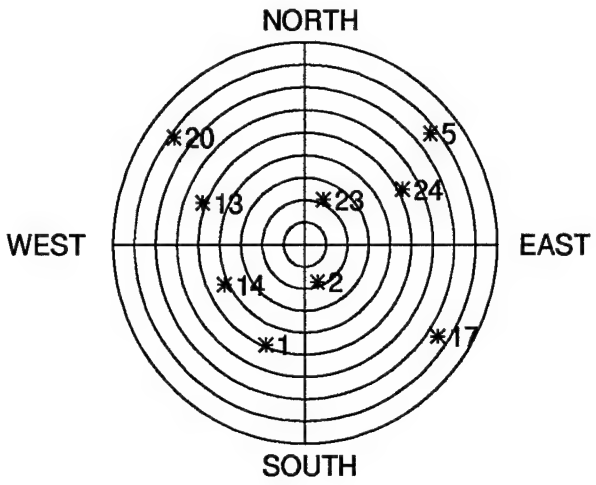

Figure 4.6 Skyplot, Scenario 1

Table 4.1 Monte Carlo Simulation Results, Scenario 1

	Closed Form	Maximum Likelihood	Kalman Update	Iterative	
				Least Squares	Best Four
Estimated σ	61.69				
GDOP				1.81	2.45
Condition H	482.80			5.43	4.16
Error x	25.50	0.36	0.43	0.29	0.21
Error y	94.51	-0.17	0.07	-0.64	-0.82
Error z	-83.29	-1.13	-1.33	-0.77	0.38
Error bias	453.44	1.12	2.25	-0.03	0.02
Miss distance	128.53	1.20	1.40	1.05	0.93
Estimated std x	719.34				
Estimated std y	2707.30				
Estimated std z	2349.87				
Estimated std bias	12930.87				
Experimental std x	1137.75	56.14	56.35	55.56	107.56
Experimental std y	4289.53	99.39	101.73	97.07	140.85
Experimental std z	3723.09	116.77	118.24	114.77	140.61
Experimental std bias	20433.70	106.34	130.63	84.56	95.91
Expected std x	1166.00		57.39	55.83	106.36
Expected std y	4388.33		91.82	97.83	142.60
Expected std z	3808.97		105.55	114.32	139.72
Expected std bias	20959.97		120.56	83.93	95.10

EXPERIMENTAL SCENARIO DATA

GPS time: t = 38700 sec
User Position: 40 N, 105 W, 300 m
Satellite Availability: N = 8
Satellites for best GDOP: 1 19 20 22

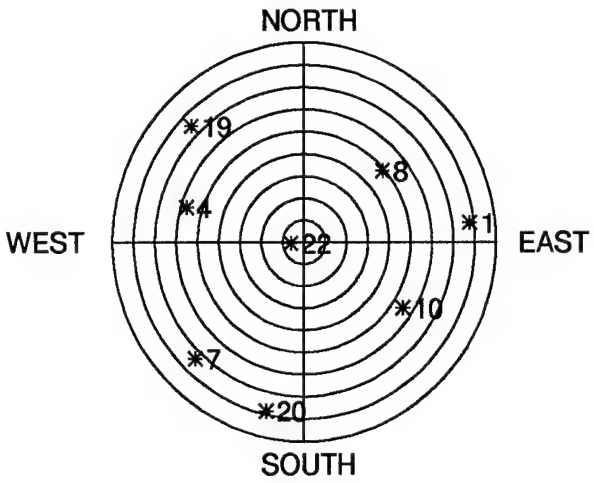

Figure 4.7 Skyplot, Scenario 2

Table 4.2 Monte Carlo Simulation Results, Scenario 2

	Closed Form	Maximum Likelihood	Kalman Update	Iterative	
				Least Squares	Best Four
Estimated σ	64.01				
GDOP				1.82	2.09
Condition H	675.34			4.95	3.63
Error x	9.82	-0.62	-0.60	-0.68	-0.77
Error y	37.60	-1.38	-1.31	-1.45	-1.67
Error z	-32.21	1.27	1.21	1.30	1.15
Error bias	185.69	-0.03	0.35	0.30	-0.07
Miss distance	50.47	1.98	1.88	2.07	2.17
Estimated std x	707.00				
Estimated std y	2637.00				
Estimated std z	2264.56				
Estimated std bias	12554.94				
Experimental std x	1078.08	64.09	64.35	63.49	85.23
Experimental std y	4011.12	122.82	124.25	119.93	129.71
Experimental std z	3442.63	95.38	96.59	93.21	113.51
Experimental std bias	19014.42	101.86	113.86	75.56	80.50
Expected std x	1104.56		60.16	64.12	85.13
Expected std y	4119.82		126.32	121.01	131.65
Expected std z	3537.94		89.79	92.59	112.85
Expected std bias	19614.72		106.06	75.51	80.72

EXPERIMENTAL SCENARIO DATA

GPS time: t = 13500 sec
User Position: 40 N, 105 W, 300 m
Satellite Availability: N = 8
Satellites for best GDOP: 3 10 15 24

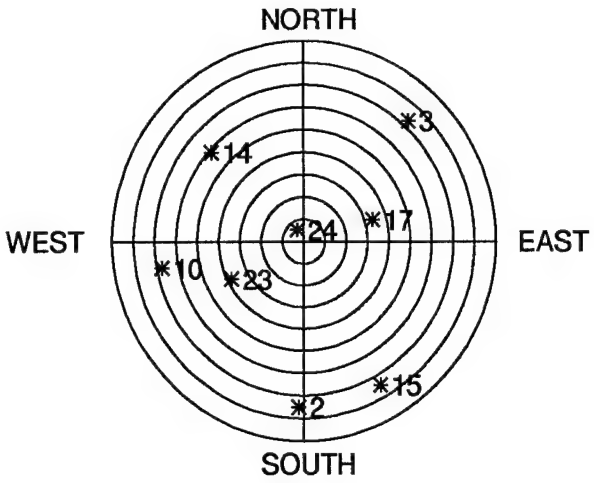

Figure 4.8 Skyplot, Scenario 3

Table 4.3 Monte Carlo Simulation Results, Scenario 3

	Closed Form	Maximum Likelihood	Kalman Update	Iterative	
				Least Squares	Best Four
Estimated σ	62.95				
GDOP				1.85	2.39
Condition H	1071.20			5.17	4.49
Error x	-23.65	0.87	0.86	0.87	0.98
Error y	-92.07	1.73	1.69	1.69	3.88
Error z	79.90	-0.35	-0.32	-0.36	-1.58
Error bias	-440.27	-0.73	-0.92	-1.28	-2.15
Miss distance	124.18	1.97	1.92	1.94	4.31
Estimated std x	1291.51				
Estimated std y	4938.60				
Estimated std z	4225.10				
Estimated std bias	23139.21				
Experimental std x	1929.29	68.49	68.56	68.13	82.90
Experimental std y	7374.58	125.44	125.97	123.81	161.19
Experimental std z	6308.96	87.66	88.19	86.69	119.05
Experimental std bias	34510.60	104.48	109.77	84.05	100.16
Expected std x	2051.48		63.71	67.02	81.89
Expected std y	7844.66		140.00	122.84	161.37
Expected std z	6711.31		89.08	87.20	120.19
Expected std bias	36755.24		86.79	83.42	100.47

EXPERIMENTAL SCENARIO DATA

GPS time: t = 6300 sec
User Position: 40 N, 105 W, 300 m
Satellite Availability: N = 7
Satellites for best GDOP: 10 11 15 21

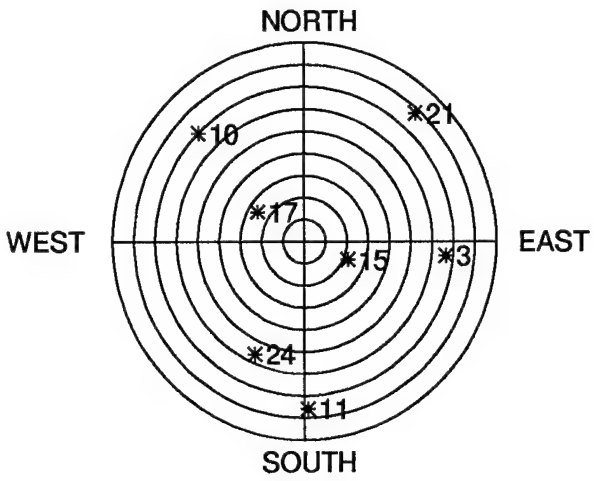

Figure 4.9 Skyplot, Scenario 4

Table 4.4 Monte Carlo Simulation Results, Scenario 4

	Closed Form	Maximum Likelihood	Kalman Update	Iterative	
				Least Squares	Best Four
Estimated σ	54.13				
GDOP				1.89	2.34
Condition H	483.67			4.81	4.25
Error x	-30.88	-1.44	-1.48	-1.32	-2.11
Error y	-110.95	0.32	0.19	0.65	0.21
Error z	96.27	-0.13	-0.01	-0.52	0.94
Error bias	-528.90	-1.00	-1.64	-0.06	0.77
Miss distance	150.11	1.48	1.49	1.56	2.32
Estimated std x	864.05				
Estimated std y	3263.67				
Estimated std z	2827.15				
Estimated std bias	15479.98				
Experimental std x	1619.75	68.97	69.09	68.75	108.93
Experimental std y	6121.03	116.08	117.33	114.85	130.93
Experimental std z	5304.14	106.57	107.74	104.87	130.06
Experimental std bias	29006.92	105.45	125.04	81.97	89.33
Expected std x	1596.27		65.01	69.37	110.06
Expected std y	6029.36		115.04	114.30	130.54
Expected std z	5222.94		113.60	104.46	132.20
Expected std bias	28598.00		96.66	82.28	90.70

EXPERIMENTAL SCENARIO DATA

GPS time: t = 56700 sec
User Position: 40 N, 105 W, 300 m
Satellite Availability: N = 7
Satellites for best GDOP: 3 4 9 13

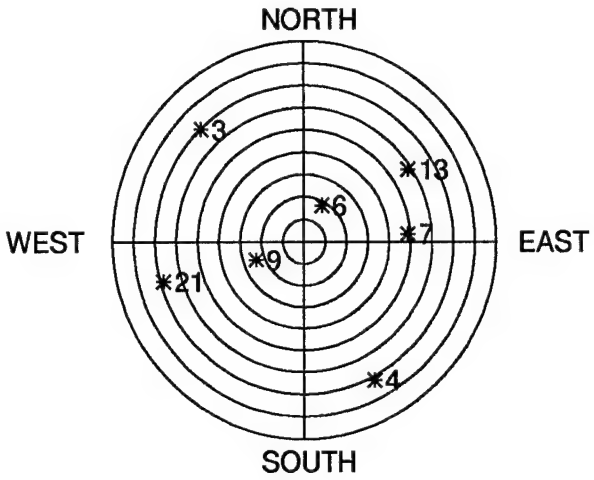

Figure 4.10 Skyplot, Scenario 5

Table 4.5 Monte Carlo Simulation Results, Scenario 5

	Closed Form	Maximum Likelihood	Kalman Update	Iterative	
				Least Squares	Best Four
Estimated σ	56.26				
GDOP				2.13	2.83
Condition H	850.41			5.70	5.63
Error x	46.31	-0.26	-0.25	-0.34	-0.67
Error y	172.78	2.11	2.17	1.93	3.12
Error z	-146.70	-0.26	-0.31	-0.08	-1.57
Error bias	795.08	-0.43	-0.13	-0.75	-1.90
Miss distance	231.34	2.14	2.20	1.96	3.55
Estimated std x	1499.53				
Estimated std y	5493.08				
Estimated std z	4713.29				
Estimated std bias	25600.41				
Experimental std x	2694.47	76.40	76.47	76.08	97.90
Experimental std y	9857.39	134.06	134.25	133.17	170.02
Experimental std z	8461.39	111.63	111.87	110.75	162.96
Experimental std bias	45921.95	115.69	118.06	99.73	126.19
Expected std x	2665.27		83.14	76.08	98.30
Expected std y	9763.41		150.57	134.95	170.91
Expected std z	8377.40		110.55	108.26	159.81
Expected std bias	45502.20		98.12	98.79	125.21

EXPERIMENTAL SCENARIO DATA

GPS time: t = 85500 sec
User Position: 40 N, 105 W, 300 m
Satellite Availability: N = 7
Satellites for best GDOP: 8 12 15 18

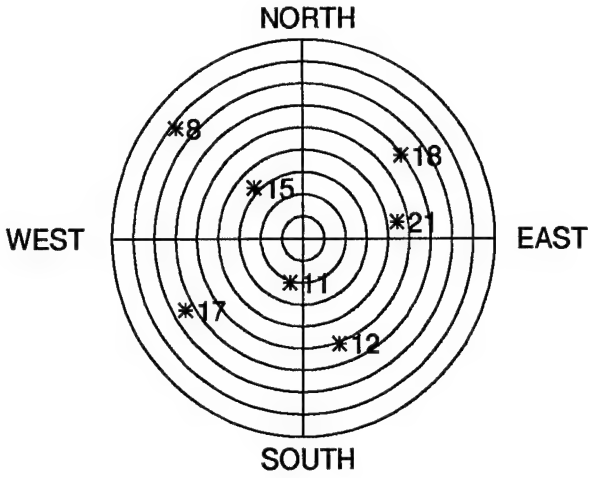

Figure 4.11 Skyplot, Scenario 6

Table 4.6 Monte Carlo Simulation Results, Scenario 6

	Closed Form	Maximum Likelihood	Kalman Update	Iterative	
				Least Squares	Best Four
Estimated σ	55.60				
GDOP				2.48	3.14
Condition H	792.75			7.01	6.52
Error x	-2.58	-2.32	-2.32	-2.33	-2.18
Error y	-3.47	-2.53	-2.54	-2.49	-2.74
Error z	2.36	1.54	1.54	1.52	1.75
Error bias	-2.04	2.39	2.36	2.52	2.56
Miss distance	4.93	3.76	3.77	3.73	3.91
Estimated std x	1148.74				
Estimated std y	4132.45				
Estimated std z	3614.97				
Estimated std bias	19524.84				
Experimental std x	2053.96	87.66	87.67	87.49	117.39
Experimental std y	7398.57	124.98	124.91	124.23	163.45
Experimental std z	6462.19	154.15	154.18	153.81	190.61
Experimental std bias	34910.46	134.45	135.37	121.56	147.44
Expected std x	2066.11		91.89	86.96	115.34
Expected std y	7432.62		127.00	124.90	163.45
Expected std z	6501.87		173.01	153.29	191.49
Expected std bias	35117.32		108.68	122.17	147.89

EXPERIMENTAL SCENARIO DATA

GPS time: t = 53100 sec
User Position: 40 N, 105 W, 300 m
Satellite Availability: N = 7
Satellites for best GDOP: 4 7 14 21

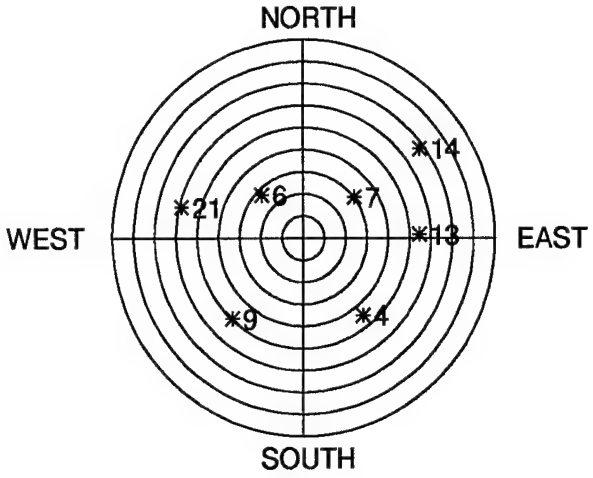

Figure 4.12 Skyplot, Scenario 7

Table 4.7 Monte Carlo Simulation Results, Scenario 7

	Closed Form	Maximum Likelihood	Kalman Update	Iterative	
				Least Squares	Best Four
Estimated σ	52.87				
GDOP				2.96	3.90
Condition H	2179.74			8.67	8.66
Error x	14.49	0.04	0.02	0.06	-0.13
Error y	54.32	0.22	0.17	0.26	-0.29
Error z	-48.62	-1.36	-1.33	-1.40	-0.15
Error bias	251.92	-0.89	-1.12	-0.70	0.07
Miss distance	74.32	1.38	1.34	1.42	0.35
Estimated std x	2621.91				
Estimated std y	9811.00				
Estimated std z	8569.22				
Estimated std bias	45828.57				
Experimental std x	5096.16	69.62	69.61	69.56	100.28
Experimental std y	19066.07	175.85	175.83	175.24	198.45
Experimental std z	16649.71	168.33	168.38	167.98	251.23
Experimental std bias	89017.21	162.90	167.95	152.54	194.91
Expected std x	4958.95		65.48	69.45	101.08
Expected std y	18556.05		173.72	174.60	199.25
Expected std z	16207.40		186.88	169.99	252.49
Expected std bias	86677.93		146.43	153.94	196.20

EXPERIMENTAL SCENARIO DATA

GPS time: t = 45900 sec
User Position: 40 N, 105 W, 300 m
Satellite Availability: N = 6
Satellites for best GDOP: 4 6 14 22

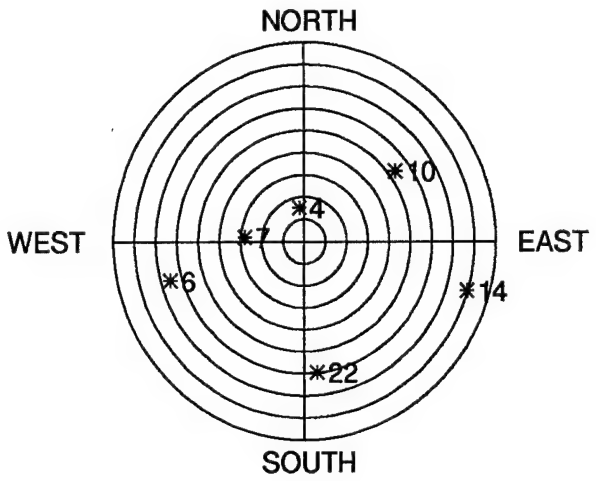

Figure 4.13 Skyplot, Scenario 8

Table 4.8 Monte Carlo Simulation Results, Scenario 8

	Closed Form	Maximum Likelihood	Kalman Update	Iterative	
				Least Squares	Best Four
Estimated σ	23.51				
GDOP				2.84	3.19
Condition H	337.28			7.45	6.60
Error x	-19.42	-0.19	-0.23	-0.14	-0.34
Error y	-73.93	-0.69	-0.85	-0.18	-0.49
Error z	64.35	1.12	1.25	0.73	-1.41
Error bias	-347.06	-0.98	-1.73	-0.29	0.42
Miss distance	99.92	1.32	1.53	0.76	1.53
Estimated std x	287.39				
Estimated std y	1094.28				
Estimated std z	944.04				
Estimated std bias	5165.26				
Experimental std x	1246.90	66.20	66.71	65.55	85.69
Experimental std y	4738.02	216.20	217.87	214.81	236.33
Experimental std z	4084.66	108.34	110.45	106.83	125.90
Experimental std bias	22298.07	144.68	171.07	136.72	150.91
Expected std x	1222.25		67.52	65.60	85.50
Expected std y	4653.81		221.57	215.38	236.35
Expected std z	4014.87		100.53	106.96	125.58
Expected std bias	21967.14		126.23	136.69	151.20

EXPERIMENTAL SCENARIO DATA

GPS time: t = 71100 sec
User Position: 40 N, 105 W, 300 m
Satellite Availability: N = 6
Satellites for best GDOP: 9 12 16 19

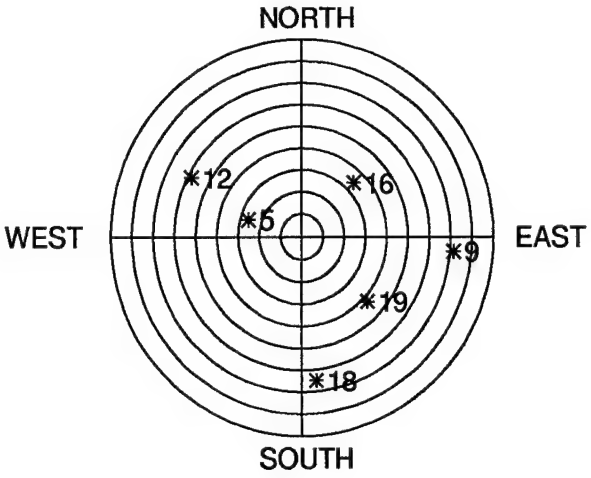

Figure 4.14 Skyplot, Scenario 9

Table 4.9 Monte Carlo Simulation Results, Scenario 9

	Closed Form	Maximum Likelihood	Kalman Update	Iterative	
				Least Squares	Best Four
Estimated σ	26.29				
GDOP				2.82	3.60
Condition H	987.14			7.41	7.23
Error x	20.25	0.72	0.74	0.75	2.06
Error y	80.04	5.98	6.05	5.97	6.78
Error z	-67.76	-3.68	-3.74	-3.51	-0.86
Error bias	344.95	-3.58	-3.24	-4.02	-2.80
Miss distance	106.81	7.06	7.15	6.97	7.13
Estimated std x	770.86				
Estimated std y	2920.93				
Estimated std z	2526.94				
Estimated std bias	13741.87				
Experimental std x	2851.21	87.03	87.23	86.21	119.07
Experimental std y	10778.94	186.99	187.56	186.53	212.71
Experimental std z	9322.34	132.66	133.13	132.24	208.80
Experimental std bias	50673.38	144.76	152.38	142.11	166.60
Expected std x	2932.02		80.72	85.56	119.03
Expected std y	11109.87		207.21	186.80	212.20
Expected std z	9611.34		142.42	131.61	206.77
Expected std bias	52267.75		87.99	141.49	165.36

EXPERIMENTAL SCENARIO DATA

GPS time: t = 81900 sec
User Position: 40 N, 105 W, 300 m
Satellite Availability: N = 6
Satellites for best GDOP: 15 18 19 21

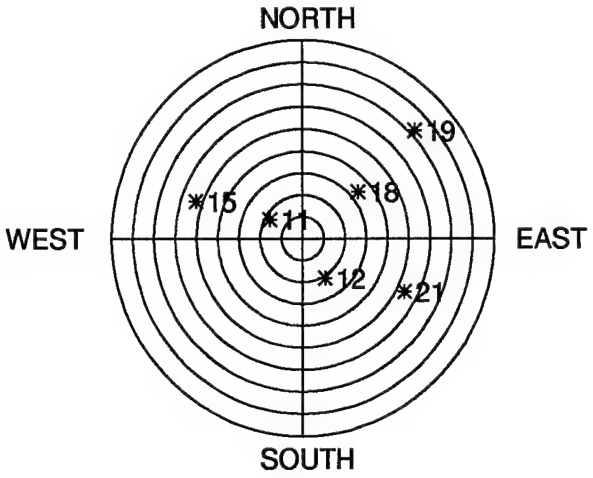

Figure 4.15 Skyplot, Scenario 10

Table 4.10 Monte Carlo Simulation Results, Scenario 10

	Closed Form	Maximum Likelihood	Kalman Update	Iterative	
				Least Squares	Best Four
Estimated σ	26.09				
GDOP				3.26	3.92
Condition H	490.73			9.02	8.69
Error x	-6.54	0.05	0.05	0.02	0.17
Error y	-25.03	0.06	0.06	0.09	-0.34
Error z	22.86	0.88	0.88	1.06	-0.14
Error bias	-115.74	0.79	0.79	0.63	0.14
Miss distance	34.52	0.89	0.88	1.06	0.40
Estimated std x	538.12				
Estimated std y	2048.11				
Estimated std z	1795.61				
Estimated std bias	9513.75				
Experimental std x	2027.26	77.76	77.88	77.36	89.65
Experimental std y	7697.27	147.44	147.92	146.93	205.44
Experimental std z	6736.57	215.51	215.53	215.25	250.14
Experimental std bias	35719.62	177.29	180.92	175.89	197.01
Expected std x	2062.54		68.85	77.84	89.96
Expected std y	7850.15		168.66	149.38	207.83
Expected std z	6882.36		230.58	215.45	251.05
Expected std bias	36465.09		124.86	177.02	198.61

EXPERIMENTAL SCENARIO DATA

GPS time: t = 74700 sec
User Position: 40 N, 105 W, 300 m
Satellite Availability: N = 6
Satellites for best GDOP: 11 12 16 18

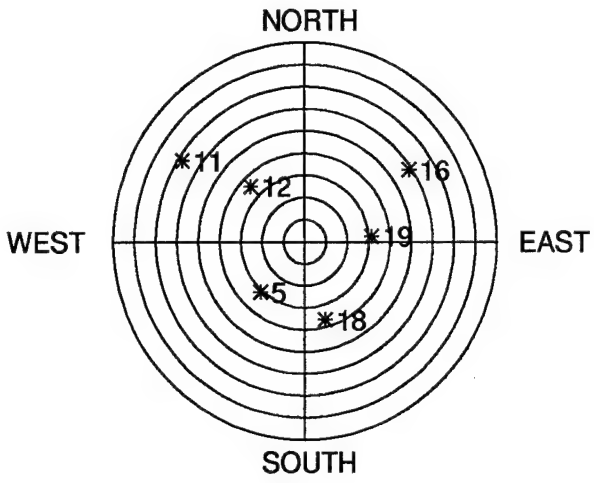

Figure 4.16 Skyplot, Scenario 11

Table 4.11 Monte Carlo Simulation Results, Scenario 11

	Closed Form	Maximum Likelihood	Kalman Update	Iterative	
				Least Squares	Best Four
Estimated σ	39.08				
GDOP				3.97	4.39
Condition H	2442.63			11.34	9.93
Error x	-145.85	-0.70	-0.72	-0.72	-0.92
Error y	-540.48	-5.62	-5.68	-5.34	-7.86
Error z	467.22	5.96	5.99	5.70	8.23
Error bias	-2500.71	4.84	4.51	5.52	7.25
Miss distance	729.17	8.22	8.29	7.84	11.42
Estimated std x	2540.03				
Estimated std y	9358.44				
Estimated std z	8071.08				
Estimated std bias	43840.47				
Experimental std x	6472.81	97.25	97.26	97.25	107.88
Experimental std y	23864.01	175.63	176.13	175.05	208.54
Experimental std z	20581.58	263.56	263.82	263.30	290.40
Experimental std bias	111746.08	223.90	227.19	218.73	233.39
Expected std x	6499.87		97.35	96.90	108.92
Expected std y	23948.04		172.89	174.18	206.69
Expected std z	20653.72		281.93	265.02	290.10
Expected std bias	112186.77		178.45	218.69	231.89

EXPERIMENTAL SCENARIO DATA

GPS time: t = 89100 sec
User Position: 40 N, 105 W, 300 m
Satellite Availability: N = 5
Satellites for best GDOP: 12 15 17 21

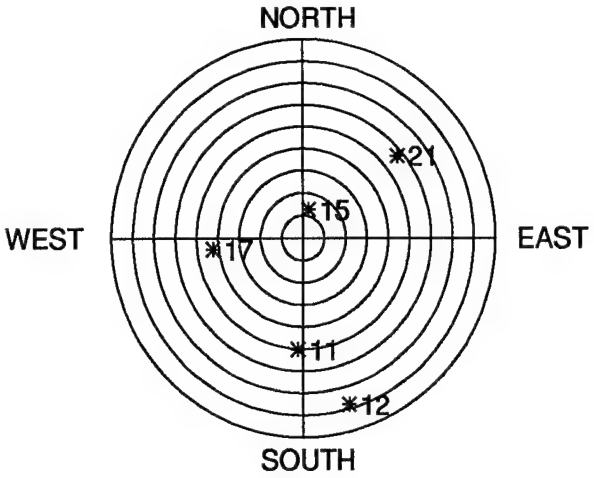

Figure 4.17 Skyplot, Scenario 12

Table 4.12 Monte Carlo Simulation Results, Scenario 12

	Closed Form	Maximum Likelihood	Kalman Update	Iterative	
				Least Squares	Best Four
Estimated σ					
GDOP				3.89	4.66
Condition H	220.92			9.81	10.54
Error x	-9.38	-2.49	-2.50	-2.48	-2.48
Error y	-26.46	-0.04	-0.08	0.08	1.02
Error z	22.53	0.05	0.08	-0.05	-0.21
Error bias	-123.96	-0.89	-1.05	-0.73	-1.21
Miss distance	36.00	2.49	2.50	2.48	2.69
Estimated std x					
Estimated std y					
Estimated std z					
Estimated std bias					
Experimental std x	1333.94	102.45	102.57	102.43	102.43
Experimental std y	5128.78	290.92	292.34	289.14	366.57
Experimental std z	4356.99	134.99	137.14	132.57	138.12
Experimental std bias	23750.81	204.84	221.34	201.19	230.79
Expected std x	1344.70		103.09	101.49	101.51
Expected std y	5146.84		278.26	288.12	367.33
Expected std z	4374.34		126.54	131.95	137.47
Expected std bias	23947.62		281.68	200.68	230.91

4.11 Experimental Results, Ground-Based Pseudolite Test Environment

The Monte Carlo simulation results associated with the ground-based pseudolite test environment are presented in Table 4.13. This test environment includes three test scenarios A, B, and C as described in Section 4.3.

4.11.1 Analysis of Results, Conventional Iterative Least Squares Algorithm.

The results for the conventional ILS algorithm are discussed first, as they will serve as a baseline for comparison. The results in Table 4.13 show that the ILS algorithm is capable of producing fairly good estimates of the four GPS estimation parameters. The results also show that the accuracy of the z user position coordinate estimate degrades as the GPS-like transmitter or pseudolite below the user position is moved away from directly below the user. In this given experimental test environment, with the user at an altitude of 10000 m, it was observed experimentally that there must be a pseudolite within approximately 500 m from the user's projection on ground in order to produce a geometry that can be handled by the iterative algorithm. As the user altitude decreases, the problem is amplified and a smaller offset can be tolerated. This problem associated with using the ILS algorithm in ground-based planar arrays is known and led to the following recommendations by McKay [20]:

- The radius of the outer pattern must be as large as possible, essentially at the horizon.
- The user altitude must be kept as large as possible essentially at its flight envelope limit.
- The user must be flown along a known ground array test pattern which guarantees that a pseudolite is always close to being directly below the user.

Table 4.13 Monte Carlo Simulation Results, Ground Test Environment

	Scenario	A	B	C
Closed Form	Estimated σ	99.86	95.56	95.22
	condition H	953483.12	1216172.19	1204038.42
	Error x	0.03	-0.53	0.12
	Error y	0.08	0.64	-0.14
	Error z	1309728.17	293416.35	1113025.86
	Error bias	260.13	264.20	259.60
	Miss distance	1309728.17	293416.35	1113025.86
	Estimated std x	30.65	28.81	28.73
	Estimated std y	30.17	28.81	28.72
	Estimated std z	19937827.70	25016822.93	24938973.83
	Estimated std bias	312.19	295.77	296.26
	Experimental std x	33.18	33.17	33.15
	Experimental std y	32.66	32.10	33.33
	Experimental std z	21254961.40	28646390.13	28058282.43
	Experimental std bias	251.55	235.98	239.60
Kalman Update	Error x	9.85	-0.52	0.17
	Error y	56.98	0.44	-0.90
	Error z	-9632.47	-10151.91	-9872.20
	Error bias	312.34	264.59	260.17
	Miss distance	9632.65	10151.91	9872.20
	Estimated std x	542.53	33.27	33.27
	Estimated std y	3086.50	37.84	38.47
	Estimated std z	12170.60	9904.77	9903.54
	Estimated std bias	4376.00	238.59	241.33
	Experimental std x	36.80	28.89	28.79
	Experimental std y	124.68	33.05	32.89
	Experimental std z	498.92	367.70	368.40
	Experimental std bias	368.13	296.89	297.28
Iterative	Error x		-0.57	0.27
	Error y		0.68	0.19
	Error z		0.39	11.46
	Error bias		-2.68	-10.62
	Miss distance		0.97	11.47
	Experimental std x		33.73	33.71
	Experimental std y		32.61	33.91
	Experimental std z		341.74	347.54
	Experimental std bias		244.70	249.12

The results for Scenario C show the case when the pseudolite below the user is offset by 400 m, which is close to the largest offset that can be tolerated without producing a singular geometry. In a singular geometry, a solution cannot be obtained, as was the case in Scenario A when no pseudolite was available directly below the receiver or in the vicinity. Scenario B whose layout is shown in Figure 4.1, in Secion 4.3, represents an optimum geometry; consequently, the estimated parameter errors were all small. The results for Scenario C show little change on the estimates of the x and y user position coordinates and the range-equivalent user clock bias, but the error in the z user position coordinate estimate increases form 0.39 m to 11.46 m. The standard deviation on the z user position coordinate estimation error was one order of magnitude larger than for the x and y coordinate; however, there was no impact on the z user position coordinate error standard deviation caused by the 400 m offset in the pseudolite below the user.

4.11.2 Analysis of Results, Closed-Form Algorithm. The results in Table 4.13 indicate that, in this test environment, the *closed-form* algorithm produces excellent estimates of the pseudorange measurement noise strength σ. The σ produced by the algorithm ranged from 95.22 m to 99.86 m compared with the true value of 100 m used in simulating the measurement noise. This test environment was intentionally simulated using ground-based planar arrays of 36 or 37 pseudolites because from the experimental results presented in Figure 4.5, in Section 4.8.2, it was anticipated that this number of transmitters would be required to obtain reliable estimates of σ. The pseudolite availability in this test environment is greater than the satellite availability that can be achieved in conventional NAVSTAR GPS scenarios. High availability is favorable for the estimation of σ since the validity of the ergodic assumption invoked in Equation (3.20), which formed the basis of the estimation of σ, is strengthened by increasing transmitter availability. Furthermore, Scenario A yielded the most favorable conditions for estimating the measurement noise strength since the pseudoranges to all transmitters were essentially the same,

validating the average pseudorange approximation used in Equation (3.5). Unlike the results obtained for the simulated GPS test environment, the estimation of u_x and u_y user position coordinates are extremely good, with errors marginally smaller than those obtained with the conventional ILS algorithm; however, the u_z user position coordinate estimation error is outrageously large, ranging from 2.9×10^5 meters to 1.3×10^6 meters. It is evident from the results that the *closed-form* algorithm has a serious observability problem along the z coordinate axis. The problem is marginally worst in Scenario A where there is no transmitter below the user along the z coordinate axis. The miss distance results are not used for comparison purpose because they reflect the overly dominant error in the z coordinate estimates. Given the algorithm's ability to estimate σ accurately, the estimation of the standard deviation of the estimation error is also extremely good, where the estimates were all within 20.24 percent of the experimentally derived standard deviations for all four estimation parameters, in the three scenarios. For the x and y coordinates, the experimental standard deviation is slightly lower than that achieved with the ILS algorithm. The standard deviation on the bias estimation error is slightly larger than that achieved with the ILS algorithm. Whether or not a transmitter is directly below the user, had virtually no effect on the effect on the performance of the *closed-form* algorithm. The *closed-form* algorithm is not dependent on having a transmitter directly below at all times, which would be physically impossible. The *closed-form* algorithm is capable of producing x and y position coordinate estimates better than the conventional iterative algorithm; however, it does significantly worse at estimating the z position coordinate and slightly worse at estimating the range-equivalent user clock bias. In addition, given the extremely low estimation errors in the x and y user position coordinate estimates, it appears that the geometry produced by a spread-out ground-based planar array of pseudolites is more favorable to the *closed-form* algorithm than any geometry that can be produced considering strictly the 24 satellite NAVSTAR GPS constellation. If it was necessary to estimate

only the x and y user position coordinates from signals obtained from pseudolites in a ground-based planar array, this *closed-form* algorithm would be the algorithm of choice.

4.11.3 Analysis of Results, Kalman Update. The results indicate that, starting from the four GPS parameter estimates produced by the *closed-form* algorithm and applying the *Kalman update* algorithm twice, there is a potential for marginal improvement or corruption of the estimates, of the x and y user position coordinates and the range-equivalent user clock bias. The small changes in the estimates of the x and y user position coordinates allowed the *Kalman update* algorithm to produce greatly improved estimate of the z user position coordinate. The standard deviation of x and y user position coordinates and the range-equivalent user clock bias estimates are also effected very little, sometimes for the worse, other times for the better. The algorithm's capability to estimate the standard deviation on the x and y user position coordinates and the range equivalent user clock bias also works well. The estimation errors for the z user position coordinate range from 9632.47 m to 10151.91 m, representing two orders of magnitude in error reduction compared to the *closed-form* algorithm. Despite this improvement, the error in the z coordinate is still too large to render this algorithm useful. The improvement in the experimental standard deviation in the z coordinate estimate is more significant than the improved estimate itself; however, the algorithm is grossly overestimating its error on the z coordinate estimate. Based on the results, the *Kalman update* algorithm does not prove very useful in this ground-based planar array test environment, as it does not provide any significant improvement over the *closed-form* algorithm; moreover, the risk of corrupting the x and y user position coordinate estimates exists.

4.12 Summary of Experimental Results

In typical near-earth GPS scenarios, the root mean square miss distances associated with the *closed-form* algorithm, ranging from 4.93 m to 729.17 m, were

much worse than the baseline ILS algorithm's results, which produced a maximum miss distance of 7.84 m. However, when the *closed-form* algorithm is assisted by a supplementary algorithm, the miss distances were reduced to the baseline level, within 8.22 m and 8.29 m for the *maximum likelihood* and *Kalman update* algorithms respectively. Based only on miss distance, the deficiency in the unassisted *closed-form* algorithm is evident; however, the experimental standard deviations associated with the four GPS solution parameters, which are much more reliable performance indicators, clearly reveal the seriousness of the problem. The experimental standard deviation, on the three position parameter estimates, yielded by the *closed-form* algorithm ranged from 1078.08 m to 23864.01 m, compared to the baseline ILS results, which ranged from 55.56 m to 289.14 m. The experimental standard deviation on the range-equivalent user clock bias estimates were much worse, ranging from 19014.42 m to 111746.08 m. The *maximum likelihood* and *Kalman update* algorithms yielded experimental standard deviations comparable to the baseline ILS results for the three position parameter estimates but consistently slightly larger than the baseline ILS results for the user clock bias. The *closed-form* algorithm's performance is inadequate for stand-alone use; however, its results are used as initialization for the supplementary algorithms, to achieve performance comparable to that of the baseline ILS algorithm. The estimation error covariance prediction performance of the closed-form algorithm is dependent on how well the pseudorange measurement noise variance (σ^2) can be estimated, which is a function of satellite availability. Under typical satellite availability conditions it was not possible to retrieve good data-driven estimates of σ, but as satellite availability is increased, the estimates of σ improve. Using a scenario concatenation scheme, a mean estimated σ of 92.5 m was retrieved, which compares well with the true value of 100 m used to generate the experimental measurement noise.

The unconventional geometries in the ground-based planar array scenarios using pseudolites, produced results that were more favorable to the *closed-form* al-

gorithm. The horizontal positioning performance of the *closed-form* algorithm was marginally better than the baseline ILS results both in terms of mean errors and experimental standard deviation. The biggest attribute of the *closed-form* algorithm was that, unlike the ILS algorithm which is highly dependent on having a pseudolite directly below the user, the *closed-form* algorithm can produce good horizontal positioning results under any geometry. Given the large pseudolite availability in the ground-based planar array, excellent estimates a σ, between 95.2 m and 99.9 m, were retrieved. As a result, the *closed-form* algorithm's error covariance prediction performance was very good.

V. *Conclusions and Recommendations*

This chapter presents a brief summary of the performance related issues of the *closed-form* algorithm and the supporting algorithms developed for this thesis research. Emphasis is placed on the identifying the areas of strength for the algorithms and suggesting applications for which they are best suited. The shortcomings seen in the Chapter IV related to algorithm deficiency and inconclusive findings are discussed, and potential approaches to correcting the problems are presented. The chapter sums up with recommendations for future work that can prove rewarding in bringing the concept of using a stochastic closed-form GPS position determination algorithm closer to reality.

5.1 Typical Near-Earth GPS Applications

When compared to the current linear iterative algorithms using approximative linearization, the use of stochastic modeling and estimation techniques applied to GPS, describes a more correct approach to solving the system of nonlinear GPS pseudorange equations from a mathematical perspective. Although the concept is sound, the results yielded by this research indicate that there are no benefits to be gained in terms of estimation accuracy when dealing with the most typical GPS application of near-earth navigation using strictly the satellites available in the NAVSTAR GPS 24 satellite constellation. Under near-earth, large SNR conditions, the research demonstrates that the stand-alone *closed-form* algorithm is incapable of producing a reasonable GPS solution estimate without being supplemented by either the *maximum likelihood* or the *Kalman update* algorithm. The performance of both supplementary algorithms is essentially equivalent but the latter is the preferred algorithm because it is closed-form in nature and because it possesses the capability of predicting its estimation error covariance. For these reasons, the conclusions will emphasize results associated with the *Kalman update* algorithm.

This research clearly indicates that the developed algorithm, consisting of the *closed-form* algorithm as supplemented by the *Kalman update* algorithm, does not offer any significant performance improvements over the conventional ILS algorithm in typical near-earth navigation applications. The relative performance of the developed algorithm can be summed up by the following points:

1. The performance in terms of accuracy, based on mean miss distance, of the developed algorithm is equivalent to that of the conventional ILS algorithm. In all the realistic near-earth test scenarios analyzed in this thesis, the miss distances yielded by the developed algorithm were a fraction of a meter either above or below those yielded by the ILS algorithm.

2. The performance in terms of experimental standard deviation of the GPS parameter estimates of the developed algorithm is, at best, slightly degraded when compared to that of the conventional ILS algorithm. This performance indicator is a measure of how sensitive the algorithm is to pseudorange measurement noise and establishes the estimation error bounds. The experimental standard deviation associated with the three position parameter estimates (u_x, u_y, u_z) produced by the developed algorithm where marginally larger; all within 4.6 percent above the ILS results. The performance degradation of the experimental standard deviation associated with the estimate of the range-equivalent user clock bias was more significant, ranging from 2.8 to 35.3 percent above the ILS results.

3. Considering only satellites available in the NAVSTAR GPS constellation, there is insufficient satellite availability, preventing the *closed-form* algorithm from producing a reliable estimate of the pseudorange measurement noise strength. The research showed improvement in estimating the noise strength, σ, with increasing satellite availability; however, an availability of at least 36 satellites is needed to produce a reliable estimate. Since this number is not achievable in

typical near-earth GPS applications, the developed algorithm cannot predict a reliable estimation error covariance, under these conditions.

4. When the algorithms are artificially informed of the pseudorange measurement noise strength, σ, the developed algorithm as well as the conventional ILS algorithm performed extremely well at producing the estimation error covariance matrix. The diagonal elements of the covariance matrix were used to calculate the expected standard deviation of the individual GPS parameter estimates for comparison to the experimentally derived values. The developed algorithm performed slightly worse than the conventional ILS algorithm. The expected standard deviations for the position parameters for the developed algorithm were all within 14.0 percent of the experimental values and the standard deviations on the clock bias were off by as much as 44.2 percent. These results do not compare very well to the maximum of 2.25 percent on all four parameters achieved by the ILS algorithm.

The largest deficiency for the developed algorithm is associated with the estimation of the clock bias, which is not an issue if only positioning accuracy is considered. It is suspected that this deficiency is a direct result of the composition of the regressor matrix. The closed-form regressor matrix is such that the last column is made up of differenced pseudorange measurements, whereas the the first three columns are made up of differenced satellite position coordinates. This composition scheme leads to an ill-conditioned regressor that is unfavorable to the estimation of the last GPS parameter, namely the range-equivalent user clock bias.

5.2 Unconventional GPS Applications

The developed algorithm which consists of the basic *closed-form* algorithm as supplemented by the *Kalman update* algorithm is, as a whole, a closed-form algorithm. Inherently, it does not require any form of user initialization in order to produce a GPS solution. One direct benefit of a closed-form GPS position deter-

mination algorithm is the ability to produce a solution in geometrical conditions very different from the typical near-earth applications for which GPS is known to be best suited. These uncommon geometrical conditions can be encountered in deep space applications and in pseudolite ground-based arrays, both of which can lead to difficulties for the conventional iterative algorithms. In these applications, the developed algorithm alleviates any concern of multiple solutions or of convergence towards the wrong solution as a result of incorrect initialization, as is the case for the conventional iterative algorithms.

This thesis research did not include any deep space simulated scenarios for testing purpose; hence, no comments can be made on performance issues in deep space. However, the developed algorithm was tested in simulated pseudolite ground-based array scenarios and it was found to be much more tolerant to geometrical conditions than was the conventional ILS algorithm. The developed algorithm is not dependent on having a pseudolite in the vicinity of user's position projection on the ground. The conventional ILS algorithm was incapable of producing a solution if a pseudolite was not present virtually directly below the user position. The acceptable offset tolerance for the receiver directly below the user is proportional to the ground array size and the user altitude. In a small size ground array with the user at low altitudes, the tolerance would be extremely small, requiring that a pseudolite always be precisely below the user. This condition is extremely restrictive on the flight pattern and would require pseudolite placed in close proximity to each others below the intended flight pattern. All these concerns are alleviated by using the developed algorithm.

In estimating strictly the horizontal user position coordinates u_x and u_y, the *closed-form* algorithm on its own without the assistance of a supplementary algorithm was the best performing algorithm. The mean error on these two estimation parameters was smaller as was the experimental standard standard deviation, when compared to the results yielded by the baseline ILS algorithm. The algorithm's in-

sensitivity to ground array geometry and its extremely good horizontal positioning accuracy makes it well suited for test range applications. Nonetheless, the *closed-form* algorithm suffers from serious observability problems along the vertical axis, as was observed from the extremely poor accuracy in the estimation of vertical user position coordinate, u_z. The observability problem along the vertical axis is a result of how the planar array is constructed. If the array were truly planar, the z coordinates of all the pseudolites would be exactly the same, which would result in a singular regressor matrix. Recalling that the third column of the regressor is made up of differenced satellite z position coordinates, in a truly planar array the third column would be a column of zeros. Fortunately, the world is not perfectly flat and it was necessary to introduce some small random variations in the simulated pseudolite z position coordinates to reflect terrain perturbations. As the variations in the pseudolite altitudes is increased, the accuracy of the estimated vertical user position coordinate improves at the expense of slightly degrading horizontal positioning accuracy. It is probably best to maintain the horizontal positioning accuracy at the highest achievable level and solving the vertical positioning accuracy problem by using an extremely accurate altitude measuring instrument such as a radar altimeter in conjunction with the *closed-form* algorithm in the GPS receiver. This combination is generally beneficial, since GPS, in general, produces vertical errors that are larger than the horizontal errors.

5.3 Estimation Error Covariance

One of the driving motivations to this thesis research, in applying stochastic modeling and estimation techniques to the GPS pseudorange equations, was the possibility of producing an estimate of the estimation error covariance. This capability would provide a confidence factor associated with the GPS solution in real time. The research demonstrated that it is possible to estimate the pseudorange measurement noise strength (σ) accurately, using the developed algorithm, if satellite availability is

greater than 36. Once the value of σ is known, the estimation error covariance can be calculated for both the closed form algorithm developed in this thesis or for the conventional iterative algorithms. Due to the deterministic nature of the conventional iterative algorithms, they have no way of estimating the pseudorange measurement noise strength. Two ways of estimating σ were shown: one using the concatenation of realistically simulated satellite scenarios and the other using simulated ground-based pseudolite planar array scenarios.

The concatenation of realistic satellite scenarios at one hour intervals to obtain an effective satellite availability of 42 proved to be effective for the estimation of σ. Using this approach while maintaining the user position stationary produced a mean estimated σ of 92.5 meters which compares very well to the σ of 100 meters that was used to simulate the experimental noise. This approach is extremely restrictive due to the fact that the user position is maintained stationary at the *measurement point*; therefore, its use for navigation in flight appears limited. Although the algorithm can't be used for estimation purposes during flight in real time, it could be used to calibrate the receiver if it is known that it will be used in the vicinity of the *measurement point.* Receiver calibration can assist in improving the receiver's accuracy by compensating for noise associated with the measurements as well as the noise that it is responsible for in itself. Obviously, the closer the user is to the *measurement point*, the greater the benefits of the receiver calibration.

The approach of estimating the noise strength from a fixed *measurement point* is very well suited for GPS applications in which the user position is stationary, such as in site surveying. Site surveying, is becoming an increasingly popular application for GPS. In site surveying, accuracy is of extreme importance. The use of the measurement noise estimation scheme will allow for the calculation of the estimation error covariance which can be used as a confidence indicator as well as a means to demonstrate that a desired level of accuracy has been achieved. Once the

measurement noise strength has been estimated, it can be used within the algorithm of choice to produce the estimation error covariance.

Using a ground array with 36 pseudolites in a circular pattern produced a mean estimated σ of 99.86 meters which is remarkably close to the actual experimental noise strength of 100 meters. This concept could prove extremely useful in test range arrangements such as the SARS [25], [20]. It has the potential of being useful in a Wide Area Augmentation Systems (WAAS) [15] which is due to become operational in the near future. The WAAS is a wide-area DGPS concept being developed by the Federal Aviation Administration (FAA) to increase GPS availability in support of flight operations from en-route navigation through Category I precision approaches. WAAS will consist of a ground-based communications network and several geosynchronous satellites to provide global coverage. Differential corrections and additional ranging data will be broadcast to users from geostationary satellites using a signal similar to the NAVSTAR GPS signal [15]. The integrated use of GPS, GLONASS, and the proposed WAAS could form a Global Navigation Satellite System (GNSS) that would guarantee much improved satellite availability that would allow reliable estimations of the pseudorange measurement noise strength using the concepts presented in this thesis. In addition to the WAAS, the possibility of other GPS augmentation systems may be implemented for other specific purposes, further improving satellite availability.

5.4 Condition Number of the Regressor

For the conventional iterative algorithms, this research demonstrated that there exists a direct relationship between the estimation accuracy and the GDOP. This relationship extended very well to the condition number of the regressor, H, where both measures were essentially equivalent indicators of geometrical strength. In the case of the closed-form algorithms, although GDOP is defined mathematically, it has no physical meaning, since it is formulated for use specifically with the matrix

of direction cosines associated with iterative algorithms; hence, the only suitable measure is the condition number of the regressor. The sensitivity of the closed-form algorithms to geometrical conditions is not well known or understood but it is obvious that what constitutes good geometry for the conventional iterative algorithms does not necessarily constitute good geometry for the *closed-form* algorithm. A loose relationship between the condition number of the regressor and the achievable estimation accuracy was observed for the *closed-form* algorithm. This relationship cannot be generalized into an error bound concept, as is the case for iterative algorithms, because the algorithm's behavior changes drastically for different scenarios or applications. The pseudolite ground-based array scenarios were extremely favorable to the *closed-form* algorithms, in the estimation of horizontal user position coordinates, despite the extremely large condition number associated with the regressor matrix. The manifestation of the ill-conditioned regressor was obvious from the poor accuracy in estimating the range-equivalent user clock bias.

5.5 Recommendations

This section presents areas that remain to be explored that can be taken on as follow on research. The results produced by this research, although not very favorable for the implementation of the stochastic closed-form algorithm, has brought to light many interesting issues that deserve further investigation. Given that this area of research is relatively new when compared to the iterative algorithms, further research is required to assess the viability of applying stochastic mathematical modeling to solve the system of GPS pseudorange equations.

5.5.1 GPS Measurement Noise Levels Investigation. In view of the outcome of this research, the most intriguing dilemma that remains unsolved is, why the conventional ILS algorithm performs so well despite the approximative nature of the linearization used and the deterministic approach taken, both of which are sources of error. This dilemma is more intuitively solved by rationalizing why the stochastic

closed-form algorithm in this thesis performed more poorly than anticipated. The explanation to this dilemma is related to the level of noise that is being considered. The low noise levels considered in this research, which are typical of GPS, are too small to gain any benefit from a weighted minimum variance estimate. The inverse covariance weighting actually introduced weighting errors into the stochastic estimate. Preliminary testing indicated that, an unweighted least squares estimate may produce marginally better results at the expense of losing the capability of producing the estimation error covariance. Under degraded operating conditions, with larger pseudorange measurement noise strengths, stochastic estimation may lead to better solutions, in terms of both mean estimation error and experimental standard deviation, than the conventional iterative approaches. Research is required to determine the noise levels at which conditions become favorable to the stochastic modeling approach and, more importantly, determining if those noise levels can ever be encountered with GPS in its current state of technology.

5.5.2 Alternate Stochastic Closed-Form Algorithms. The derivation of the two closed-form algorithms in this thesis make use of an average pseudorange approximation in order to simplify the noise statistics. The approximation is also needed to obtain an expression for the covariance that is not dependent on any of the four GPS parameters being estimated. This approach enabled the algorithm to maintain a true closed-form structure. The derivation of the algorithm needs to be revisited without the use of any approximations in order to evaluate the impact of using the approximation through experimental analysis. In addition, new approaches to deriving alternate stochastic closed-form solutions to the system of pseudorange equations must be investigated in an attempt to obtain an algorithm that possesses the following qualities:

- The regressor matrix should have a low condition number to maintain the estimation error amplification bounds to a minimum.

- The algorithm should be capable of producing an estimate of the four GPS estimation parameters using only four pseudorange measurements, as is the case for deterministic solutions both iterative and closed-form.
- The algorithm should be capable of producing an accurate GPS solution with a single application without the use of a supplementary algorithm.

It must be noted that the existence of, or feasibility of developing, an algorithm that possesses all or any of the above qualities is not guaranteed.

5.5.3 Computational Effectiveness. Another area that remains to be explored is computational effectiveness of the closed-form algorithms. Given current state of computational power, this issue is not one of high priority. Nonetheless, consideration must be given to the computational effectiveness to assess the viability of using the algorithms in real-time applications. The closed-form algorithms are expected to be more effective from a computational standpoint than the iterative algorithms due to the non-recursive nature; however, the rewards of the closed-form algorithm may be offset by an overly complex algorithm that requires computationally demanding mathematical operations.

Bibliography

1. Abel, J. and J. Chaffee. "Existence and Uniqueness of GPS Solutions," *IEEE Transactions on Aerospace and Electronic Systems*, *27*(6):952–956 (November 1991).
2. Bancroft, S. "An Algebraic Solution of the GPS equations," *IEEE Transactions on Aerospace and Electronic Systems*, *21*(1):56–59 (November 1985).
3. Brown, James M. *Optimal Inputs for System Identification*. Dissertation, AFIT/DSG/ENG/95-S-04, School of Engineering, Air Force Institute of Technology, Wright-Patterson AFB, OH, June 1995.
4. Campbell, S.L. and C.D. Meyer, Jr. *Generalized Inverses of Linear Transformations*. New York: Dover Publications, Inc., 1979.
5. Canadian GPS Associates. *Guide to GPS Positioning*. Fredericton, N.B., Canada: University of New Brunswick Graphic Services, 1987.
6. Chaffee, J. and J. Abel. "On the Exact Solutions of Pseudorange Equations," *IEEE Transactions on Aerospace and Electronic Systems*, *30*(4):1021–1030 (October 1994).
7. Chaffee, J. and K. Kovach. "Bancroft's Algorithm is Global Nonlinear Least Squares." *Proceedings of ION GPS-96*. 431–437. September 1996.
8. Dailey, D. J. and B. M. Bell. "A Method for GPS Positioning," *IEEE Transactions on Aerospace and Electronic Systems*, *32*(3):1148–1154 (July 1996).
9. DeLory, Stephen J. *Design and Analysis of a Navigation System Using the Federated Filter*. MS Thesis, AFIT/GSO/ENG/95D-02, School of Engineering, Air Force Institute of Technology, Wright-Patterson AFB, OH, December 1995.
10. GPSoft, Athens, OH. *Satellite Navigation Toolbox for Matlab*, January 1997.
11. Hoshen, J. "The GPS Equations and the Problem of Apollonius," *IEEE Transactions on Aerospace and Electronic Systems*, *32*(3):1116–1124 (July 1996).
12. Kalman, R. E. "A New Approach to Linear Filtering and Prediction Problems," *Transactions of the ASME, Series D: Journal of Basic Engineering*, *82*:34–45 (1960).
13. Kalman, R. E. and R. S. Bucy. "New Results in Linear Filtering and Prediction Theory," *Transactions of the ASME, Series D: Journal of Basic Engineering*, *83*:95–108 (1961).
14. Krause, L. O. "A Direct Solution to GPS-Type Navigation Equations," *IEEE Transactions on Aerospace and Electronic Systems*, *23*(2):223–232 (March 1987).

15. Leick, Alfred, Professor of Spatial Information Science and Engineering. Ohio State University, Department of Geodetic Science, 1997. Internet Site - http://www.spatial.maine.edu/leick.html.

16. Lewantowicz, Z. H. and R. N. Pashcall. Air Force Institute of Technology, Wright-Patterson AFB, OH. Paper - Deep Integration of GPS, INS, SAR and Other Sensor Information - Final Draft.

17. The MathWorks, Inc., Natick, MA. *MATLAB (registered trademark)* (Version 4.2c Edition), November 1994.

18. Maybeck, Peter S. *Stochastic Models, Estimation, and Control, I*. New York: Academic Press, Inc., 1979. Republished, Arlington, VA: Navtech, 1994.

19. Maybeck, Peter S., Professor of Electrical Engineering. Air Force Institute of Technology, Wright-Patterson AFB, OH, 1996. Course Notes - EENG 844, Computational Aspects of Modern Control.

20. McKay, Jason B. *Optimization of a GPS-Based Navigation Reference System*. MS Thesis, AFIT/GE/ENG/96D-12, School of Engineering, Air Force Institute of Technology, Wright-Patterson AFB, OH, December 1996.

21. Milliken, R. J. and C. J. Zoller. "Principles of Operation of NAVSTAR and System Characteristics," *Navigation, Journal of the Institute of Navigation*, *25*(2):3–14 (Summer 1978).

22. Pachter, Meir., Professor of Electrical Engineering, Air Force Institute of Technology, Wright-Patterson AFB, OH. Personal Notes. October, 1996.

23. Papoulis, Athanasis. *Probability, Random Variables and Stochastic Processes*. McGraw-Hill, Inc., 1991. Third Edition.

24. Parkinson, B. W. "GPS Error Analysis." *Global Positioning System: Theory and Applications Volume 1*, edited by B. W. Parkinson et al. Washington, D.C.: American Institute of Aeronautics and Astronautics, 1996.

25. Raquet, J. et al. "Development and Testing of a Mobile Pseudolite Concept for Precise Positioning," *Proceedings of ION GPS-95*, 1–11 (September 1995). Palm Springs.

26. Riggins, Robert N., Assistant Professor of Electrical Engineering. Air Force Institute of Technology, Wright-Patterson AFB, OH, 1996. Course Notes - EENG 534, Global Positioning System.

27. Siouris, George M. *Aerospace Avionics Systems: A Modern Synthesis*. San Diego: Academic Press, Inc., 1993.

28. Spilker, J. J. Jr. "Satellite Constellation and Geometric Dilution of Precision." *Global Positioning System: Theory and Applications Volume 1*, edited by B. W. Parkinson et al. Washington, D.C.: American Institute of Aeronautics and Astronautics, 1996.

29. Spilker, J. J. Jr. and B. W. Parkinson. "Overview of GPS Operation and Design." *Global Positioning System: Theory and Applications Volume 1*, edited by B. W. Parkinson et al. Washington, D.C.: American Institute of Aeronautics and Astronautics, 1996.

30. van Graas, F. and M. S. Braasch. "Satellite Constellation and Geometric Dilution of Precision." *Global Positioning System: Theory and Applications Volume 1*, edited by B. W. Parkinson et al. Washington, D.C.: American Institute of Aeronautics and Astronautics, 1996.

Vita

Salvatore Nardi was born on 22 December 1963 in Montreal, Quebec, Canada. After graduating from Laurier McDonald High School in 1981, he pursued his studies in Electrotechnology at Vanier College. Upon his graduation from Vanier College in 1984, he began his undergraduate studies in Electrical Engineering at Concordia University. After graduation, he worked in industry for one year before deciding to join the Canadian Forces as an Aerospace engineer. Upon completion of his occupational training he was employed in the Directorate Maritime Aircraft Engineering and Maintenance in Ottawa as an avionics project officer for the CP-140 aircraft.

He was selected to pursue post graduate studies at AFIT beginning in June 1996. While at AFIT, he worked on a Masters of Science Degree in Electrical Engineering with a concentration in navigation, guidance, and control. Upon graduation from AFIT in March 1998, Salvatore will return to Ottawa where he will assume his new responsibilities as a navigation systems technical authority in the Directorate General Aerospace Equipment Program Management (DGAEPM).

Permanent address: 5820 Thierry
St-Leonard, QC
Canada, H1P 1K8

REPORT DOCUMENTATION PAGE

Form Approved
OMB No. 0704-0188

Public reporting burden for this collection of information is estimated to average 1 hour per response, including the time for reviewing instructions, searching existing data sources, gathering and maintaining the data needed, and completing and reviewing the collection of information. Send comments regarding this burden estimate or any other aspect of this collection of information, including suggestions for reducing this burden, to Washington Headquarters Services, Directorate for Information Operations and Reports, 1215 Jefferson Davis Highway, Suite 1204, Arlington, VA 22202-4302, and to the Office of Management and Budget, Paperwork Reduction Project (0704-0188), Washington, DC 20503.

1. AGENCY USE ONLY *(Leave blank)*	2. REPORT DATE	3. REPORT TYPE AND DATES COVERED
	March 1998	Master's Thesis

4. TITLE AND SUBTITLE
IMPROVED MATHEMATICAL MODELING
FOR GPS BASED NAVIGATION

5. FUNDING NUMBERS

6. AUTHOR(S)
Salvatore Nardi
Captain, Canadian Forces

7. PERFORMING ORGANIZATION NAME(S) AND ADDRESS(ES)
Air Force Institute of Technology, WPAFB OH 45433-6583

8. PERFORMING ORGANIZATION REPORT NUMBER
AFIT/GE/ENG/98M-01

9. SPONSORING/MONITORING AGENCY NAME(S) AND ADDRESS(ES)
Captain Jeff Hebert
746th TS/TGGED
1644 Vandergrift Rd.
Holloman AFB, NM 88330-7850

10. SPONSORING/MONITORING AGENCY REPORT NUMBER

11. SUPPLEMENTARY NOTES

12a. DISTRIBUTION/AVAILABILITY STATEMENT
Approved for public release; Distribution Unlimited

12b. DISTRIBUTION CODE

13. ABSTRACT *(Maximum 200 words)*
This thesis is concerned with the development of new closed-form GPS position determination algorithms that work in the presence of pseudorange measurement noise. The mathematical derivation of two closed-form algorithms, based on stochastic modeling and estimation techniques, is presented. The algorithms provide an estimate of the GPS solution parameters (viz., the user position and the user clock bias) as well as the estimation error covariance. The experimental results are analyzed by comparison to the baseline results from the conventional Iterative Least Squares (ILS) algorithm. In typical GPS scenarios, the closed-form algorithms are extremely sensitive to noise, making them unsuitable for stand-alone use; however, they perform very well at estimating horizontal position parameters in ground-based pseudolite planar array scenarios where the ILS algorithm breaks down due to poor geometry. For typical scenarios, the use of a supplementary algorithm is required to refine the solution. Thus, the derivation of two supplementary algorithms is presented; the first based on a maximum likelihood approach and the second uses a Kalman-like update approach. Both supplementary algorithms produce results comparable to the ILS results, but the Kalman update approach is preferred. The advantages introduced by the closed-form, supplemented by the Kalman update, algorithm are: 1) The capability to estimate its estimation error covariance, and 2) The potential for computational efficiency due to the closed-form nature of the solution.

14. SUBJECT TERMS	15. NUMBER OF PAGES
Global Positioning System, GPS, Direct Solution, Closed Form, Stochastic Modeling, Stochastic Estimation	144
	16. PRICE CODE

17. SECURITY CLASSIFICATION OF REPORT	18. SECURITY CLASSIFICATION OF THIS PAGE	19. SECURITY CLASSIFICATION OF ABSTRACT	20. LIMITATION OF ABSTRACT
UNCLASSIFIED	UNCLASSIFIED	UNCLASSIFIED	UL

GENERAL INSTRUCTIONS FOR COMPLETING SF 298

The Report Documentation Page (RDP) is used in announcing and cataloging reports. It is important that this information be consistent with the rest of the report, particularly the cover and title page. Instructions for filling in each block of the form follow. It is important to ***stay within the lines*** to meet ***optical scanning requirements***.

Block 1. Agency Use Only *(Leave blank)*.

Block 2. Report Date. Full publication date including day, month, and year, if available (e.g. 1 Jan 88). Must cite at least the year.

Block 3. Type of Report and Dates Covered. State whether report is interim, final, etc. If applicable, enter inclusive report dates (e.g. 10 Jun 87 - 30 Jun 88).

Block 4. Title and Subtitle. A title is taken from the part of the report that provides the most meaningful and complete information. When a report is prepared in more than one volume, repeat the primary title, add volume number, and include subtitle for the specific volume. On classified documents enter the title classification in parentheses.

Block 5. Funding Numbers. To include contract and grant numbers; may include program element number(s), project number(s), task number(s), and work unit number(s). Use the following labels:

C	- Contract	**PR**	- Project
G	- Grant	**TA**	- Task
PE	- Program Element	**WU**	- Work Unit Accession No.

Block 6. Author(s). Name(s) of person(s) responsible for writing the report, performing the research, or credited with the content of the report. If editor or compiler, this should follow the name(s).

Block 7. Performing Organization Name(s) and Address(es). Self-explanatory.

Block 8. Performing Organization Report Number. Enter the unique alphanumeric report number(s) assigned by the organization performing the report.

Block 9. Sponsoring/Monitoring Agency Name(s) and Address(es). Self-explanatory.

Block 10. Sponsoring/Monitoring Agency Report Number. *(If known)*

Block 11. Supplementary Notes. Enter information not included elsewhere such as: Prepared in cooperation with...; Trans. of...; To be published in.... When a report is revised, include a statement whether the new report supersedes or supplements the older report.

Block 12a. Distribution/Availability Statement. Denotes public availability or limitations. Cite any availability to the public. Enter additional limitations or special markings in all capitals (e.g. NOFORN, REL, ITAR).

- **DOD** - See DoDD 5230.24, "Distribution Statements on Technical Documents."
- **DOE** - See authorities.
- **NASA** - See Handbook NHB 2200.2.
- **NTIS** - Leave blank.

Block 12b. Distribution Code.

- **DOD** - Leave blank.
- **DOE** - Enter DOE distribution categories from the Standard Distribution for Unclassified Scientific and Technical Reports.
- **NASA** - Leave blank.
- **NTIS** - Leave blank.

Block 13. Abstract. Include a brief *(Maximum 200 words)* factual summary of the most significant information contained in the report.

Block 14. Subject Terms. Keywords or phrases identifying major subjects in the report.

Block 15. Number of Pages. Enter the total number of pages.

Block 16. Price Code. Enter appropriate price code *(NTIS only)*.

Blocks 17. - 19. Security Classifications. Self-explanatory. Enter U.S. Security Classification in accordance with U.S. Security Regulations (i.e., UNCLASSIFIED). If form contains classified information, stamp classification on the top and bottom of the page.

Block 20. Limitation of Abstract. This block must be completed to assign a limitation to the abstract. Enter either UL (unlimited) or SAR (same as report). An entry in this block is necessary if the abstract is to be limited. If blank, the abstract is assumed to be unlimited.

★U.S.GPO:1993-0-336-043